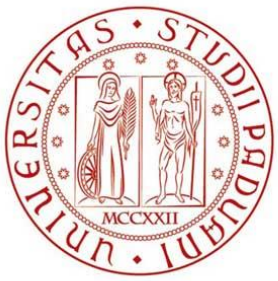

UNIVERSITÀ DEGLI STUDI DI PADOVA

Universita' degli Studi di Padova
Dipartimento di Scienze Chirurgiche, Oncologiche e Gastroenterologiche

DOTTORATO DI RICERCA IN ONCOLOGIA E ONCOLOGIA CHIRURGICA
XXIX CICLO

CHRONIC LYMPHOCYTIC LEUKEMIA: ANALYSIS OF MICROENVIRONMENTAL INFLUENCE ON NEOPLASTIC CLONE SURVIVAL AND IgM SIGNALING DURING IBRUTINIB THERAPY

Tesi redatta con il contributo finanziario della Fondazione Cariparo

Coordinatore: Ch.ma Prof. PAOLA ZANOVELLO
Supervisore: Dr. MONICA FACCO
Co-Supervisore: Ch.mo Prof. LIVIO TRENTIN

Dottoranda: GIORGIA CHIODIN

Table of Contents

ABBREVIATIONS

Ab	Antibody
Ag	Antigen
AID	Activation-Induced Deaminase
ALC	Absolute Lymphocyte Count
ALL	Acute Lymphoblastic Leukemia
AML	Acute Myeloid Leukemia
APC	Allophycocyanin
ATM	Ataxia Telangectasia Mutated
BAD	BCL-2 Associated Death Promoter
BCL-2	B-Cell Lymphoma 2
BCR	B-Cell Receptor
BLNK	B-cell Linker
BM	Bone Marrow
BMF-4	Bone Morphogenic Factor-4
BMSC	Bone Marrow Stromal Cell
BTK	Bruton's Tyrosine Kinase
CCL	Chemokine (C-C motif) Ligand
CCR	Chemokine (C-C motif) Receptor
CD	Cluster of Differentiation
CDR	Complementarity Determining Region
CLL	Chronic Lymphocytic Leukemia
CTL	Cytotoxic T lymphocytes
CR	Complete Remission
CSK	C-terminal Src tyrosine Kinase
CXCL	Chemokine (C-X-C motif) Ligand
CXCR	Chemokine (C-X-C motif) Receptor
DAG	Diacylglycerol
DD	Death Domain
EDTA	Ethylenediaminetetraacetic Acid
ERK	Extracellular signal Regulated Kinase
F/H	Fycoll/Hypaque
Fab	Antigen binding Fragment
FADD	FAS-associated Death Domain
FAS	Fibroblast Associated Antigen
FBS	Fetal Bovine Serum
Fc	Crystallizable fragment
FCS	Fetal Calf Serum
FISH	Fluorescence *in situ* hybridization
FITC	Fluorescein isothiocyanate
FL	Follicular Lymphoma
FR	Framework Region
G-CSF	Granulocyte Colony Stimulating Factor
GC	Germinal Center
GM-CSF	Granulocyte Macrophage Colony Stimulating Factor
GSK3	Glycogen Synthase Kinase 3
GVHD	Graft versus host disease
Hb	Hemoglobin

HCL	Hairy Cell Leukemia
HGF	Hepatocyte Growth Factor
HLA	Human Leukocyte Antigen
HSC	Hematopoietic Stem Cell
HSP90	Heat shock protein 90
hTERT	human Telomerase reverse Transcriptase
iCA^{2+}	Intracellular Calcium
IDO	Indoleamine 2,3-dioxygenase
IFN	Interferon
Ig	Immunoglobulin
IGHV	Immunoglobulin heavy chain variable region
IL	Interleukin
IP$_3$	Inositol Triphosphate
ITAM	Immunoreceptor Tyrosin-based Activation Motif
ITIM	Immunoreceptor Tyrosine-based Inibitory Motif
LN	Lymph node
mAb	monoclonal Antibody
MAPK	Mitogen Activated Protein Kinase
MBL	Monoclonal B-lymohocytosis
MCL	Mantle Cell Lymphoma
MCL-1	Myeloid Cell Leukemia-1
MDS	Myelodysplastic Syndrome
MHC	Major Histocompatibility Complex
MM	Multiple Myeloma
MSC	Mesenchymal Stromal Cell
MZL	Marginal Zone Lymphoma
NF-κB	Nuclear Factor-kappa B
NHL	Non-Hodgkin Lymphoma
NLC	Nurse-like cell
NK	Natural Killer
ORR	Overall Response Rate
OS	Overall Survival
OSM	Oncostatin M
PARP	Poli-ADP-Ribose Polymerase
PB	Peripheral lood
PBMC	Peripheral Blood Mononuclear Cell
PBS	Phosphate Buffered Saline
PCR	Polymerase Chain Reaction
PDGF	Platelet-Derived Growth Factor
PE	Phycoerythrin
PFS	Progression Free Survival
PGE-2	Prostaglandin E-2
PH	Pleckstrin-Homology
PI3K	Phosphatidylinositol 3-Kinase
PIP$_2$	Phosphtidylinositol 4,5-bisphsphate
PIP$_3$	Phosphtidylinositol 3,4,5-triphsphate
PKC	Protein Kinase C
PLCγ2	Phospholipase Cγ2
PLL	Prolymphocytic Leukemia

PS	Phosphatidylserine
PTK	Protein Tyrosine Kinase
RAG	Recombinant-Activating-Genes
SCF	Stem Cell Factor
SCT	Stem Cell Transplantation
SD	Standard Deviation
SDF-1α	Stromal Derived Factor-1α
SDS-PAGE	Sodium Dodecyl Sulphate-PolyAcrylamide Gel electrophoresis
SFKs	Src Family Kinases
SH	Src-Homology
SHM	Somatic Hypermutation
sIgM	surface Immunoglobulin M
SLL	Small Lymphocytic Leukemia
SMZL	Splenic Marginal Zone Lymphoma
STAT	Signal Transducer and Activator of Transcription
SYK	Spleen tyrosine Kinase
TA	Telomerase activity
TGF-β	Transforming Growth Factor-β
TH	TEC-Homology
TNF-R	Tumor Necrosis Factor-Receptor
TK	Thymidine Kinase
VCAM-1	Vascular Cell Adhesion Molecule-1
VEGF	Vascular Endothelial Growth Factor
WB	Western Blotting
WBC	White Blood Cells
XLA	X-Linked Agammaglobulinemia
ZAP-70	Zeta-Associated Protein of 70kDa

SUMMARY

Chronic lymphocytic leukemia (CLL) is a lymphoproliferative disorder characterized by the accumulation of mature B cells in the peripheral blood, bone marrow and lymphoid organs. Malignant lymphocytes are small clonal CD19+/CD5+/CD23+ cells maintained largely in the G0/G1 phase of the cell cycle, able to escape apoptosis through intrinsic features of the neoplastic clone, including genetic abnormalities and overexpression of anti-apoptotic proteins. However, their survival advantage is due also to extrinsic factors that influence the behavior of neoplastic cells in the tissue microenvironment. Mesenchymal stem cells (MSCs) represent a major component of the marrow stroma. MSCs are commonly found in secondary lymphatic tissues of CLL patients, providing survival and migration signals to leukemic cells.

During the last years, the modulation of the interaction of tumor cells with microenvironmental elements has become a promising therapeutic strategy in CLL treatment. Recently, several small molecules have been designed against specific kinases involved in the propagation of B cell receptor (BCR) signaling, in order to block the activation of multiple survival pathways.

Bafetinib (INNO-406) is a dual BCR-ABL/LYN inhibitor initially designed for treatment of chronic myeloid leukemia. In CLL, it has been demonstrated that the src-kinase LYN is overexpressed and constitutively active, thus Bafetinib is an interesting potential target for CLL treatment.

Ibrutinib (PCI-32765) is a potent BTK (Bruton's tyrosine kinase) inhibitor that covalently binds to the cysteine 481 (C481) of the protein active site, thus preventing its complete activation. The consequences *in vitro* are inhibition of basal and induced BTK phosphorylation, with broad inhibition of downstream pathways. However, the functional consequences on signaling in response to sIgM stimulation during Ibrutinib therapy *in vivo* are not completely elucidated.

In the first part of this thesis (Chapter 2), we evaluated the effect of *in vitro* treatment with kinase inhibitors (Ibrutinib and Bafetinib) on CLL cells in the presence of MSCs, challenging the ability of the stromal cells to protect neoplastic lymphocytes from drug-induced apoptosis, and the influence of the microenvironment on CLL migration, adhesion and chemokine receptor

expression. This research has demonstrated that the MSC co-cultures represent a reproducible *in vitro* system, with functional similarities to the *in vivo* marrow environment. In the presence of kinase inhibitors, leukemic B cells lose not only their ability to proliferate and survive, but also to interact with the protective marrow microenvironment. Thus, the impairment of the cross-talk between stromal cells and CLL cells seems an important and necessary condition to target for the eradication of the disease. Moreover, in this project, the LYN inhibitor Bafetinib has been shown to exert an effect similar to Ibrutinib in blocking MSC/CLL B cell cross-talk, for the first time in *in vitro* CLL cultures.

In the second part (Chapter 3), developed during a research period at the University of Southampton, the effect of *in vivo* Ibrutinib therapy on surface IgM (sIgM) expression and signaling capacity in CLL patients was investigated, aiming to understand the behavior of tumor cells in the early phases of therapy. This study has shown that, after one week of treatment, IgM levels are increased on CLL cell surface and associate with cell signaling capacity, as shown by the increased pSYK inducibility during therapy. The inhibition of BTK activation is responsible for the decrease of iCa^{2+} and ERK phosphorylation at week 1, but the variability of the response and the residual signaling activity observed suggest that there may be other pathways that could take part in the signaling process, bypassing BTK blockade.

Chapter 1 – Chronic Lymphocytic Leukemia

1.1 Introduction

1.1.1 Epidemiology and etiology

Chronic lymphocytic leukemia (CLL) is a lymphoproliferative disorder characterized by the progressive accumulation of mature B cells in the peripheral blood, bone marrow and lymphoid organs. Malignant B lymphocytes are small clonal cells mainly in the G_0/G_1 phase of the cell cycle that display a highly distinctive immunophenotype, with positivity for B-cell markers cluster of differentiation 19 (CD19), CD20, CD23 plus the CD5 antigen, in the absence of other pan-T-cell surface markers [1]. CLL is the most common leukemia in the Western world [2], and is more prevalent in men than in women, with a male to female ratio of 2:1. CLL is considered a disease of the elderly, with a mean age at diagnosis of 70 years; however, it can be diagnosed also in younger individuals. The incidence increases rapidly with an increase in age [3].

Etiology is still unknown; the exposure to common carcinogens does not seem to be associated with disease progression. More studies are in progress to assess a potential relation between CLL, inflammation, and autoimmune conditions[4]. Moreover, it has been demonstrated that anticipation, a phenomenon whereby an inherited disease is diagnosed at an earlier age in each successive generation of a family, occurs in familial CLL and a genetic mechanism is suggested as the cause [5].

1.1.2 Clinical features

The clinical course and the survival of CLL patients are quite variable: some patients remain asymptomatic without any treatment requirement, while others present an aggressive disease course that is difficult to control with chemotherapy.

CLL is often determined with routine laboratory tests, and is frequently diagnosed in asymptomatic patients. In other cases, the pathology occurs with asthenia, weight loss, fever, lymphadenopathy, splenomegaly and hepatomegaly. Some patients can show autoimmune phenomenon, such as hemolytic anemia (11%

of cases) or autoimmune thrombocytopenia (2% of cases), which occur in advanced and multi-treated disease. Moreover, the hypogammaglobulibemia typical in CLL can induce immunodeficiency and high mortality due to infections [6, 7].

Although the causes of death are often attributed to the underlying disease, in some cases progressing syndromes with a poor prognosis can occur; for example, Richter's syndrome, in which CLL disease changes into a fast-growing diffuse large B cell lymphoma, or B-cell prolymphocytic leukemia (B-PLL), is more aggressive and characterized by larger malignant B cells. The occurrence of acute lymphoblastic leukemia (ALL) is very rare, while acute myeloid leukemia (AML) could be correlated with the immunological deficit and the chemotherapy associated with CLL[8]. CLL is always a disease of neoplastic B cells, while the formerly described T-CLL is now called T-cell prolymphocytic leukemia (T-PLL).

1.1.3 Diagnosis

In contrast to other indolent lymphoproliferative disorders, diagnosis of CLL is based on examination of peripheral and marrow blood and flow cytometry to evaluate the blood count, differential counts, blood smear and immune phenotype [9]. The National Cancer Institute diagnostic criteria include:

1) **The presence of at least $5x10^9$/L B-lymphocytes in the peripheral blood for the duration of at least 3 months.** Leukemic cells in the blood appear as small, mature lymphocytes with a narrow border of cytoplasm and dense nucleus, lacking of discernible nucleoli and with partially aggregated chromatin. These cells may be found mixed with larger or atypical cells, broken cells, or prolymphocytes, up to a 55% of the peripheral lymphocytes [9]. Finding a higher percentage of prolymphocytes would favor a B-PLL diagnosis. Other morphological features of neoplastic lymphocytes are the smudge cells (or Gumprecht shadows), which are CLL cells that have been ruptured during peripheral blood smear preparation, and their presence and aspect is related to the content of the cytoskeletal protein vimentin in leukemic cells (Figure 1) [10]. In the absence of lymphadenopathy, cytopenia, or disease-related symptoms, the presence of <5,000 B-lymphocytes/μl is defined as monoclonal B-lymphocytosis (MBL) [11].

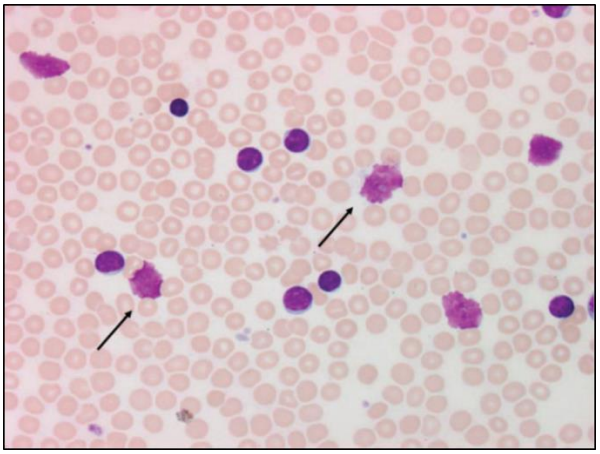

Figure 1. Peripheral blood smear from a CLL patient. The arrows indicate examples of smudge cells (Gumprecht shadows), which are pathognomonic of the disease [10].

2) **Bone marrow lymphocytic infiltration >30%**. This criterion is not essential in the case of a blood count <5,000/μl. However, the diagnosis should be confirmed by histopathologic evaluation of a lymph node or bone marrow biopsy where possible. Marrow infiltration can be diffuse, nodular, interstitial or mixed. The nodular pattern suggests an early stage of the disease, while the diffuse and interstitial infiltration patterns are typical of advanced stages. The presence of cytopenia caused by a typical marrow infiltrate defines the diagnosis of CLL regardless of the number of peripheral blood B-lymphocytes or of the lymph node involvement (Figure 2) [12].

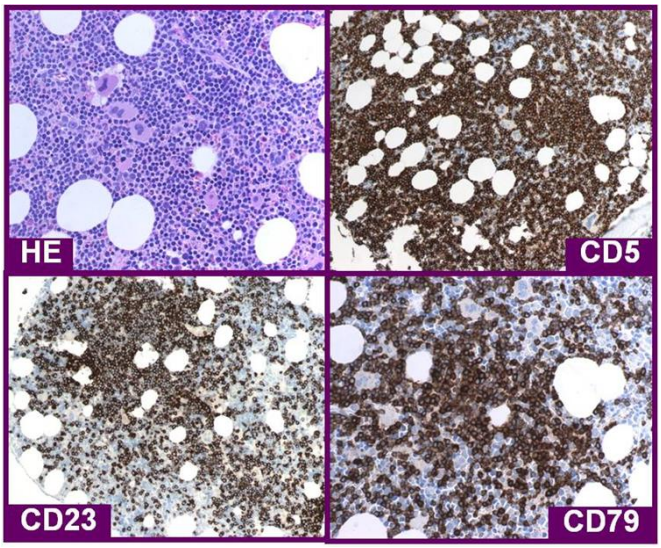

Figure 2. Bone marrow biopsy of CLL patient. Example of bone marrow tissue staining with hematoxylin-eosin (HE), and immunohistochemistry staining for three diagnostic markers (CD5, CD23 and CD79).

3) **Immunophenotyping**. CLL B cell phenotype is characterized by:
   a) the expression of a unique type of immunoglobulin light chain (κ or λ) [13];
   b) the co-expression of the T-cell antigen CD5 and the B-cell surface antigens CD19, CD20 and CD23. CD23 is of particular importance in the differential diagnosis of mantle cell lymphoma, which is CD5+ but CD23- (Figure 3) [9];
   c) low levels of CD79b [13] and surface immunoglobulins (sIg) compared to nomal B cells. In CLL sIg appear to be mainly IgM; however, most cases of CLL co-express IgM and IgD, and a very small proportion of cases have undergone isotype switching.

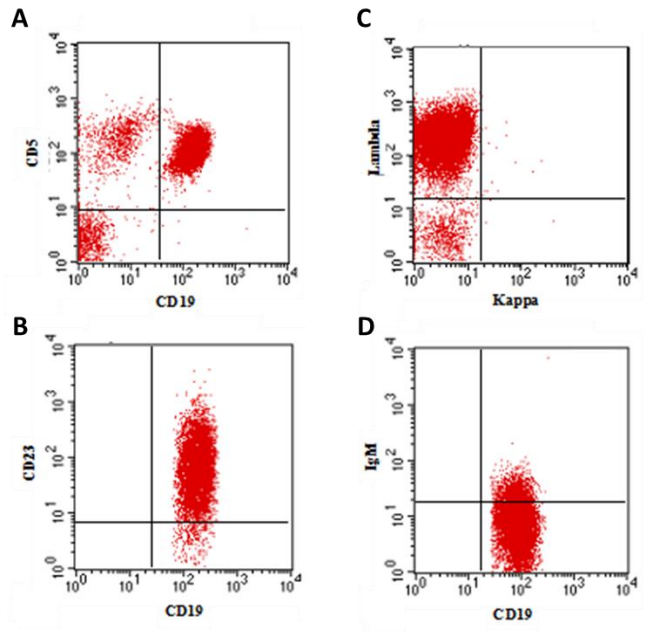

Figure 3. Representative immunophenotype of CLL peripheral blood cells. B lymphocytes analyzed (CD19+) are positive for CD5 (panel A) and CD23 (panel B), express one type of immunoglobulin light chain (example λ, panel C), and surface IgM (sIgM) at low density (panel D).

In CLL, T lymphocytes, in particular CD8+ T cells, are often increased, with a consequent reduction in the CD4/CD8 ratio. T lymphocytes show activation markers such as CD25 and HLA-DR. Natural-Killer (NK) cells (CD16+/CD56+) are present at high levels.

Further analyses are performed to confirm the diagnosis and to prevent complications: serum protein electrophoresis, Ig levels, Coombs' test, and analysis of renal and hepatic functionality.

It is crucial to verify that the CLL diagnosis is correct because there are other lymphoproliferative diseases that can masquerade as CLL, such as hairy cell leukemia (HCL) or leukemic manifestations of mantle cell lymphoma (MCL), marginal zone lymphoma (MZL), splenic marginal zone lymphoma (SMZL) with circulating villous lymphocytes, or follicular lymphoma (FL). CLL is distinguishable from small lymphocytic leukemia (SLL) only by its leukemic appearance.

1.1.4 Prognosis

It is difficult to predict the course of the disease at the time of diagnosis. However, several different parameters and prognostic factors are used to help predict the clinical course of CLL.

1.1.4.1 Clinical prognostic factors

1) **Clinical staging:** the clinical staging systems by Rai [14] and Binet [15] serve as a standard for the assessment of prognosis in CLL. They are based on simple and widely available methods, like physical examination, complete blood count and standard laboratory tests. However, further refinement of individual prognosis requires more detailed laboratory assessment [9]. The original Rai classification was modified to reduce the number of prognostic groups from 5 to 3. Now, both systems describe 3 major subgroups with different clinical outcomes (Table I).

   The Rai system is defined as the following:

   - **low-risk disease (formerly stage 0):** lymphocytosis with leukemia cells in the blood and/or marrow (absolute lymphocytosis>15,000/μl and marrow lymphocytosis >30%)
   - **intermediate-risk disease (formerly stage I or II):** lymphocytosis, enlarged nodes at any site, and splenomegaly and/or hepatomegaly (lymph nodes being palpable or not)
   - **high-risk disease (formerly stage III or IV):** disease-related anemia (hemoglobin (Hb)<110g/L) or thrombocytopenia (as defined by platelet count $<100x10^9$/L)[16].

The Binet system is based on the number of involved areas, as defined by the presence of lymph nodes with a diameter greater than 1 cm or organomegaly, and the presence of anemia or thrombocytopenia. It is divided as:

- **Stage A**. Hb≥10g/dL, platelets≥$100x10^9$/L, and up to 2 lymph node areas involved.
- **Stage B**. Hb≥10g/dL, platelets≥$100x10^9$/L and 3 or more areas of nodal or organ enlargement.

- **Stage C**. All patients who have Hb<10g/L and/or a platelet count <100x10^9/L, irrespective of lymphoadenopathy [15].

Table I. Rai and Binet staging system.

		Stage	Definition	Survival (years)
RAI SYSTEM	Low risk	0	Lymphocytosis	14.5
	Intermediate-risk	I	Lymphadenopathy	7.5
		II	Hepatomegaly and/or splenomegaly	
	High-risk	III	Anemia, hemoglobin <110g/L	2.5
		IV	Thrombocytopenia <100x10^9/L	
BINET SYSTEM		A	<3 involved areas	14
		B	≥3 involved areas	5
		C	Anemia (hemoglobin <100g/L) and/or thrombocytopenia <100x10^9/L	2.5

2) **Lymphocyte doubling time:** If lower than 12 months, it is associated with a worse clinical course.
3) **Bone marrow infiltration:** A diffuse infiltration pattern correlates with a poor prognosis.

1.1.4.2 Biological prognostic factors

Several biological factors used for the prognosis of CLL patients correlate with leukemic clone expansion, and only become indicative when the disease is worsening. These biological factors include:

1) **Percentage of circulating prolymphocytes (PL):** If the percentage is less than or equal to 10%, the probability of PLL is very low; if the percentage is between 11% and 55% there is an intermediate risk of CLL/PL leukemia, and if it is greater than 55% the transformation to PLL may occur [17].
2) **β_2-microglobulin:** Inversely correlated with survival, this parameter is related to the lymphocyte doubling time, so that an increase in β_2-microglobulin indicates a high neoplastic cell proliferation rate [17].
3) **Thymidine kinase (TK) level:** It has been shown that elevated serum levels of thymidine kinase (s-TK) are predictive of disease progression in CLL. Patients with s-TK values greater than 7.1U/L have a median progression free survival

(PFS) of 8 months, whereas patients with s-TK values ≤7.1U/L show a longer PFS[18].

4) **Soluble CD23 level (sCD23):** Serum CD23 levels provide additional prognostic information in terms of overall survival (OS) in CLL. Among patients with disease at an early stage, sCD23 determination at diagnosis and during the course of the disease may help the identification of individuals who will rapidly progress to advanced stages. Functions ascribed to sCD23 include the prevention of apoptosis of germinal center (GC) B cells, proliferation of myeloid precursors, co-stimulation of interferon-γ (IFN-γ) production by T cells and triggering of cytokine release by monocytes [19].

The progressive discoveries on CLL pathogenesis have allowed the identification of new prognostic markers that can better determine the clinical course of the disease. They describe biological characteristics of the leukemic clone that are crucial to evaluate its proliferative potential. These markers can be studied by flow cytometry, and by cytogenetic and molecular biology techniques. The main markers are:

1) **Somatic hypermutations (SHM) of the Ig heavy chain variable region (IGHV) genes.** Based on the percentage of somatic mutations detected in these genes, CLL cases can be divided into 2 categories: “unmutated” (SHM-, U-CLL) and “mutated” (SHM+, M-CLL). Conventionally, patients with <2% differences from the most similar germline gene in the expressed variable heavy (V_H) genes are defined as unmutated; whereas M-CLL cases show ≥2% differences in the V_H gene [20]. The two subsets are associated with different clinical outcome. Unmutated V_H genes are usually associated with a malignant disease, while M-CLL cases usually have a more stable disease with a longer median survival and better prognosis (Figure 4) [21].

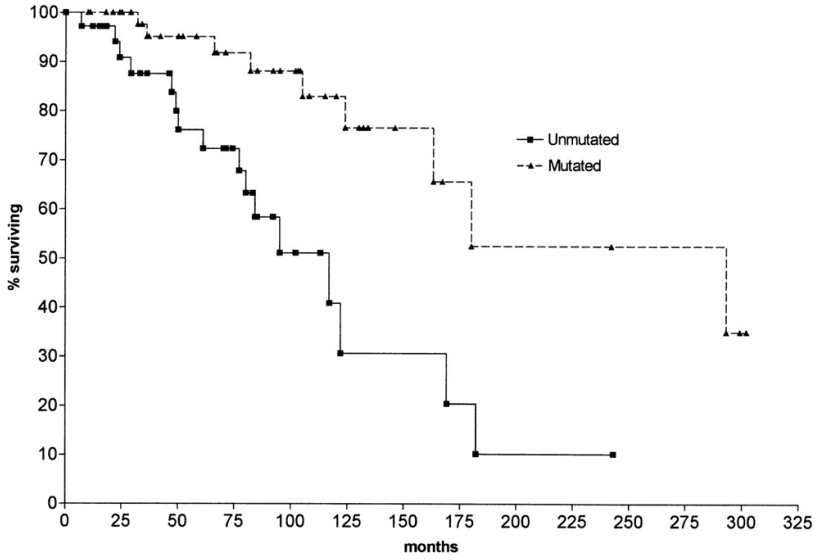

Figure 4. Survival curves comparing U-CLL (unmutated) and M-CLL (mutated) cases. The survival curves show the association of the V_H gene status with the clinical outcome of the disease. The median survival for U-CLL was 117 months, while the median survival of mutated V_H gene cases was 293 months [21].

2) **CD38 expression.** CD38 is a transmembrane glycoprotein expressed on the surface of cells in a significant percentage of CLL patients. A study has suggested that CD38 expression has a prognostic value for this disease, in fact cases with >30% CD38+ cells show worse prognosis [20]. However, the cut-off to discriminate CD38+ and CD38- cells is not unanimously defined: some authors place it at 20% [22], others at 7% [23]. A limit of this marker is its variability, in particular after treatment; for example, chemotherapy affects mainly CD38- cells, determining an increase of CD38+ cells in a second time [20].
3) **Intracytoplasmatic expression of ZAP-70.** Zeta chain-associated protein kinase 70kDa (ZAP-70) is a cytoplasmic tyrosine which is a key signaling molecule for T lymphocytes and NK cells [24, 25]. ZAP-70 expression may reflect an activation state of the malignant clone associated with progressive disease, or may be involved in CLL progression because of its function as a tyrosine kinase that can signal downstream of surface receptors [25, 26]. In CLL, protein levels of ZAP70 are highly associated with U-CLL [27] and the expression may change overtime, in particular during clinical progression, suggesting an interest in the evaluation of ZAP-70 during the evolution of the disease [28]. ZAP-70 expression analysis can be performed by different

methods: flow cytometry, immunohistochemistry, western blotting, and Real-Time Polymerase Chain Reaction (PCR). Among these, flow cytometry is the most advantageous method for its ease of application. However, the values are subjected to inter-laboratory variation, and there is neither a consensus nor a regulatory approved methodology [29].

4) **Chromosomal alterations.** Deletions (11q22-23, 17p13, 13q14) and chromosome 12 trisomy are the most frequent chromosomal alterations in CLL. Clonal genomic aberrations can be identified in approximately 80% of CLL patients by fluorescence *in situ* hybridization (FISH). The del13q represents the single most frequently observed cytogenetic aberration in CLL (55% of all cases), and it is typically characterized by a benign course of the disease [30]. Deletions of chromosome 11 (del11q) can be found in approximately 25% of patients with advanced disease stages and in 10% of patients with early stage disease [31]. These aberrations usually involve the gene *ATM* (ataxia telangiectasia mutated), proximal DNA damage response kinase. Trisomy 12 is observed in 10-20% of CLL patients, but genes implicated in the pathogenesis of CLL involving this aberration are unknown [32]. Deletions of the short arm of the chromosome 17 (del17p) are found in 5-8% of patients, and include the section where the tumor suppressor gene *TP53* (tumor protein 53) is located. CLL clones that carry this mutation have been associated with treatment failure and with a very poor prognosis (ultra-high risk), showing a marked resistance to genotoxic chemotherapies [16]. The presence of high-risk chromosome alterations justifies the use of a more aggressive treatment [33]. Del17p and del11q are independent prognostic factors that identify subgroups of patients with rapid disease progression and short survival times in multivariate analysis, whereas del13q as a single aberration shows favorable outcome (Figure 5). Chromosome alterations are independent from IGHV mutational status, though it is evident that there is a higher frequency of del11q and del17p in U-CLL, and of del13q in M-CLL cases. Thus, the cytogenetic analysis could be used as a further risk stratification system, together with the other prognostic factors [34].

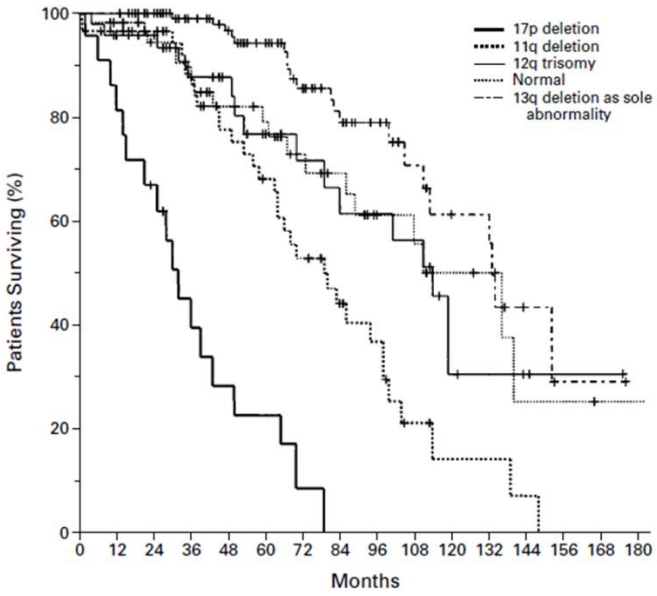

Figure 5. Survival curves of CLL patients carrying the most common chromosomal aberrations. The median survival times for the groups with del17p, del11q, trisomy 12, normal karyotype and del13q as sole abnormality were 32, 79, 114, 111 and 133 months, respectively [35].

5) **Telomerase expression and telomere length.** Telomeres are protective structures at the end of eukaryotic chromosomes that are progressively shortened during cell replication cycles because of end-replication problems of the DNA polymerase [36]. The regulation of telomere length is important for the control of the cellular replicative potential; after a critical point of telomere erosion, cells undergo senescence or apoptosis [37]. Telomerase reverse transcriptase (hTERT) is essential to maintain telomere length by adding TTAGG repeats to the chromosome ends, and plays a critical role in tumorigenesis [38]. The levels of telomerase activity (TA) and/or hTERT expression have been related to clinical aggressiveness, and may be a prognostic indicator of overall survival in CLL [38, 39]. The analysis of hTERT levels and telomere length, related to the IGHV mutational status and to chromosomal aberrations of CLL patients, has shown that U-CLL cases with high-risk chromosomal aberrations were more frequently characterized by high telomerase levels and short telomeres [40], and these parameters correlated with a poor clinical outcome (Figure 6). The evaluation of hTERT and telomere length might help in the management of CLL patients with mutated IGHV and/or high-risk chromosomal aberrations, since cases with high

hTERT/short telomere length will progress more rapidly and might require earlier treatment than cases with low hTERT/long telomeres [40].

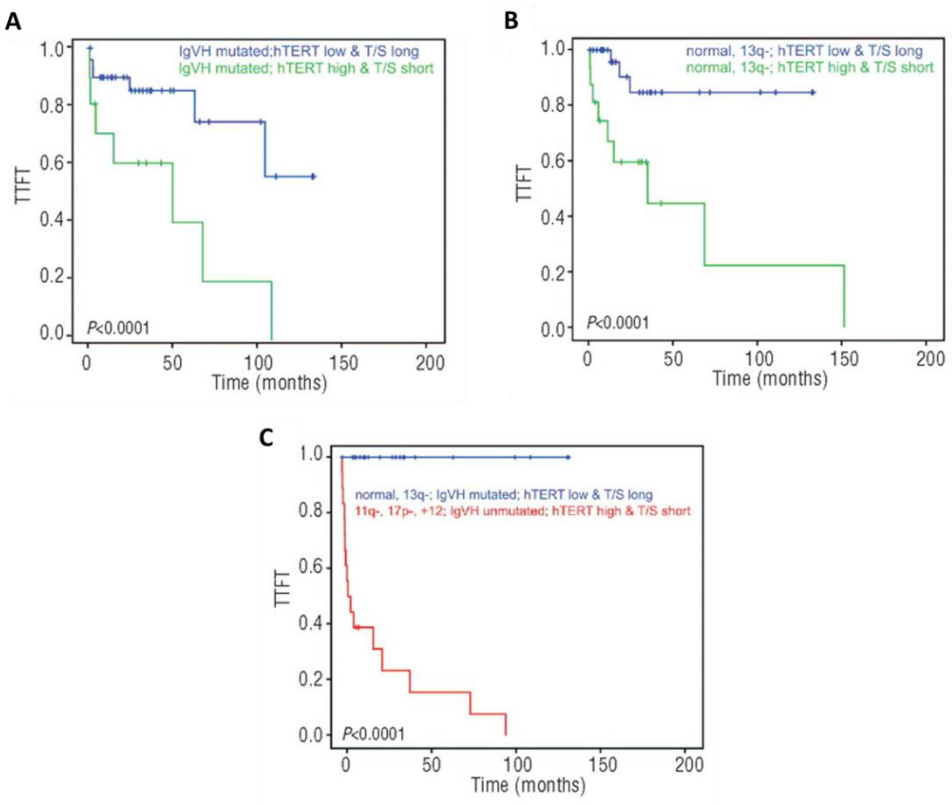

Figure 6. Curves of treatment-free survival of CLL patients in relation to hTERT levels. Treatment-free survival curves according to hTERT level/telomere length profile and (**A**) IGHV mutational status, (**B**) chromosomal categories, and (**C**) IGHV mutational status and chromosomal aberrations [40]. TTFT, time to first treatment. hTERT low: ≤median value; hTERT high: >median value; T/S short ≤median value; T/S long: >median value.

6) **MicroRNAs (miRNA).** MicroRNAs have been proposed as prognostic markers for several human cancers, including CLL. MicroRNAs are small non-coding RNAs (20-22 nucleotides) involved in the regulation of gene expression via translational repression or transcript degradation and gene silencing [41]. Expression profiling revealed that miRNA signatures can distinguish normal B cells from malignant CLL cells, and are associated with prognosis, disease progression and drug resistance [42, 43]. Moreover, it has been shown that aggressive and indolent CLL exhibit a different miRNA profile [44], and that specific miRNA signatures can predict refractoriness to treatment [43]. Current studies aim to detect which miRNAs are involved in CLL, in order to discover new prognostic markers and to develop new targeted gene therapy.

1.1.5 Treatment

The criteria for initiating treatment depend on clinic symptoms, stage and disease activity. In general practice, newly diagnosed patients with asymptomatic early-stage disease (Rai 0, Binet A) should be monitored without therapy, unless they have evidence of progression. On the contrary, patients at intermediate (I and II) and high risk stages (III and IV), or at Binet stage B or C, usually benefit from treatment from the start. Some of these patients (in particular Rai intermediate risk or Binet stage B) can be monitored without therapy until they have evidence of progressive or symptomatic disease [9]. Anyway, the choice of therapy is based on patient age and general health conditions.

Therapeutic possibilities range from drugs with different mechanisms of action to stem cells auto/allotransplantation. Since CLL is an incurable disease, current therapy is intended to control the expansion of the neoplastic clone.

Alkylating agents and purine analogues

In older patients (>65 years), primary treatment consists of Chlorambucil alone or in association with Prednisone, while in other cases therapy is based on Fludarabine alone or in association with Cyclophosphamide. Treatment with the alkylating agent Chlorambucil induces a response in 70% of the cases, but only 10% show a complete response (CR) and has no effect on survival, making it suitable for palliative treatment.

From the 1990's, the first line treatment for CLL has been the use of purine analogous. This class of drugs includes Pentostatin, an adenosine deaminase inhibitor, Clabridine, Fludarabine, and DNA-polymerase inhibitors. The most effective treatment for CLL turned out to be Fludarabine; 80% of the cases showed overall response, and 30% a complete remission. Moreover, the time of remission is greater than that obtained with Chlorambucil plus Prednisone [45]. Despite the positive overall response, Fludarabine and purine analogous are no more effective in improving the survival rate than alkylating agents [46-48]. Since purine analogues and alkylating agents have different mechanisms of action and partially non-overlapping toxicity profiles, a number of studies were designed to determine the effects of their combination. Preclinical studies showed that the exposure of CLL cells to Fludarabine and Cyclophosphamide resulted in

synergistic cytotoxicity [49]. The US Intergroup Trial has demonstrated that the combination of Fludarabine and Cyclophosphamide (FC), compared to Fludarabine alone, gives higher overall responses (OR) (74.3% *vs* 59.5%), CR (23.4% *vs* 4.6%), and progression free survival (PFS, 31.6 *vs* 19.2 months). Conversely, the combination of the two drugs resulted in a greater bone marrow toxicity, neutropenia, anemia and thrombocytopenia with infectious complications [50].

Bemdamustine is a unique cytostatic agent with combined properties of an alkylating agent and purine analogue. An international phase III study has shown that Bendamustine induced a significantly higher OR/CR and PFS compared to Chlorambucil [51]. These results led to the approval of Bendamustine for the first-line treatment of CLL patients ineligible for FCR (Fludarabine, Cyclophosphamide, Rituximab). Bendamustine has also been successfully combined with Rituximab, an anti-CD20 monoclonal antibody [52].

Monoclonal antibodies

Monoclonal antibodies have provided a significant advantage in the treatment of hematological malignancies. CD20, a glycosylated phosphoprotein expressed on the surface of mature B cells, has become the preferred target for immunotherapy. The chimeric mouse anti-human monoclonal antibody Rituximab (IDEC-C2B8) is specific for the CD20 antigen and has been used in clinical trials to treat patients with Non-Hodgkin Lymphoma (NHL). Preclinical studies identified the ability of Rituximab to increase the effectiveness of cytotoxic drugs in resistant cell lines, blocking the anti-apoptotic signaling. The combination of Rituximab with other drugs results in a synergistic cytotoxicity and apoptosis [53]. In fact, Fludarabine down-modulates the complement-resistance proteins CD46, CD55 and CD59 on leukemic lymphocytes, making cells potentially more vulnerable to Rituximab-induced complement mediated lysis [54]. The combination of Rituximab with Fludarabine/Cyclophosphamide (FCR) in previously untreated patients showed an OR rate of 95%, with CR in 72% of the cases [55]. A subsequent randomized trial (CLL8 protocol) showed that the positive effect of FCR applied for most prognostic subgroups, but it did not improve the survival of patients with del17p [56]. The use of FCR therapy has

now become very promising, leading to complete remissions and possible cures for patients with mutated IGHV.

Alemtuzumab (Campath-1H) is a humanized anti-CD52 antibody; CD52 is expressed at high levels on most of the normal and malignant mature lymphocytes, but not on hematopoietic stem cells. Alemtuzumab can be administrated subcutaneously and is very effective in inducing remission in relapsing CLL patients [57]. The association with Fludarabine and Cyclophosphamide is burdened by significant toxicity to the bone marrow, so precautions are necessary during Alemtuzumab administration.

Bone marrow transplantation

Allogeneic and autologous stem cell transplantation (SCT) are gaining increasing consideration for treatment of CLL. With appropriate supportive care, SCT is safe and can induce long-lasting clinical and molecular remission. Feasibility of autologous SCT appears to be best in the early stages of the disease, but there is only limited hope that autotransplantation can cure the disease [58]. Allogeneic stem cell transplantation (alloSCT) currently represents the only potentially curative treatment option in patients with CLL.

BH3-mimetics

The expression of the anti-apoptotic protein BCL-2 **(**B-cell lymphoma-2) is associated with the pathogenesis of CLL. As a negative regulator of intrinsic apoptotic pathways, overexpression of BCL-2 confers chemoresistance in a number of hematologic cancers and solid tumors [59]. Although protein levels vary among cells and patients, BCL-2 is expressed in virtually all CLL patients and its upregulation plays a critical role in the disease. Deletion of miRNA regulators of BCL-2 expression is frequently found in CLL cells, causing the upregulation of the protein. High BCL-2 and high MCL-1 expression levels have been reported to mediate resistance to Chlorambucil, Fludarabine and Rituximab [60-62].

BCL-2 inhibitors have recently been developed and have demonstrated considerable activity against CLL cells in both preclinical models and clinical trials [63, 64]. The so-called BH3-mimetics (e.g. ABT-737, ABT-199/Venetoclax,

Navitoclax) disrupt the interactions between BCL-2 family anti-apoptotic members and the pro-apoptotic BH3-only proteins, favoring the activation of the apoptotic machinery [65]. An anti-apoptotic member of the BCL-2 family is MCL-1 (myeloid cell leukemia-1), for which the BH3-mimetics have shown so far a low affinity rate [66]. It has been shown that acquired resistance to the ABT-737 occurs via elevated levels of MCL-1 that sequesters the pro-apoptotic protein BIM [67], impairing the activation of the apoptotic signaling.

Inhibitors of the interactions with the microenvironment

Cytokine support from the malignant microenvironment prolongs CLL cell survival, immune evasion and resistance to therapy. Interrupting these pro-survival effects coming from the microenvironment is a new approach in treating CLL patients, with the administration of compounds that affect molecules involved in the compartmentalization of tumor cells (e.g. Thalidomide, Lenalidomide, Plerixafor) [68, 69], or that target kinases of the BCR signaling pathway important for CLL cells survival (e.g. Ibrutinib, Idelalisib, Dasatinib) [70].

Lenalidomide, a second generation thalidomide analogue, is an immunomodulating drug with antitumor and antiangiogenic activity reported in various malignant disorders, including multiple myeloma (MM) and myelodysplastic syndrome (MDS). Lenalidomide is also reported to have an immunomodulatory action through the activation of the immune effectors (T and NK cells), directly inducing apoptosis in tumor cells. These properties make Lenalidomide an attractive therapeutic agent to add to Rituximab treatment [71]; in fact, this combination seems to increase the response rate without a higher risk of toxicity, even in patients with del17p and/or unmutated IGHV-status [72]. Moreover, Lenalidomide showed encouraging results in the treatment of high-risk patients including carriers of a del17p [73].

BCR-signaling kinase inhibitors

New generation kinase inhibitors are drugs directed against key molecules of the BCR signaling pathway, for example Bruton's tyrosine kinase (BTK), phosphatidylinositol 3-kinase (PI3K), LYN and spleen tyrosine kinase (SYK)

(Figure 7). Due to their potential to inhibit specific signaling pathways in malignant cells, the kinase inhibitors are continuously under investigation, both as single agents and in combination with other drugs.

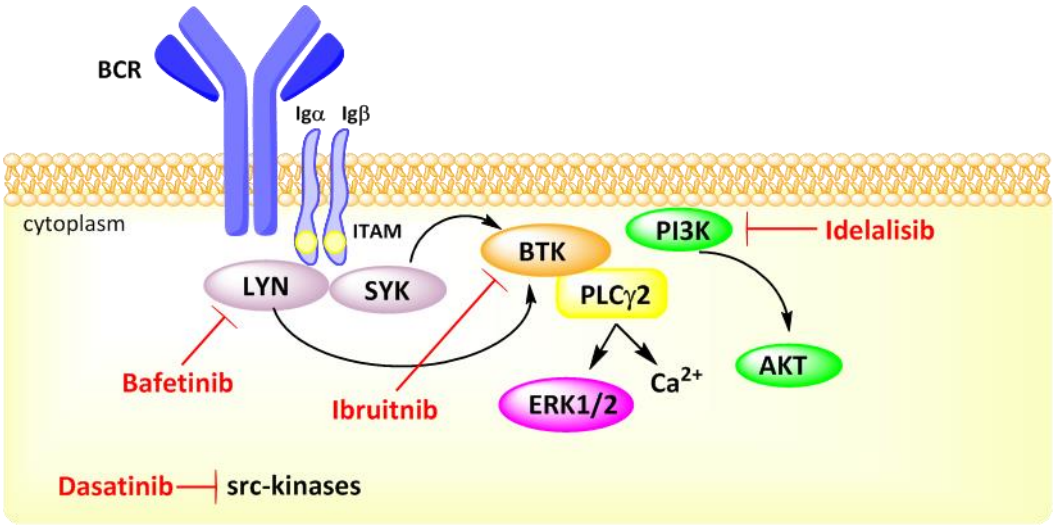

Figure 7. BCR signaling inhibitors. Schematic representation of the kinase inhibitor targets in the BCR signaling pathway.

Ibrutinib (PCI-32765) is the first BTK inhibitor that binds specifically and irreversibly to a cysteine residue in the BTK kinase domain, inhibiting the autophosphorylation and activation of the protein [74, 75]. Ibrutinib has shown encouraging clinical activity particularly in patients with CLL and MCL [76-78]. The clinical activity of the drug is characterized by CLL cell redistribution from the tissues to peripheral blood, with an initial transient lymphocytosis [79]. Ibrutinib was tested in combination with Rituximab in patients with high-risk disease, showing an encouraging safety and activity profile for high-risk patients [80]. A more extended clinical and biological characterization of Ibrutinib will be described in Chapter 3 of this thesis (Section 3.1.2).

PI3K is able to integrate signals coming from BCR, chemokine receptors and adhesion receptors [81, 82]. Different isoforms of PI3K have been discovered, allowing a classification of the kinases based on their role and cell expression. Idelalisib (GS-1101, CAL-101) is a highly selective inhibitor of the isoform PI3Kδ [83], which expression is restricted to hematopoietic cells, and plays an important role in B-cell homeostasis and function [84]. It has been shown that Idelalisib can induce apoptosis in tumor cells, in particular in patients with CLL,

MCL and MM [83, 85, 86]. As for Ibrutinib, patients treated with Idelalisib also have a transient lymphocytosis with a decrease in lymph node (LN) size, supporting the *in vitro* results of inhibition of CLL cell migration toward CXCL12 and CXCL13, and beneath stromal cells (pseudoemperipolesis) in the presence of Idelalisib [87]. Administered alone or in combination with other agents, Idelalisib showed promising activity in the treatment of relapsed CLL patients in phase I trials [88]. Idelalisib plus Rituxmab was more effective than Idelalisib alone in patients with relapsed CLL who were unable to receive standard cytotoxic therapy [89].

Dasatinib is a pan-Src kinase inhibitor used for treatment of Imatinib-resistant CML, but it has also shown activity against several kinases that are activated in CLL cells, such as LYN, c-Abl and BTK [90-92]. *In vitro* studies showed that Dasatinib can inhibit the activation of anti-apoptotic proteins of the BCL-2 family, and restores the sensitivity to Fludarabine [93]. Dasatinib as a single agent in a phase II study showed activity in relapsed CLL/SLL, also in subgroups with poor prognostic features, with acceptable toxicity [94]. In another phase II study, Dasatinib in combination with Fludarabine in patients with refractory CLL showed reduction of LN sizes, low overall response rate (ORR) (18%), and median PFS of 6.3 months with an overall survival (OS) of 11.6 months [95]. Interestingly, a temporary increase in the lymphocyte counts occurred in 61% of the patients shortly after the start of the treatment, suggesting that therapy may target the BCR- and chemokine-induced integrin-mediated adhesion and homing of malignant cells in the LN.

Finally, the second-generation tyrosine kinase inhibitor Bafetinib is under investigation as a possible new treatment for CLL. Bafetinib (INNO-406) was initially developed as a BCR-ABL inhibitor for treatment of CML; it has a chemical structure similar to Imatinib, but with potentiated efficacy against the fusion protein BCR-ABL. Moreover, Bafetinib efficiently inhibits the src-family kinase (SFK) member LYN, which has been associated to Imatinib resistance in CML patients [96]. It has been demonstrated that LYN is overexpressed and constitutively active in CLL cells, and its high basal activity has been correlated with defects in apoptosis [97]. For this reason, the use of Bafetinib may suppress the growth of CLL cells by inhibition of LYN kinase, thus having clinical activity.

A phase 2 trial of single agent Bafetinib showed promise in patients with relapsed/refractory CLL; no treatment-limiting toxicity was observed [98]. However, more investigations are needed to test Bafetinib effects *in vitro* and the possible combinations with monoclonal antibodies and chemotherapy *in vivo*.

1.2 Leukemic B cells

1.2.1 B cell biology

B lymphocytes are central components of the humoral immunity. After binding of an antigen (Ag) by the specific B-cell receptor (BCR), B lymphocytes are able to proliferate and differentiate into plasma cells specialized in antibody (Ab) production [99]. B cells can also differentiate into "memory" B lymphocytes, which are ready for rapid response to repeated exposure to the antigen.

The BCR is a multimeric complex composed of a membrane-bound homodimer linked to the plasma membrane through its constant region (Fc), which is non-covalently linked to the heterodimer Igα/Igβ (CD79a/CD79b) [100]. The surface immunoglobulin (sIg) consists of two identical light chains (L) and two identical heavy chains (H), each one containing a variable region (V) at the N-terminal that contributes to the shape of the antigen binding site, and a constant (C) region that defines the isotype (Figure 7) [101]. The antigen binding region (Fab) of the sIg consists of the variable regions of light and heavy chains. In the V domains, three short polypeptide sequences that show exceptional variability, the so-called hypervariable regions or complementarity-determining region (CDR), have been identified. When the V_H and V_L domains are paired in the Ig, they create a single hypervariable site that binds specifically to one antigen. Conversely, the segments in between the hypervariable regions (framework regions, FR) show less variability, and contain invariant peptide sequences that support the CDR [102]. Light chains can be κ or λ, and an Ig expresses exclusively one of them. The isotype of the heavy chains determines the functional properties of the sIg and defines 5 principal classes of immunoglobulins: IgM, IgD, IgG, IgA and IgE, which carry the μ, δ, γ, α and ε heavy chain, respectively.

In cells committed to become B lymphocytes, the Ig genes are assembled through the somatic recombination of germline DNA fragments. The diverse set of BCRs is established through the rearrangement of V and J gene segments at the IgL *loci*, and of V, D and J genes at the IgH *loci* [103-105]. The rearrangement consists of the generation of one single functional V-region for the heavy chain and one for the light chain through a similar mechanism (Figure 8). DNA

segments are joined by the recombinant-activating-genes (RAG) enzymes. Subsequently, the primary RNA transcript is generated and, after differential splicing, the mature mRNA is translated into the heavy or light chain to obtain the receptor protein [106, 107]. When a successful V_HDJ_H recombination event occurs at the IgH, the resulting heavy chain product pairs with a surrogate light chain to form the pre-BCR, which is trafficked to the plasma membrane and associated with the signaling components Igα and Igβ.

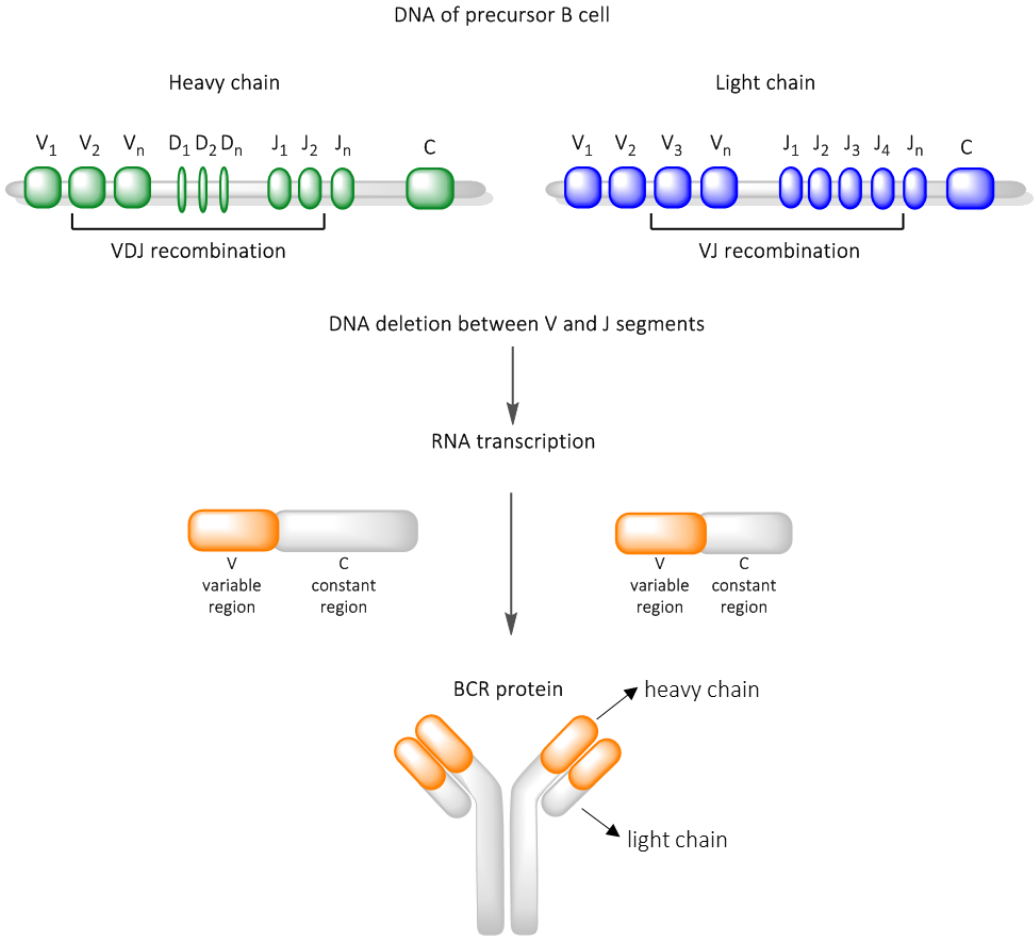

Figure 8. Gene rearrangement of the immunoglobulin heavy and light chain. Schematic representation of VDJ and VJ gene rearrangement at the heavy and light chain loci, respectively (modified from Wiestner A., Haematologica, 2015 [108]). DNA of a precursor B cell is recombined by random deletion of segments between V and J. The resulting rearranged DNA generates a transcript, which comprehends variable and constant region, and is then translated into the BCR protein.

Genes of the rearranged V region are further differentiated by somatic hypermutation, i.e. high rate of point mutations that occur in the V region of the rearranged heavy and light chain genes, inducing diversity in the antigen-binding

site. The enzyme that initiates this mutation process is the activation-induced deaminase (AID), which has been shown to be upregulated in germinal center (GC) B cells [109, 110]. Somatic hypermutation occurs in the peripheral lymphoid organs, in particular when antigen-activated B cells enter the lymphoid follicles and form the GCs, which are characterized by highly proliferating cells. The aim of the hypermutation is the generation of new BCRs that can bind the antigen more strongly and more specifically. In GCs, B lymphocytes are in contact with dendritic cells expressing antigens, and their fate is determined by selective competition: lymphocytes that show a high-affinity antigen binding will undergo clonal proliferation and increased antibody synthesis, while the rest of the cells with low or null antigen binding capacity will die [111]. Thus, the result is affinity maturation of the receptor, which increases the binding efficiency of the antibodies to the antigen.

CLL B cells

CLL lymphocytes are small B cells blocked in G_0/G_1 phase of the cell cycle, and are characterized by the expression of B-related surface markers, such as CD19 and CD21, and other antigens not specific for the B lineage, like CD5, CD23, CD25 and the human leukocyte antigen D-related (HLA-DR) (Figure 9).

Studies have shown that 50-70% of CLL harbor somatic mutations of IGHV genes, a phenomenon that characterizes normal B cells in a T cell-dependent GC reaction [112]. This and other findings led to the hypothesis that M-CLL cases may derive from a cell that had transited through the GC, so with a post-follicular origin, whereas those cases with germline IGHV (U-CLL) may derive from a pre-GC CD5+ B cell [20, 113, 114]. In fact, unmutated cases have relative conserved IGHV genes similar to those of naïve innate B cells. This hypothesis has both biological and clinical relevance, since the two subgroups have different prognosis, with IGHV-mutated CLL displaying a better clinical course [115] (Section 1.1.4.2).

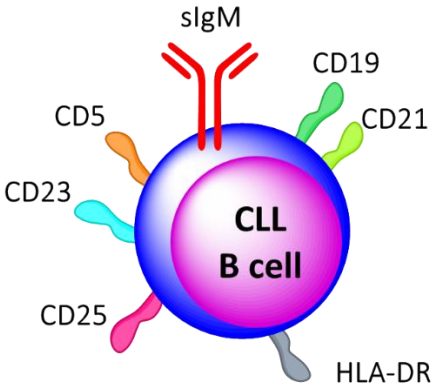

Figure 9. Characteristic membrane phenotype of CLL B lymphocytes. Schematic representation of surface molecules expressed by CLL B cells.

1.2.1 BCR-mediated signal transduction

The B-cell receptor is the complex required to start the cascade of events that leads to the transduction of signals for cell survival, proliferation and apoptosis. It has two main roles: to transmit signals for B-cell fate regulation and to mediate antigen processing and presentation to T cells, allowing full activation of B lymphocytes. However, the BCR of CLL cells shows a reduced ability to capture, present and respond to antigens, but it abnormally regulates the intracellular signals mediated by tyrosine phosphorylation of different substrates [116].

Signal initiation

The BCR multiprotein structure consists of membrane-bound immunoglobulin heavy and light chains associated with the heterodimer Igα and Igβ. Igα and Igβ each contain a single immunoreceptor tyrosine-based activation motif (ITAM) in the cytoplasmic tail that transduce signals after BCR ligation [99]. The ITAM is a conserved motif composed of two tyrosine residues surrounded by consensus sequences that provide specific binding sites for Src-homology2 (SH2) domain-containing proteins [117]. Aggregation and engagement of the BCR by antigens results in the phosphorylation of ITAM domains; most evidence support the idea that, during development and following Ag-induced aggregation of the BCR, the ITAM phosphorylation is mediated in particular by LYN, which is the predominant Src-family kinase expressed by B cells [118, 119]. Dual phosphorylation of ITAM tyrosines is necessary to create a

specific, spatially-defined binding site for tandem SH2 domains, thus allowing the subsequent recruitment, phosphorylation and activation of additional effector molecules, such as SYK [120]. Igα and Igβ seem to give a different contribution to BCR signaling; it has been suggested that Igβ could play a role in BCR expression [121], while Igα could be directly involved in protein tyrosine kinase (PTK) activation and in negative signaling functions [122, 123].

SYK is essential to couple the BCR to distal signal transduction molecules. Once activated, SYK can phosphorylate and interact with the adaptor molecule B-cell linker (BLNK, also known as SLP-65) [124]. BLNK acts as a scaffold for the recruitment of other proteins, allowing the activation of different signaling pathways [125].

The initiation of BCR signaling is indirectly regulated by two non-receptor molecules, CD45 and C-terminal src tyrosine kinase (CSK). The glycoprotein CD45 is a transmembrane tyrosine phosphatase that acts on different molecules of the BCR signaling pathway, maintaining src-family kinases in a partially active state [126]. Its primary function may be the control of the relative threshold of sensitivity to an antigenic stimulus. Conversely, CSK phosphorylates the inhibitory tyrosine of src-family PTKs, keeping them in an inactivated status [127]. Thus, the balance between CD45 and CSK signals regulate LYN activity and, consequently, BCR signal initiation.

Signal amplification, propagation and integration

BCR engagement leads to the generation of second messengers for signal propagation, in particular inositol triphosphate (IP_3) and diacylglycerol (DAG), to the release of intracellular calcium (iCa^{2+}), and to the activation of important downstream pathways (Figure 10).

The activation of LYN and SYK is essential for the phosphorylation of BTK at Tyr551 and proper BCR signal transduction. It has been shown that deficiencies in one or more of the PTKs (represented by LYN, SYK, and BTK) results in defective or aberrant B-cell function and development [128-130]. Moreover, the full activation of BTK requires not only the phosphorylation at Y551 mediated by LYN and SYK, but also the consequent autophosphorylation at Y223 [131].

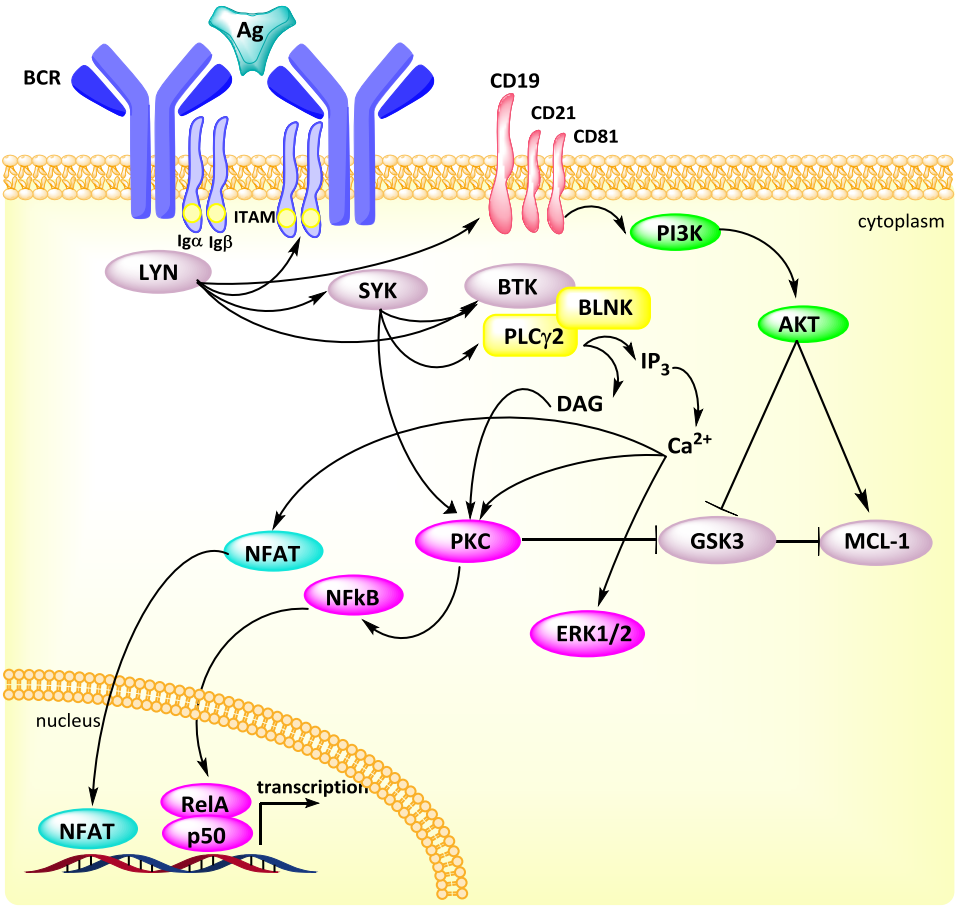

Figure 10. BCR signaling. Simplified representation of the main intracellular pathways that result in activated B cells after BCR engagement by an antigen.

PI3K, a molecule that phosphorylates the plasma membrane lipid phosphatidylinositol 4,5-bisphosphate (PIP_2) to create phosphatidylinositol 3,4,5-triphosphate (PIP_3), is also activated after BCR ligation. The production of PIP_3 is important to recruit to the plasma membrane pleckstrin-homology (PH)-domain containing proteins, like BTK, in order to favor their enzymatic activity [132].

One of the best understood activation mechanisms of PI3K involves the glycoprotein CD19. On B cells, CD19 has been shown to associate with CD21, a complement receptor, and with CD81, a member of the tetraspan family [133]. CD19 plays two important roles in B-cell activation: it serves as an adaptor protein to localize signaling proteins to the membrane, and it acts as a transduction subunit for the CD19/CD21 cluster [134]. Upon BCR ligation, the tyrosines of the cytoplasmic tail of CD19 become phosphorylated by LYN, creating docking sites for cytoplasmic molecules containing SH2 domains, such as the p85 adaptor subunit of PI3K [135]. Moreover, the phosphorylation of

different tyrosine sites on the cytoplasmic tail of CD19 leads to the recruitment of several other proteins, such as VAV (vav guanine nucleotide exchange factor), PLCγ2 (phospholipase Cγ2) and GRB2 (growth factor receptor bound protein 2) [136], thus promoting the activation of protein kinase C (PKC) and mitogen activated protein kinase (MAPK pathways), and the release iCa^{2+} [137].

Once LYN, SYK and BTK are activated, the signal is propagated through a number of effector proteins. BLNK, working as an adaptor molecule, has been identified as important mediator of PLCγ2 recruitment to the plasma membrane, where it can be phosphorylated by BTK and transmit the signal downstream [125]. The activated lipase PLCγ2 is responsible for PIP_2 cleavage and generation of IP_3 and DAG, which mediate, respectively, the release of intracellular calcium and the activation of downstream proteins, such as the PKC and ERK [138, 139]. Elevated iCa^{2+} levels are required for activation of transcriptional factors like NF-κB, while PKC has been shown to promote the activation of VAV, GRB2, and the MAPK pathway. Thus, signals coming from the BCR are connected with the activation of transcription factors and the regulation of gene expression.

A primary signaling integration point is mediated by the MAPK family, which comprises the proteins ERK, C-Jun N-terminal kinases (JNKs) and p38 MAPK [140]. After activation, MAPK family members can phosphorylate different transcription factors, regulating cell fate by gene expression modulation. ERK is able to regulate ELK-1 (ETS-domain containing protein) and c-MYC (myelocytomatosis proto-oncogene) activity, while JNK and p38 MAPK act on ATF-2 (activating transcription factor-2), JUN proto-oncogene and MAX (MYC-associated factor X).

ERK is a key molecule involved in different pathways. Its activation is dependent on RAC and RAS/RAF/MEKK cascade [141], which can be induced by the SYK/BLNK axis or by PKC after generation of DAG [142, 143].

Through the generation of IP_3 and DAG, PLCγ2 has been related to the activation of JNKs and p38 MAPK, which are usually activated in response to stress stimuli and are involved in apoptosis, differentiation and cytokine production [144].

Another molecule that links the BCR signals with the events that happen in the nucleus is AKT (or protein kinase B, PKB), a serine/threonine kinase that

plays a role in the regulation of cell survival. After PI3K activation, AKT is recruited to the plasma membrane and phosphorylated at Ser437 and Thr308, both sites are required for full activation of the protein. In B cells, AKT inhibits the activation of the pro-apoptotic BCL-2-family member BAD and the glycogen synthase kinase 3 (GSK3). In unstimulated cells, the constitutively active GSK3 phosphorylates and destabilizes MCL-1, MYC and cyclin D, proteins involved in the control of apoptosis and cell-cycle progression. Moreover, upon activation, AKT translocates to the nucleus and acts as a transcription factor for anti-apoptotic molecules. In this way, AKT functions as a promoter of BCR-induced cell proliferation, as well as survival [145].

BCR engagement also leads to the activation of the NF-κB family of transcription factors via BTK/PI3K pathway, in particular through PLCγ2-dependent activation of PKC [146]. The NF-κB family is composed of p50, p52, RelA, c-Rel and RelB members, and is important for B cell development, proliferation and immunoglobulin class switching [147]. Usually sequestered by IκB proteins in the cytoplasm, upon activation NF-κB dimers are able to translocate to the nucleus. In addition to NF-κB, the transcription factor NF-AT is also important for downstream BCR signaling. Like NF-κB, NF-AT is influenced by the elevation of iCa^{2+}, and its activation can be mediated by the beta-isoform of PKC [148, 149].

Signal modulation

In B cells, quantity and quality of BCR-mediated signals can be influenced by multiple receptor-associated accessory molecules and co-receptors (Figure 11).

As previously described in this chapter, the glycoprotein CD19 positively contributes to BCR signaling by recruitment and activation of LYN, PI3K and VAV [137].

In addition, it has been demonstrated that while LYN positive activity is redundant in B cells, its negative role as a BCR signaling regulator is indispensable. LYN exerts its inhibitory function by phosphorylation of the immunoreceptor tyrosine-based inhibitory motifs (ITIM) on the molecules FCγRIIB (CD32) and CD22, which are then able to recruit phosphatases and suppress the BCR positive response [150]. CD22 exerts its negative effects

recruiting SH2-containing tyrosine phosphatase-1 (SHP-1), which substrates are molecules like Igα, Igβ, SYK, BLNK and CD22 itself [151]. The low-affinity receptor for IgG, FcγRIIB, blocks antigen-induced signaling, primarily by preventing PIP_3 accumulation through promotion of SH2-containing inositol 5'phosphatase-1 (SHIP-1) activation and CD19 dephosphorylation [152, 153]. SHIP can also recruit the adaptor molecule downstream of kinase (DOK), which is able to inhibit downstream signaling pathways, such as RAS and ERK [154].

BCR signaling can also be regulated by the signaling components organization on the plasma membrane. Literature data have proposed that in the absence of antigen binding, the BCR is already pre-assembled into oligomeric receptor complexes, which generate a basal level of signaling that is essential for B-cell maintenance [155]. During B cell activation, ligand-aggregated BCR molecules tend to partition into microdomains called lipid rafts, which are rich in glycosphingolipids and cholesterol, and create a liquid-ordered phase within the plasma membrane to allow lateral diffusion of proteins and lipids [156]. In addition, lipid rafts are constitutively enriched in certain types of proteins such as glycosphingolipids-linked proteins and lipid chain-modified proteins, including heterotrimeric G proteins, the src kinases LYN and Fyn, and other molecules involved in signal transduction, such as BLK, RAS, c-ABL, and actin [157].

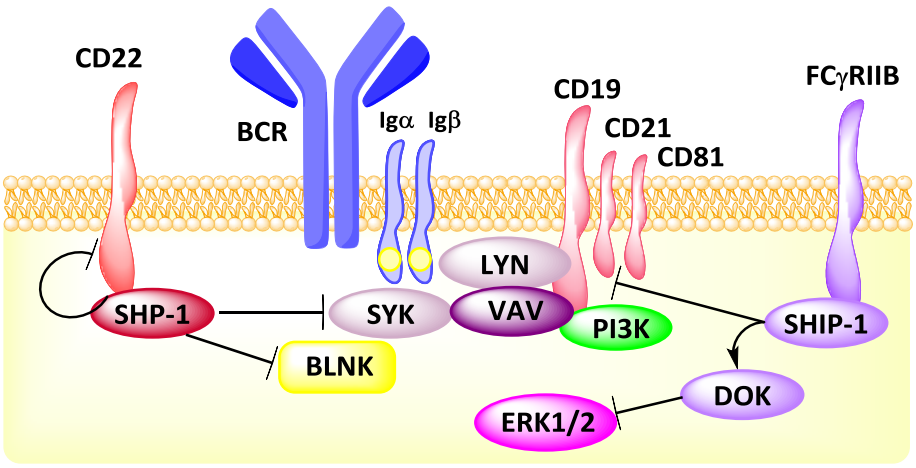

Figure 11. BCR signaling modulation. Simplified representation of the events initiated by CD19, CD22 and FCγRIIB, molecules involved in BCR signaling modulation.

BCR signaling in CLL cells

BCR signaling is heterogeneous in CLL, and the expression of sIgM seems to be the factor that drives the heterogeneity. It has been shown that U-CLL cases display a higher expression of sIgM and a retained ability to signal. Conversely, the strong down-modulation of sIgM has been related to reduced signaling responses, and it has been found mostly in CLL cases with mutated IGHV [25]. The biological effect of the variable immunoglobulin expression on the CLL cell surface reflects the clinical behavior of the disease, where clones with increased IgM expression and consequent maintained signaling capacity (typically U-CLL cases) show a poorer prognosis than the more indolent disease found in mutated patients [21] [158].

The predominant tumor status in terms of BCR response in CLL seems to be anergy, a mechanism whereby autoreactive B cells do not respond to activation via surface BCRs [159]. In CLL, the anergic state is characterized by low expression of sIgM, together with increased ERK1/2 and NFAT phosphorylation, and elevated iCa^{2+}, in absence of other features of BCR activation, such as AKT phosphorylation [160, 161]. These characteristics plus the constitutive SHIP-1 phosphorylation are usually observed in ZAP-70-negative cells, making anergy a typical characteristic of M-CLL cases associated with a relative good prognosis [162]. LYN plays a dual role in favoring and inhibiting BCR signaling, and its activation is not associated with IGHV status or ZAP-70 expression [97, 163], increasing the complexity in the interpretation of its involvement in anergy.

Our group has previously demonstrated that in CLL, as compared to normal B cells, LYN protein is upregulated and shows a different subcellular localization [97]. Moreover, it displays a remarkable constitutive activity associated to an increased basal tyrosine phosphorylation and a low responsiveness to BCR ligation. In normal B cells, LYN is located in membrane lipid rafts, whereas in CLL cells it is present all over the cell surface, and it has been detected also in the cytoplasm of malignant clones. Upon caspase-dependent cleavage at its N-terminal region, LYN is released into the cytosol and this has been described as a general mechanism in hematopoietic cells during induction of apoptosis [164].

LYN activity is critically regulated through its C-terminal Tyr507, which is phosphorylated by the tyrosine kinase CSK and dephosphorylated by the receptor tyrosine phosphatase CD45. In resting B lymphocytes, LYN is present in its inactive conformation, as a result of CSK phosphorylation of Tyr507 [165]. CSK is similarly expressed in normal and CLL cells, thus the constitutive activity of LYN could be due to the low amount of CSK insufficient to phosphorylate and downregulate its overexpressed substrate. Furthermore, the high concentration of LYN in CLL cells could promote the kinase intermolecular autophosphorylation at Tyr396, which in turn induces LYN activation [166].

SFK level is regulated by the balance of two opposing mechanisms: degradation by ubiquitination or rescue by association with HSP90 (Heat shock protein of 90kDa), a chaperone molecule interacting with the N-terminal lobe of the SFK catalytic domain [167]. Our group has previously demonstrated that, in CLL cells, LYN is part of a cytosolic 600 kDa complex, where it is associated with HS1 (Hematopoietic lineage cell Specific protein 1), SHP-1, and HSP90 [168]. The complex, stabilised by HSP90, maintains LYN in an active conformation and prevents its degradation.

1.2.2 Control of apoptosis (programmed cell death)

CLL is not a static disease that results only from the accumulation of long-lived lymphocytes, but it is a dynamic process of cells that also proliferate and die [169]. However, the dysregulation of programmed cell death is now widely recognized as one of the main mechanisms in the pathogenesis of many tumors, including CLL; the accumulation of leukemic cells is related to intrinsic features of the clone that allow escape from apoptosis, thus failing the homeostatic mechanism that normally limits the number of circulating cells.

Even though genetic lesions and intrinsic characteristics of tumor lymphocytes may be important for their prolonged survival and persistence *in vivo*, CLL cells from peripheral blood cultured *in vitro* typically undergo apoptosis, indicating that factors originating from the microenvironment play a major role in preventing cell death [170]. Thus, it is becoming increasingly clear that the defects in apoptosis have to be ascribed not only to intrinsic traits of the neoplastic

cells, but also to extrinsic factors that influence their behavior. Malignant cells retain the ability to respond to microenvironmental signals, showing a specific sensitivity to anti-apoptotic stimuli that favor their survival, and becoming insensitive to pro-apoptotic signals [23].

Apoptosis pathways can be initiated by stimuli received at the mitochondria (intrinsic pathway) or at the plasma membrane (extrinsic pathway). The principal apoptosis regulators are proteins of the BCL-2 family, which includes anti-apoptotic proteins (BCL-2, BCL-XL, and MCL-1), apoptotic effectors (BAX and BAK) and pro-apoptotic members called BH3-only proteins (BIM, BID, PUMA, BAD and NOXA) [171].

The antiapoptotic molecule MCL-1 (myeloid cell leukaemia-1) is constitutively upregulated in CLL, and its overexpression has been related to a worse prognosis and resistance to treatment [61, 172]. MCL-1 exerts its anti-apoptotic function by repressing the oligomerization of the pro-apoptotic proteins BAX and BAK, sequestering and maintaining them in an inactive form. The induction of the intrinsic mechanism of apoptosis is guided by BH3-only proteins, which compete with the pro-survival members of the BCL-2 family for the binding of the proteins BAX and BAK [173]. The oligomerized apoptotic effectors BAX and BAK can then bind the outer mitochondrial membrane, thus causing its permeabilization and the release of cytochrome c from the mitochondrial inter-membrane space into the cytoplasm, allowing the caspase activation that leads to cell death [174, 175] (Figure 12). BCL-2 has been shown to be an independent prognostic factor in CLL [176], while constitutive expression of MCL-1 has been associated with IGHV mutational status, CD38 expression and ZAP70 expression [61]. BCL-2 is also a target of BH3-mimetics (Section 1.1.5), aim to induce apoptosis by favouring the release of BH3-only proteins and enabling the oligomerisation of apoptotic effectors (Figure 12B).

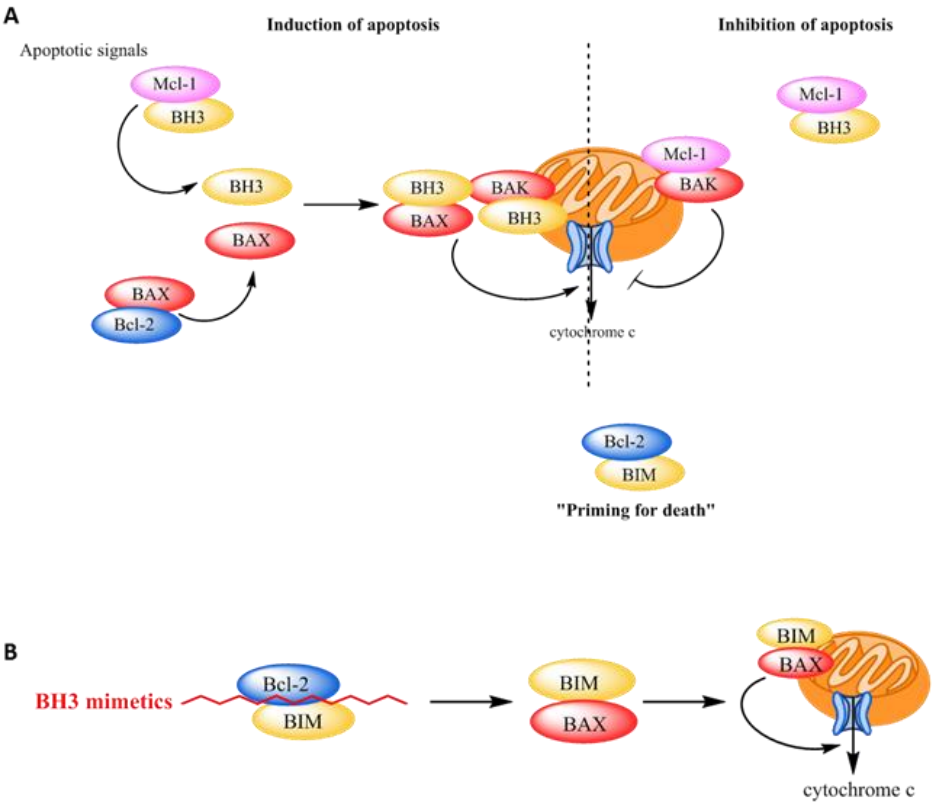

Figure 12. MCL-1 and BH3-mimetics mechanism of action. A) The anti-apoptotic proteins MCL-1 and BCL-2 sequester apoptotic effector BAX and the pro-apoptotic BH3-only proteins, preventing their oligomerization. In the presence of apoptotic signals, MCL-1 releases the BH3-only proteins, which can compete with BCL-2 for the binding of BAX, with subsequent polymerization of BAX and BAK. This leads to the permeabilization of the mitochondrial outer membrane, with consequent release of cytochrome c into the cytoplasm and activation of caspase, followed by cell death. In CLL cells, BCL-2 is bound to the pro-apoptotic BH3-only protein BIM, making cells "primed for death". **B)** BH3-mimetics show high affinity for BCL-2. These compounds disrupt the binding of BCL-2 to BIM, allowing BIM to activate BAX and to form pores in the mitochondrial membrane, with consequent cell death.

The extrinsic apoptotic pathway is activated by extracellular ligands that bind specific receptors located at the plasma membrane of cells destined to apoptosis. Typical death receptors are CD95/FAS (fibroblast associated antigen) and TNF-R (tumor necrosis factor receptor), which contain a cytosolic domain called death domain (DD). The ligation of these receptors induces the recruitment of the adaptor protein FAS-associated death domain (FADD) and the activation of caspase-8 or -10 (initiators of the apoptosis pathway) [177, 178].

In CLL, CD95 is down-modulated and the FAS-mediated apoptotic pathway is inactive, as opposed to normal B cells from healthy individuals [179, 180]. TOSO (also known as FAS-inhibitory molecule 3) is a transmembrane protein that inhibits FAS-mediated apoptosis by binding FADD via its intracellular

domain. TOSO was identified as a candidate gene overexpressed in CLL, and its high expression has been correlated with a more aggressive disease [181].

Other intrinsic factors, which are critical for the control of apoptosis, are the 17p13 and 11q23 deletions. The deleted chromosomic regions contain two prominent tumor suppressor genes: *TP53* and *ATM*, respectively. The proteins p53 and ATM are central regulators of the DNA-damage response pathways, and their activation leads to cell-cycle arrest and DNA repair, apoptosis or senescence, depending on the cellular context. Impaired p53 function through mutations and/or deletions is the best characterized factor associated with chemoresistance in CLL [182].

1.2.3 Cytokine and chemokine receptors

The contact with the microenvironment plays an important role in B cell trafficking, homing and survival. Stromal cells in secondary lymphoid tissues produce high amounts of chemokines and cytokines that provide guidance for homing in a protective environment [183], or the recruitment of effector cells in inflammatory conditions [184].

Lymphocyte cell trafficking is mainly mediated by chemokine receptors and adhesion molecules, which expression on B cell surface is modulated during differentiation and activation [185]. It has been demonstrated that, in B cell leukemia/lymphomas, neoplastic cells maintain their ability to respond to chemoattractant stimuli, modulating the expression of chemokine receptors and adhesion molecules on their cell surface [186, 187].

One of the most characterized chemokine receptors is chemokine (C-X-C motif) receptor 4 (CXCR4), which is expressed by all B cell subsets [188]. Present at high levels on the surface of circulating tumor cells, G protein-coupled CXCR4 mediates CLL lymphocyte migration *in vivo* and *in vitro* toward the specific ligand chemokine (C-X-C motif) ligand 12 (CXCL12), and actin polymerization [186]. CXCR4 modulation is mediated by CXCL12 via receptor endocytosis, in particular in tissues, where the ligand is present at high concentrations. In addition, BCR engagement may also be able to modulate CXCR4 levels; literature data report that increased signaling through the BCR may lead to increased chemotaxis toward CXCL12 [189]. CXCR4 stimulation

mediates the phosphorylation and activation of BTK and PLCγ2, key components of the signaling pathway that controls cell migration [190]. Consequently, receptor binding induces intracellular calcium mobilization, ERK and signal transducer and activator of transcription 3 (STAT3) activation, and prolonged cell survival *in vitro* [186, 191, 192]. High levels of CXCR4 positive cells in the peripheral blood of CLL patients have been associated with higher risk of tissue infiltration and poor prognosis [193].

CXCR5 is a chemokine receptor mainly expressed on mature B lymphocytes [188], and it binds specifically the chemokine CXCL13, which is constitutively secreted by lymph node stromal cells [194]. CXCR5 induces the recruitment of B lymphocytes into follicles, in particular their positioning in the germinal centers [194]. It has been demonstrated in CLL cells that CXCL13 binding induces actin polymerization, chemotaxis and activation of intracellular signaling mediated by ERK [195, 196]. CXCR5 is highly expressed on CLL cells, while CXCL13 serum levels are higher in CLL patients compared to normal individuals [196].

An important receptor for lymphocyte entry into secondary lymphoid tissues is chemokine (C-C motif) receptor 7 (CCR7), which leads B cells to migrate across the vascular endothelium by binding to the ligands chemokine (C-C motif) ligand 19 (CCL19) and CCL21 [197]. These chemokines have been detected at elevated concentrations in the high endothelial venules (HEV) of lymph nodes in CLL. Expression of CCR7 on CLL cell surface is usually high, in particular in ZAP-70+ cells in patients with lymphadenopathy [197, 198]. The receptor binding induces the activation of intracellular pathways mediated by PI3K/AKT, thus regulating cell survival and trafficking [197]. Moreover, it has been proposed that ZAP-70 may be directly responsible for CCR7 cell surface expression through activation of the ERK pathway [199].

The chemokine receptor CXCR3 has been less well-characterized in CLL. Moreover, our group has previously demonstrated that CXCR3 is consistently expressed on the CLL cell surface, and its binding to the IFNγ-induced molecules CXCL9, CXCL10 and CXCL11 mediates chemotaxis to sites of inflammation [200]. Studies have reported the overexpression of the receptor in patients with early stage CLL [201], or in advanced disease stage in association with poor

prognosis [202]. The literature suggests that CXCR3 and its ligands play an important role in CLL cell trafficking, and that further investigations might be required to more clearly define their specific effects.

Although complex, cell trafficking and homing are very important steps in B cell development, activation and survival. The ability to migrate in response to external stimuli is even more crucial for CLL cells, which need to be able to escape the apoptosis process and use the microenvironment to their own advantage. Therefore, increasing understanding of this field has the potential to help the discovery and design of new therapeutic treatments for the disease.

ABSTRACT – Chapter 2

Chronic Lymphocytic Leukemia (CLL) is characterized by the monoclonal expansion of mature CD19+/CD5+/CD23+ B lymphocytes in peripheral blood, bone marrow and lymphoid tissues. When cultured *in vitro*, leukemic cells undergo spontaneous apoptosis, suggesting that their survival advantage is due not only to intrinsic features of the clones, but also to extrinsic factors that influence the behavior of neoplastic cells in the tissue microenvironment. Mesenchymal Stem Cells (MSCs) represent the major component of the stromal microenvironment and play a role in disease support and progression. In this thesis, the cross-talk and bi-directional activation between CLL cells and MSCs *in vitro* have been studied. In particular, we aimed to evaluate the influence of stromal cells on the leukemic clone survival in presence of the chemotherapeutic agents Fludarabine and Ciclophosphamide, or after treatment with BCR-signaling inhibitors. MSCs isolated from the marrow aspirate of 46 CLL patients were expanded *ex vivo*, characterized by flow cytometry and co-cultured with leukemic cells. After 7 days, we observed a relevant extended survival of leukemic cells, which could be differently dependent on the signals coming from the stromal cells. Moreover, co-culture of MSCs with CLL cells induced an increase in the production of IL-8, CCL4, CCL11 and CXCL10 chemokines. In addition, MSCs were able to counteract the cytotoxic effect of Fludarabine/Cyclophosphamide in vivo administration, confirming the important role played by microenvironment during therapy. However, the kinase inhibitors Ibrutinib and Bafetinib could induce apoptosis of leukemic cells co-cultured with MSCs, and inhibited CLL B cell CD49d-mediated adhesion and pseudoemperipolesis. These evidences suggest that the new kinase inhibitors are effective in targeting the pro-survival cross-talk between leukemic lymphocytes and stromal cells, and open the way to the identification of new targets for therapy in CLL.

Chapter 2 – Microenvironment influence on CLL cells

2.1 Introduction

Mesenchymal stromal cells (MSCs) are adherent stem-like cells for non-hematopoietic tissues, with high proliferative capacity and long term-self renewal; they are able to differentiate into cells of mesenchymal origin and into most somatic cell types [203, 204]. MSCs can retain their differentiation potential when cultured *in vitro*, thus supporting their definition as stem cells [205]. In the mid-1970s, Friedenstein cultured samples of whole bone marrow (BM) on plastic dishes and after a few hours removed the non-adherent cell fraction [206]. After 2-4 days, he observed the formation of loci of a few cells that started proliferating and were inclined to mutual confluence. After several passages in culture, they became spindle-shaped, and showed the ability to differentiate into different cell types. Extended studies were carried out to investigate the nature of the marrow progenitor cells, and in the 1980's it was demonstrated that these stromal cells could differentiate into osteoblasts, chondroblasts, adipocytes and myoblasts [207-210]. Due to this ability of generating mesenchymal lineages, bone marrow-derived stromal progenitors have been designated mesenchymal stem cells [208].

2.1.1 MSC tissue origin

MSCs were firstly isolated from the bone marrow of mice and described as fibroblast-like cells with large nuclei, evident nucleoli and clear cytoplasm [211]. In this tissue, MSCs are present in a very low concentration (about 0.01-0.0001% of all the nucleate cells), and their number is expected to decrease with age.

For the growing interest in the study of these cells, MSCs have also been isolated from other tissues, including human umbilical cord blood [212], subcutaneous adipose tissue [213], human placenta from cells of fetal or maternal origin [214], or from the periodontal ligament [215]. However, the search for MSCs in the peripheral blood (PB) gave conflicting results. Some studies reported the impossibility to get MSCs from peripheral blood stem cell collection (PBSC), demonstrating that cells from PB cultured *in vitro* gave origin to a population of non-confluent fibroblastic-like cells with a hematopoietic phenotype [216, 217].

Other studies, however, demonstrated that mesenchymal precursor cells could be obtained from the PB of normal individuals, and they could proliferate in the presence of fetal bovine serum without specific growth factors [218], or were identified in growth-factor-mobilized peripheral blood cells from breast cancer patients [219].

2.1.2 Immunophenotypic characterization

Contrary to stem cells with hematopoietic origin (Hematopoietic Stem Cells, HSCs), MSCs lack an antigenic marker for unique identification (as CD34 antigen for HSCs). Thus, the phenotypic characterization of human MSCs is based on the positivity or negativity of surface molecules not MSC-exclusive [220].

MSCs express a wide range of molecules that can be used for positive detection of the cell population. Receptor molecules used as MSC markers are CD44, hyaluronic acid receptor, and CD105, a glycoprotein that is part of the transforming growth factor-β (TGF-β) receptor complex and is recognized by SH-2 antibodies [221]. Adhesion molecules expressed on stromal cells that can be useful for MSC identification are CD90 and CD29 [222, 223], and CD54 (ICAM-1) [224]. Moreover, the ecto-5'-nucleotidase CD73, which converts extracellular adenosine monophosphate to adenosine, and is recognized by SH-3 and SH-4 antibodies [225], and STRO-1, an antigen present on non-hematopoietic precursors in the bone marrow [226], are used as positive markers for MSCs.

Antigens which should not be present on stromal cell surface also contribute to MSC identification. CD34, the hematopoietic progenitor cell antigen, functions as a cell-cell adhesion factor, and mediates the attachment of stem cells to bone marrow stroma and extracellular matrix [227]. CD45, originally called leukocyte common antigen (LCA), is a protein tyrosine phosphatase expressed by almost all the differentiated hematopoietic cells [126]. Moreover, CD14, a protein involved in detection of bacterial lipopolysaccharide (LPS) [228], and CD31 (also called platelet endothelial cell adhesion molecule, PECAM-1) [229], involved in transmigration, angiogenesis and integrin activation, are also regarded as MSC negative markers.

2.1.3 MSC culture expansion and functional characterization

MSCs are isolated *ex vivo* from cell suspensions of marrow blood or cellular components of disaggregated tissues, and are cultured in liquid media. Mononuclear cells are seeded in culture plates or flasks at the concentration of approximately 1,000cells/cm^2 in Modified Eagle Medium (α-MEM) or Dulbecco's modified Eagle medium (D-MEM), supplemented with fetal bovine serum and antibiotics.

After 24 hours, some cells may have adhered to the plastic surface, whilst the most part remains in suspension and will be removed after 7 days with the first change of medium. In the subsequent days, proliferation foci made of highly proliferative cells that tend to the mutual confluence begin to appear. If the cell layer covers the entire plastic surface, confluence is reached and the blockade of proliferation and the spontaneous differentiation in pre-adipocytes occur. Thus, when the monolayer reaches a semi-confluent level (i.e. when 70-80% of the plastic surface is covered by cells), it is necessary to remove the adherent cells by trypsin treatment and seed them into new plates or flasks to expand the culture.

After 5-7 weeks, the adherent cells form a homogenous population of spindle-shaped cells with a fibroblast-like phenotype that continues to proliferate without differentiation up to 40 generations [223]. During *in vitro* culture, MSCs do not modify their membrane phenotype nor their multilinear differentiation potential, maintaining an undifferentiated status. However, in the presence of appropriate conditioned medium, MSCs are able to differentiate in different mesodermal lineages, like adipogenic, osteogenic, chondrogenic and myogenic [230]. This property certify the stem nature of these cells.

The adipogenic differentiation is induced with media that contains dexamethasone (1μM), insulin and 3-isobutil-1-metilxantine, which are all factors that activate metabolic pathways for lipid synthesis [231]. MSCs progressively accumulate lipid drops in the cytoplasm which are detected by specific staining with Oil-red-O or Sudan black. The potential of MSCs to differentiate into adipocytes may be related to the fact that, with aging, marrow is partially replaced by adipose tissue [232] (Figure 13).

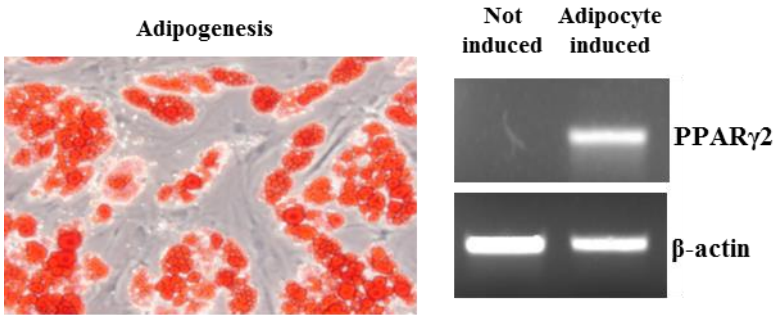

Figure 13. Adipogenic differentiation. MSC adipogenic differentiation is evaluated by Oil Red staining (10X magnification, Olympus BX60). Molecular analysis with specific primers for PPAR-γ (Peroxisome Proliferator Activated Receptor) allows to confirm the occurred differentiation of MSCs in adipocytes.

The osteogenic induction is obtained with a media containing dexamethasone (0.1μM), ascorbic acid and β-glycerophosphate. Cells assume a polygonal shape and deposit a mineralized matrix which is strongly colored by von Kossa staining or by reaction to the alkaline phosphatase (Figure 14).

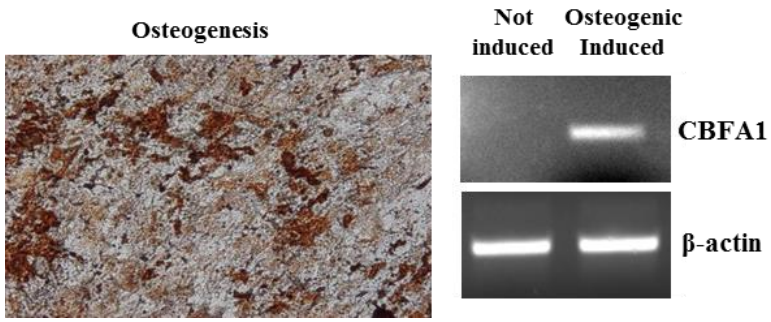

Figure 14. Osteogenic differentiation. MSC differentiation in osteoblasts is evaluated by von Kossa staining (10X magnification, Olympus BX60). The molecular analysis performed with specific primers for CBFA1 (Core Binding Factor 1) confirms the occurred differentiation.

The chondrogenic differention can be driven by the use of a specific media containing dexamethasone and ascorbic acid (as for the osteogenic differentiation), supplemented with TGF-β1 and proline [233]. Cultured cells produce abundant extracellular matrix composed of cartilage-specific molecules, such as type II collagen and aggrecan. The matrix can be colored by tolouidine blue staining, making cells positive for type II collagen by immunohistochemical analysis. The potential to differentiate into chondrocytes could be related to the process of fracture repair, since small amounts of chondrocytes appear at the fracture sites and are then replaced by bone [234].

The myogenic induction is obtained by incubation of the cells with amphotericin B or 5-fluorocytidine [235]. During differentiation, a progressive stretching of the cells occur, with generation of myotubes and the beginning of spontaneous or acetylcholine-induced contractile activity. The myogenic induction is demonstrated through the expression of myogenin, Myo D (transcription factor involved in mesenchymal cell differentiation) or myosin.

Moreover, the ability of MSCs to differentiate also in tissues of non-mesodermal origin has been reported. The use of appropriate stimuli *in vitro* can induce MSCs to generate neurons (ectodermic origin) [236], pneumocytes [237], hepatocytes [238] and epithelial cells of the renal tubule [239] (all cells of endodermic origin). Studies *in vivo* in mice have confirmed the *in vitro* results, showing that MSCs injected in rat ischemic brain assume a neuronal phenotype and improve the functional recovery of the damaged area [240]; additionally, in mice exposed to bleomycin, MSCs root in the lung and can differentiate into type I pneumocytes [237].

2.1.4 MSC functions

In vivo, MSCs are directly and actively involved in survival, quiescence and differentiation of HSCs, supporting hematopoiesis and hematopoietic-cell homeostasis [241]. This is in line with *in vitro* studies, which showed that MSCs sustain long-term hematopoietic cell cultures and that, in animal models, MSC and HSC co-transplant favors the engraftment of HSCs [242]. Stromal cells in fact maintain HSCs in specialized niches close to the marrow vasculature or to the endosteum, providing signals for self-renewal, proliferation and differentiation [243].

The interaction between MSCs and HSCs occurs through both direct cell-cell contact and production of soluble factors. MSCs produce several cytokines including Stem Cell Factor (SCF), Stromal Derived Factor 1 (SDF-1), Oncostatin M (OSM), Bone Morphogenetic Factor-4 (BMF-4), fms related tyrosine kinase (ftl-3), TGF-β, which are able to maintain the hematopoietic stem cells in a quiescent state or can promote their self-renewal [244]. Moreover, MSCs produce a wide variety of interleukins (IL), such as IL-1, IL-6, IL-7, IL-11, IL-12, IL-14, IL-15, and *in vitro* in presence of IL-1α, Granulocyte Macrophage Colony

Stimulating Factor (GM-CSF) and Granulocyte Colony Stimulating Factor (G-CSF) are involved in the hematopoietic precursor differentiation [222].

Interestingly, it has been shown that MSCs can migrate toward damaged tissues to start the healing process. This is possible through MSC binding to P-selectin, a molecule expressed on the endothelial cell surface, which allows the extravasation of stromal cells to reach the site of injury [245]. Moreover, MSCs produce a local "curtain" of bioactive molecules to protect the site of injury from the immune system, which could cause the initiation of an autoimmune response, and, at the same time, they release soluble factors to start the regeneration process [246, 247].

2.1.5 Immunomodulatory properties

The immunomodulatory capacity of MSCs has important implications in different fields. MSCs are slightly immunogenic, and can be used allogenically or xenogenically in a variety of tissue disease states [248-250]. MSCs do not express co-stimulatory molecules important for the direct stimulation of T lymphocytes, such as CD80, CD86, CD40 or CD40L [250, 251]. However, they can be induced to express MHC class II and Fas ligand, but they are not recognized and lysed by cytotoxic T cells [252, 253]. For example, it has been demonstrated that allogeneic MSC HLA-mismatched transplant in experimental animal models such as rat or baboon are not rejected [254]. Moreover, MSCs show an immunosuppressive effect on many immune cells (Figure 15). Due to these qualities, MSCs have become very attractive for stem cell-based therapy strategies in tissue repair and gene therapy, and it has been postulated that the benefit observed in cell-based therapy is due to local immune modulation by MSCs rather than differentiation and replacement of the damaged tissue [255, 256].

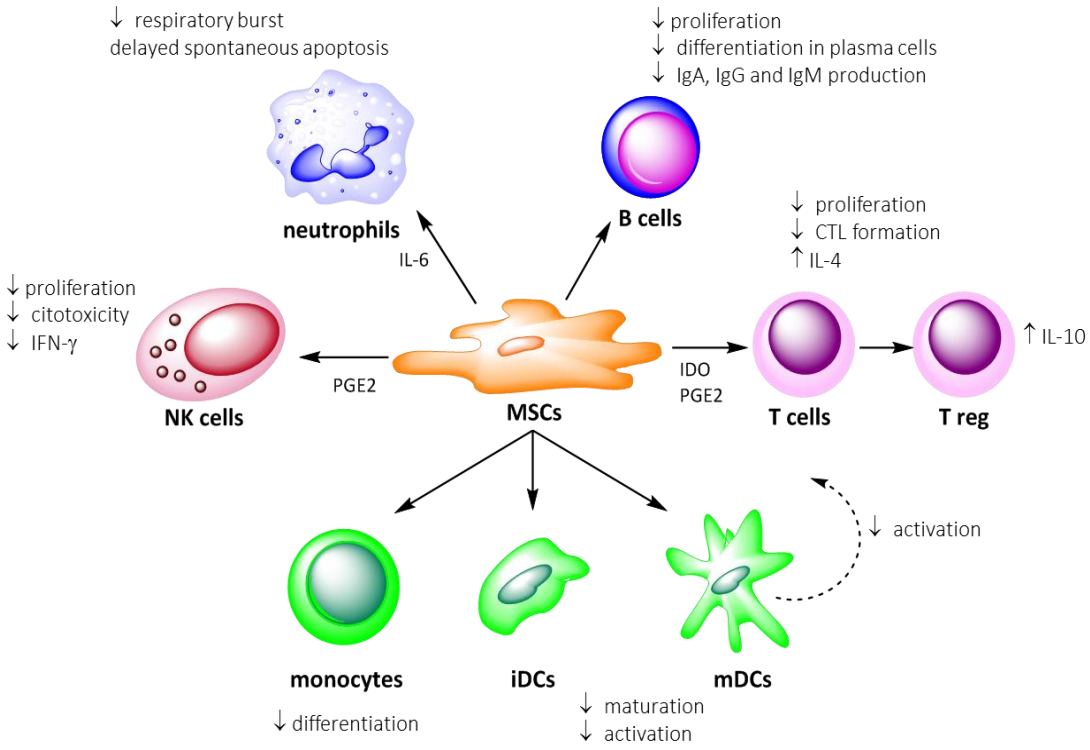

Figure 15. MSC immunomodulatory properties. Schematic representation of the immunomodulatory properties of MSCs on various immune cell subsets. Immature dendritic cells (iDC), mature dendritic cells (mDC), regulatory T cells (Treg). Modified from Nauta A.J. et al, Blood, 2007 [257].

MSCs and T cells

Studies *in vitro* on murine, human and baboon cells have shown that MSCs are able to inhibit both T cell proliferation, induced by alloantigens and mitogens [258], and T cell activation after stimulation with CD3 and CD28 antibodies [259]. The molecular mechanisms involved in the regulatory function of MSCs are still not well known. This activity is not due to a pro-apoptotic effect on proliferating T cells, but due to a block in the G0 phase of the cell cycle [260]. The inhibition of T lymphocyte proliferation could be mediated in part by cell-cell interactions, but also by the production of soluble factors such as TGF-β1, hepatocyte growth factor (HGF), Prostaglandin E-2 (PGE-2) [258] and the enzyme 2,3 dioxygenase (IDO) [261].

The immunogenic role of MSCs is also played towards regulatory T cells, which are recruited and maintained with a regulatory phenotype (CD4+/CD25+/FOXP3+) by stromal cells [262]. Moreover, it has been shown

that MSCs are able to increase the CD4+/CD25+ population when cultured with mononuclear cells from peripheral blood stimulated with mitogens [250, 263].

Studies *in vivo* about Graft Versus Host Disease (GVHD) showed that MSCs can inhibit the cytotoxic effect of cytotoxic T cells (CTL), probably suppressing their proliferation rather than interfering with their cytolytic activity [252, 264] [257]. Thus, human MSCs administered *in vivo* improve the outcome of allogenic transplantation by promoting hematopoietic engraftment and by interfering with GVHD [265].

MSCs and B cells

B cell development occurs in the bone marrow and is strictly dependent on close interaction with stromal cells, which produce different cytokines able to support progenitor B cell survival [266]. In B cell lymphopoiesis, interactions between the lymphocyte receptor CXCR4 and the stromal cell-derived CXCL12 are critical for retention of B cells in the bone marrow and their subsequent maturation [267]. MSCs, however, also affect mature B cell functions and survival, as demonstrated by *in vitro* co-culture experiments. It has been shown that human MSCs inhibit the proliferation of B lymphocytes *in vitro*, causing their arrest in the G0/G1 phase of the cell cycle without inducing apoptosis, and also they reduce the production of type A, G and M Igs, thus interfering with B cell differentiation in antibody-secreting cells [241]. In addition, the expression of chemokine receptors such as CXCR4, CXCR5 and CCR7 on the B cell surface is decreased in presence of MSCs, and consequently chemotaxis toward the respective receptor ligands CXCL12, CXCL13 and CCL19 is impaired. This modulation by stromal cells on lymphocyte function and phenotype is due to the active cross talk between the two cell types.

MSCs and Natural Killer cells (NK)

MSCs inhibit IL-2 and IL-15-induced proliferation, IFN-γ secretion and the cytotoxic activity of NK cells through different mechanisms that involve direct cell-cell contact and soluble factors [268]. It has been demonstrated that PGE-2 secretion from MSCs can partially influence NK proliferation and cytotoxic activity, but it does not interfere with the cytokine production or the expression of cell activating receptors, such as CD56. However, these effects can

be measured only when MSCs are present at a high concentration in the culture system, so in a non-physiologic condition.

Although considered only slightly immunogenic, recent studies have demonstrated that NK cells can be activated by MSCs through the binding to molecules like UL16-binding proteins (ULBP), Polio Virus Receptor (PVR) and Nectin-2 on the stromal cell surface [269].

MSCs and dendritic cells (DC)

MSCs can interfere with dendritic cell differentiation and maturation, and it has been demonstrated that mesenchymal stem cells inhibit the differentiation and function of the monocyte-derived dendritic cell population [270]. Moreover, DC generated in the presence of MSCs show a reduced efficacy in the T cell activation process; this is due to the upregulation of MHC-II and CD83 up-regulation and the expression of co-stimulatory molecules do not occur as in the normal maturational process [270, 271]. The presence of MSCs also causes a reduction in pro-inflammatory cytokine production, such as Tumor Necrosis Factor α (TNF-α), IFN-α, IFN-γ and IL-12, the increased production of the anti-inflammatory cytokine IL-10 [250, 272], as well as the blockade of the cell cycle in the G0/G1 phase [273]. These conditions lead to the generation of immature DCs with a suppressive or inhibitory phenotype and a reduced ability to activate T lymphocytes.

MSCs and neutrophils

MSCs can interfere with the respiratory burst and delay spontaneous apoptosis of both quiescent and activated neutrophils, through an IL-6-dependent mechanism [274]. Some studies hypothesize that, in the marrow stroma, MSCs protect the resident neutrophils from apoptosis, preserving their effector functions and preventing the excessive or inappropriate metabolic activation [275]. These kind of mechanisms could operate in the lung, where a resident MSC population has recently been identified.

2.1.7 MSCs in tumors

The tumor microenvironment continuously produces and releases cytokines and other mediators to create an inflammatory state in the tissue.

Attraction of MSCs to the site of inflammation and incorporation in the primary and metastatic tumor microenvironment has been observed in different types of cancer (lung, brain, breast, skin, colon, ovarian cancer) [276]. For this targeted migration, MSCs have been described to either support or inhibit tumor growth and invasion.

MSCs may be involved in regulation of immune surveillance and apoptosis during tumor development, acting as a source of different soluble factors that can promote neoplastic growth and metastasis [277], as demonstrated by *in vitro* and *in vivo* experiments with cancer cells from colon and ovarian carcinomas [278, 279]. MSCs can suppress immune response by secretion of soluble factors like nitric oxide (NO) and IL-6 for modulation of T-cell proliferation and function [280, 281], and prostaglandin E2 (PGE-2) for inhibition of monocyte differentiation [282].

Angiogenesis is an important step in the development of metastasis. In this context, MSCs can exert a paracrine activity on endothelial cells, inducing the release in the microenvironment of vascular endothelial growth factor (VEGF), platelet-derived growth factor (PDGF), IL-6, IL-8 and TGF-β, which are known to promote angiogenesis [283].

However, many studies have reported an inhibitory effect of stromal cells on tumor growth. For example, MSCs seem to downregulate the Wnt/β-catenin signaling pathway in the breast cancer MCF-7 cell-line, thus inhibiting cell proliferation [284]. Additionally, in a chemically induced hepatocarcinoma experiment it has been shown that inhibition of the Wnt/β-catenin pathway is caused by downregulation of β-catenin, cyclin D and survivin [285]. Furthermore, MSC-mediated downregulation of the Akt pathway, observed in a model of Kaposi's sarcoma, had a pro-apoptotic effect on cancer cells [286].

Since MSCs can be easily harvested in large numbers and handled *in vitro*, and most importantly can be transplanted into patients without inducing a host immune response, increasing attention has been paid to their involvement in targeted gene therapy [287]. In particular, MSCs seem to be suitable for tumor selective delivery of therapeutic agents, as they can be transduced with exogenous genes, are non-immunogenic, and possess tumor tropism. Therefore, MSCs have been studied as vehicles for therapeutic cytokines [288, 289] and prodrug gene

therapy [290], becoming very promising for safer and more efficient clinical therapy in the future.

2.1.8 MSCs in CLL

MSCs are commonly found in secondary lymphatic tissues of CLL patients, providing survival and migration signals to leukemic cells [291].

Ding and colleagues were the first to demonstrate the existence of a bi-directional activation between CLL B cells and MSCs [292]. It has since been shown that bone marrow stromal cells (BMSCs) can up-regulate aggressive disease markers in CLL cells, such as ZAP70 and CD38, and promote the activation of CD71, CD69, CD25 and CD70 [292, 293]. Moreover, the contact with MSCs has been demonstrated to down-regulate the SDF-1α receptor CXCR4 and the expression of CD20 on CLL cell surface [293, 294]. In addition, studies *in vitro* showed that MSCs co-cultured with CLL B cells have the ability to protect the tumor clone from spontaneous apoptosis, and are involved in drug-resistance [292].

Importantly, Ding demonstrated that CLL cell activation is accompanied by MSC activation. CLL cells are active players in shaping the microenvironment according to their needs. Thus, the effect of the leukemic clone on stromal cells is exerted by activation of signaling pathways in MSCs involving PKC and NF-κB, as well as ERK and AKT [292, 295]. Moreover, besides soluble factors, CLL cells release micro- and nano-vesicles enriched in activated proteins, which can stimulate BMSCs [296, 297].

MSCs from CLL patients have been expanded in order to study their characteristics and differences from the normal counterpart in healthy donors. MSCs obtained from CLL patients show morphology and immunophenotypic characteristics of the normal stromal cells, thus expressing CD29, CD44, CD73, CD90 and CD105 and being negative for CD14, CD34 and CD45, as well as being adherent in nature [220, 292, 298]. Moreover, CLL-derived MSCs are not qualitatively nor quantitatively different from normal MSCs in terms of differentiation potential [298].

The frequency of MSCs in the bone marrow of leukemic patients is lower than in the healthy donors, and as well, they display a decreased proliferative

potential compared with normal counterparts. Thus, when cultured *in vitro*, MSC growth rate over passages is significantly reduced compared to cultures of stromal cells derived from normal individuals [298].

MSCs from CLL patients show normal immunosuppressive properties, and co-cultures of CLL-MSCs and tumor B cells result in a significant increase in B-cell proliferation and survival, and IgG production [292, 298-300]. However, CLL-derived MSCs do not confer a survival advantage over normal MSCs to the leukemic cells. In addition, it has been shown that the chromosomal aberrations found in hematopoietic cells are not detected in MSCs, suggesting that the stromal population is not a part of the malignant clone [298].

2.2 Aim of the study

CLL B cells are characterized by the tendency to infiltrate the bone marrow, and this associates with clinical stage and prognosis of the disease. In the marrow, the leukemic clone can find a protective niche in which interactions with other supportive cells occur. CLL B cells are able to escape apoptosis through intrinsic (such as chromosomal mutations and overexpression of anti-apoptotic proteins) and extrinsic mechanisms, like the contact with the microenvironment. MSCs are an important component of the marrow stroma, they support hematopoietic stem cell growth and are involved in tissue repair and wound healing.

In this thesis, the effect of MSCs toward CLL B cells has been evaluated. In particular, the aim of the study was to determine whether MSCs could protect CLL B cells from spontaneous and drug-induced apoptosis, and in which way MSCs can favor neoplastic cell survival. In order to investigate this, we:

- isolated MSCs and B cells from bone marrow aspirates and peripheral blood of CLL patients and normal subjects;
- evaluated levels of leukemic and normal B cell viability in the presence/absence of supportive stromal cells;
- analyzed the cytokine/chemokine secretion profile of MSCs, CLL and normal B cells in culture alone or co-culture, through the Bio-Plex array;
- evaluated the apoptosis levels of CLL B cells exposed to Fludarabine and Cyclophosphamide therapy and co-cultured with MSCs;
- determined the effects of kinase inhibitor administration on CLL B cell viability, migration, adhesion and chemokine receptor expression in the presence of MSCs.

2.3. Materials and Methods

2.3.1 Patients

In this study, we have analyzed MSCs obtained from bone marrow samples of 46 CLL patients (32 males and 14 females, aged between 40 and 78 years), and B cells obtained from 45 CLL patients (33males and 12 females, aged between 46 and 93 years) and 11 healthy donors, enrolled by the Hematology and Clinical Immunology branch (chief Prof. G. Semenzato), Padua University School of Medicine.

Clinical characteristics of patients enrolled for MSCs isolation are listed in Table II. Clinical characteristics of patients from who we obtained peripheral blood samples are listed in Table III. B lymphocytes obtained from peripheral blood of 11 healthy subjects were used as normal controls.

Table II. Characteristics of CLL patients enrolled for MSC isolation.

Patients (number)	46
Age, (years, range)	59 (40-78)
Males/Females	32/14
Lymphocytes (%, range)	52 (35-70)
IGHV mutated[a] (%)	51
CD38[b] (%)	21
Karyotype (N[c]/13q-/12+/11q-/17p- %)	15/18/15/4/30

IGHV, immunoglobulin heavy chain variable region.

[a] samples with percentage of mutation in the IGHV gene >2% in respect to the closest germline sequence.

[b] values determined by flow cytometry (cut-off 30%)

[c] N, normal karyotype defined by the absence of cytogenetic abnormalities.

Table III. Characteristics of CLL patients enrolled for tumor B cell isolation.

Patients (number)	45
Age (years, range)	69 (46-93)
Males/Females	33/12
WBC (cells/mm^3)	52,999 (4,700-30530,000)
Lymphocytes (%, range)	69 (40-97)
IGHV mutated[a] (%)	53
CD38[b] (%)	18
Karyotype (N[c]/13q-/12+/11q-/17p- %)	17/17/13/5/33

WBC, whole blood cells. IGHV, immunoglobulin heavy chain variable region.

[a] samples with percentage of mutation in the IGHV gene >2% in respect to the closest germline sequence.

[b] values determined by flow cytometry (cut-off 30%)

[c] N, normal karyotype defined by the absence of cytogenetic abnormalities.

2.3.2. Isolation of MSCs from bone marrow

MSCs were obtained from 46 CLL patients (Table II). From each patient 2ml of iliac crest bone marrow blood were taken under local anesthesia and processed with Ficoll/Hypaque (F/H; Amersham Biosciences; Buckinghamshire, UK) to obtain mononuclear cells (Figure 16). Each sample was filtered in a 26G needle and diluted 1:3 in Phosphate Buffered Saline (PBS1X) (Euroclone; Milan, Italy). BM mononuclear cells (BMMCs) were layered slowly over the F/H solution, a method that allows the dissection of the different blood components by density gradient. Mononuclear cells (lymphocytes and monocytes) and platelets are concentrated above the F/H layer because of their low density, while red blood cells and granulocytes settle at the bottom of the tube. After centrifugation at 900g for 20 minutes at 20°C with brake off, the layer of BMMCs formed at the F/H interface was collected and washed twice in PBS1X by centrifugation at 400g for 10 minutes at 20°C. The pellet was then suspended in an adequate amount of RPMI 1640 (Sigma-Aldrich; Milan, Italy) and cells were counted in the Burker chamber.

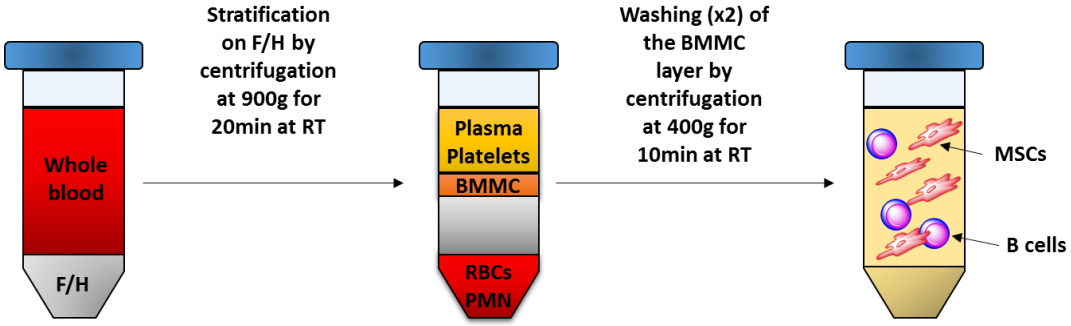

Figure 16. MSCs isolation from bone marrow blood. Blood components were stratified on Ficoll/Hipaque solution by centrifugation, depending on their density. BMMC layer was collected and cells were washed twice in PBS1X. F/H, Ficoll/Hipaque. RT, room temperature. BMMC, bone marrow mononuclear cells. RBC, red blood cells. PMN, polymorphonuclear cells. MSC, mesenchymal stromal cells.

2.3.3. *Ex vivo* MSC expansion

Mononuclear cells obtained from marrow blood were resuspended in Dulbecco's Modified Eagle Medium (DMEM) (Euroclone) supplemented with 10% heated-inactivated FBS (Fetal Bovine Serum), 1% PenStrep (100U/ml Penicillin, 100µg/ml; Life Technologies; Paisley, UK) and 10µg/ml Ciprofloxacin (Ciproxin; Bayer; Leverkusen, Germany). Cells were seeded at the concentration of 1,000cells/cm^2 and were incubated at 37°C in 5% CO_2 modified atmosphere. Cells started to adhere to the bottom of the flask after 24-48 hours, and in few days following seeding, it was possible to observe the generation of foci containing highly proliferating cells tending to reciprocal confluence. The medium was changed after 7 days of culture to remove the non-adherent fraction of cells. In order to expand the culture, flasks were washed with PBS1X and incubated at 37°C with Trypsin (Life Technologies; Carlsbad, CA, USA). Cell suspension was then transferred in fresh medium containing 10% FBS (which stops the enzymatic digestion reaction) and cells were seeded in new flasks at the concentration of 10x10^{4}cells/cm^2.

2.3.4 Isolation of B lymphocytes from peripheral blood

B lymphocytes were isolated from peripheral blood of 45 CLL patients (Table III) and 11 healthy donors. For CLL patients, a sample of heparinized venous blood was processed with a layering on F/H, as described for the isolation of MSCs from bone marrow aspirates (Section 2.3.2; Figure 17).

In most of the cases, the percentage of leukemic B cells was greater than 90% of PBMCs (peripheral blood mononuclear cells) isolated. When cell population had more than 10% T lymphocytes, further B cell purification was performed.

Untouched normal B cells from healthy donors were isolated using the RosetteSep isolation kit for B cells (STEMCELL Technologies; Vancouver, Canada).

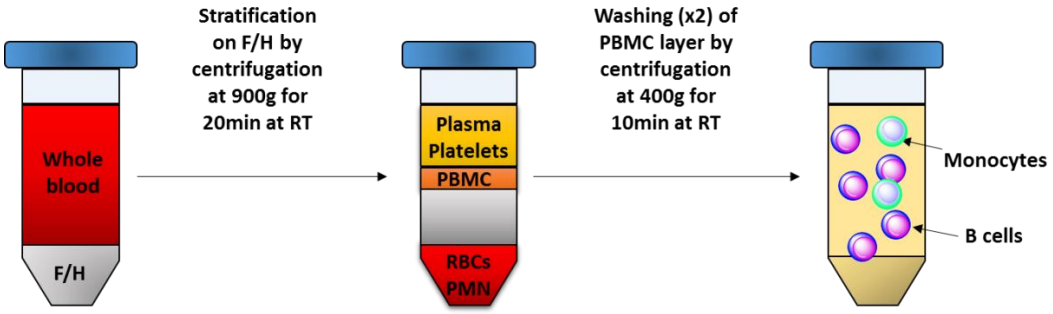

Figure 17. B cell isolation from peripheral blood. Blood components were stratified on Ficoll/Hipaque solution by centrifugation, depending on their density. PBMC layer was collected and cells were washed twice in PBS1X. F/H, Ficoll/Hipaque. RT, room temperature. PBMC, peripheral blood mononuclear cells. RBC, red blood cells. PMN, polymorphonuclear cells.

2.3.4.1 Purification of B lymphocytes using RosetteSep kit

The kit consists of a cocktail of antibodies directed against surface antigens (Ag), expressed by hematopoietic cells (CD2, CD3, CD16, CD36, CD56, CD66b), and glycophorin-A, expressed by red blood cells. This mixture of antibodies binds "not-B" and red blood cells, creating immuno-rosettes. In this way, CD19+ B lymphocytes are isolated from whole blood by negative selection (Figure 18).

Each ml of blood was incubated with 50µl of RosetteSep at room temperature for 20 minutes. The samples were then diluted 1:2 with PBS1X + 2% FBS, gently agitated, and then layered over F/H. We proceeded with a centrifugation at 900g for 30 minutes at room temperature, followed by the collection of the B cells at the F/H interface. Cells were washed in PBS1X + 2% FBS, centrifuged at 400g for 10 minutes, resuspended in PBS1X and counted in a Burker chamber.

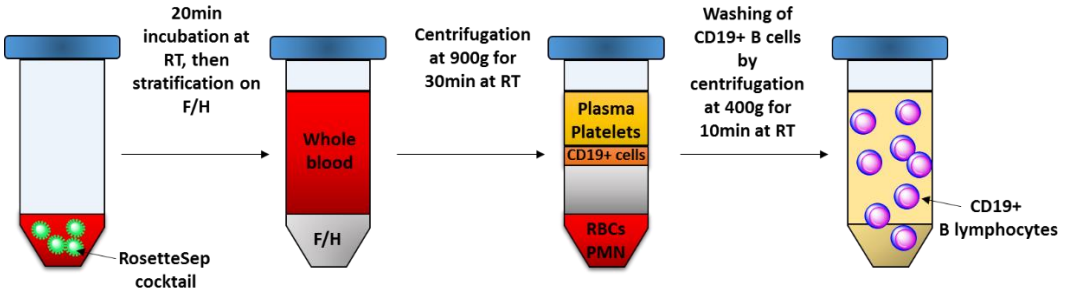

Figure 18. B cell purification by RosetteSep kit. 10ml of whole blood were incubated for 20min at RT with RosetteSep cocktail, to allow the isolation of CD19+ B lymphocytes by negative selection of the other contaminating cell types. CD19+ lymphocyte layer was collected and cells were washed in PBS1X. F/H, Ficoll/Hipaque. RT, room temperature. RBC, red blood cells. PMN, polymorphonuclear cells.

2.3.5 Immunophenotypic characterization of MSCs and CLL cells by flow cytometry

The immunophenotypic analysis on MSCs and lymphocytes obtained from marrow and peripheral blood respectively of CLL patients was performed by flow cytometry. This technique allows a multiparametric evaluation of antigenic characteristics of single cells by the analysis of visible and fluorescent light emitted when they flow through a liquid medium.

The immunophenotype assay is based on the identification of surface and intracellular Ag using monoclonal antibodies (mAbs) conjugated with fluorochromes. The presence of a certain Ag is used as an indicator of the cell type as well as its level of maturation. The fluorochromes used for this thesis were: fluorescein isothiocyanate (FITC), phycoerythrin (PE), PE-Cy5.5 (a tandem conjugate that combines phycoerythrin and the cyanine dye Cy5), allophycocyanin (APC). Samples were analyzed by flow cytometer FACSCanto (Becton Dickinson; Franklin Lakes, NJ).

To evaluate the MSCs phenotype, and so to verify the homogeneity of the population of interest, we tested the negativity for the markers CD14, CD31, CD34 and CD45, and the positivity for the typical mesenchymal markers CD73, CD90 and CD105.

Samples for FACS analysis were prepared as follows:

1) MSCs derived from each primary culture were seeded in 0.4cm^2 surface wells. Once reached confluence (about 1x10^{4}cells per well), MSCs were removed from the bottom of the well by enzymatic digestion with 500µl

Accutase (Sigma-Aldrich; Saint Louis, Mo, USA), which contains proteolytic enzymes and collagenase to break cell-cell interactions but does not degrade MSC surface molecules.

2) Cells were then resuspended in 100µl PBS 1X and stained with saturating concentrations of the following monoclonal antibodies: anti-humanCD14-FITC (BD Biosciences, Franklin Lakes, NJ, USA), anti-CD31-FITC (BD Biosciences), anti-CD34-PE (BD Biosciences), anti-CD90-FITC (Abd Serotech; Oxford, UK), and anti-CD73-PE (BD Biosciences), and 2.5µl of anti-CD45-FITC (Invitrogen; Paisley, UK) and anti-CD105-PE (Invitrogen). After staining, cells were incubated in the dark at room temperature for 13 minutes.
3) A washing step with PBS1X was performed to eliminate the excess of antibody not bound to the surface molecules. Samples were read with FACSCanto (BD Biosciences) and the data obtained were analyzed with Cell Quest program. For each analysis, 20,000 events were acquired.

CLL B cell phenotype was analyzed by flow cytometry in order to identify the proportion of the tumor population in the samples. For each sample, 50µl of whole blood were stained in the dark for 10 minutes at room temperature with saturating concentrations of the following antibodies: anti-CD5-FITC (BD Biosciences), anti-CD16-PE (BD Biosciences), anti-CD19-APC (BD Biosciences), anti-CD3-PE-Cy7 (BD Biosciences) and anti-CD38-PerCP-Cy5.5. Then cells were washed in a 0.15M NH_4Cl solution to lyse red blood cells, and samples were analyzed with FACSCanto.

For the analysis of the adhesion molecule CD49d and chemokine receptor expression on CLL cell surface, $5x10^5$ leukemic B cells were collected from the different culture conditions, washed and resuspended in PBS1X, and stained for 15 minutes in the dark at room temperature with saturating concentrations of anti-CD49d-PE (BD Biosciences), anti-CCR7-FITC (R&D Systems Inc., Minneapolis, MN; USA), anti-CXCR4-PE (R&D Systems Inc.), anti-CXCR3-PE-Cy5.5 (BD Biosciences), anti-CXCR5-FITC (R&D Systems Inc.) and anti-CD19-APC (BD Biosciences). Cells were then washed with 0.15M NH_4Cl and resuspended in PBS1X. 20,000 total events were acquired using FACSCanto, and data were

analyzed by FACSDiva 7 software. For the expression analysis, samples were gated on intact cells depending on the parameters forward scatter (FSC) and side scatter (SSC); a second gate was generated on the CD19+ population, on which the receptor levels were evaluated.

2.3.6 MSC and allogenic B cell co-cultures

B cells obtained from peripheral blood of CLL patients or healthy donors were co-cultured with:

1) MSCs isolated from CLL patients;
2) MSCs isolated from healthy donors, used as a non-pathological control;
3) HS-5 cell line, a human fibroblastoid cell line available from the American Type Culture Collection (ATCC; Manassas, VA, USA), used as a positive control, according to literature data [299].

MSCs were seeded at the concentration of $1x10^5$ onto 12-well plates ($1.2cm^2$ surface) and incubated at 37˚C in a humidified atmosphere and 5% CO_2. For co-culture experiments, B cells were added to MSCs layer at a ratio of 20:1 in complete RPMI medium. The plates were incubated at 37˚C in humidified atmosphere and 5% CO_2, and suspension cells were then collected after 3, 5 and 7 days to evaluate the degree of apoptosis.

In some experiments, CLL B cells were obtained from 10 patients before and after therapy, according to the protocol FLU-Cy (FLU $25mg/m^2$ for 3 days and Cy $350mg/m^2$ for 3 days, every 28 days), which is the standard care for patients who need therapy. For the *in vitro* treatment with FLU and Cy, CLL cells were incubated with 20μM FLU and 5μM Cy (drug concentrations were chosen from previous dose-response experiments [301]).

For experiments where kinase inhibitors were used, cells were treated with 5μM Bafetinib (Selleck Chemicals; Munich, Germany) or 5μM Ibrutinib (Selleck Chemicals) for 1 hour at 37°C and then cultured in presence and absence of MSCs, as previously described in this section. The concentration of inhibitors was chosen according to preliminary experiments with different doses.

In some experiments, HS-5 cell line was employed. $1x10^5$ HS-5 cells were plated in 12-well plates up to confluence and then leukemic B cells were added, as previously described.

In order to assess whether the anti-apoptotic effect of MSCs on CLL B cells was due to soluble factors or to cell-cell contact, experiments with a transwell system (TW) were performed using polycarbonate membranes (Corning Costar; Cambridge, UK) with 0.4μm pores. The usage of transwells prevented physical contact between B lymphocytes and MSCs, but allowed the diffusion of soluble factors secreted by the adherent layers of stromal cells (Figure 19).

Figure 19. Culture conditions of CLL cells and MSCs. In this study, CLL B cells were cultured alone and co-cultured with MSCs in close contact or separated by a porous membrane (transwell system), which prevented the direct contact of the two cell types but allowed the exchange of soluble factors.

2.3.7 SDS-PolyAcrylamide Gel Electrophoresis (SDS-PAGE) and Western Blotting

The western blotting (WB) or immunoblotting is an immunoassay able to detect traces of a specific protein in a heterogeneous mixture, combining the high resolving power of gel electrophoresis with the specificity of the antibodies. WB is a technique with high sensitivity, able to detect quantities of protein in the order of nanograms.

Western blot analysis for CLL B cells undergone to different culture conditions was performed as follows.

2.3.7.1 Cell lysates preparation

For each sample, aliquots of $5x10^5$ B lymphocytes were lysed in 50μl of the following buffer:

- 50mM Tris (hydroxymethyl) aminomethane hydrochloride (Tris-HCl) pH 6.8;

- 5mM Ethylenediaminetetraacetic acid (EDTA);
- 10% glycerol;
- 2% SDS (sodium dodecyl sulphate);
- 1% β-mercaptoethanol;
- Dye (Bromophenol blue or pyronin) (Sigma-Aldrich).

Subsequently, the lysates were vortexed, boiled at 100°C for 5 minutes and then subjected to SDS-PAGE (polyacrylamide gel electrophoresis).

2.3.7.2 Polyacrylamide gel electrophoresis in SDS (SDS-PAGE)

The polyacrylamide gel electrophoresis in SDS is one of the most used methods to separate a mixture of proteins in dependence of their molecular weight. SDS is an ionic detergent that binds tightly to proteins causing their denaturation. In presence of an excess of SDS, approximately 1.4g of detergent will bind to each gram of protein, providing a constant amount of negative charge per unit mass. Therefore, during electrophoresis, all protein-SDS complexes move toward the anode and, thanks to the molecular sieve properties of the gel, their mobility is inversely proportional to their molecular weight. Through the migration of standard proteins of known molecular weight simultaneously to samples, it is possible to determine the weight of the proteins in the samples.

SDS polyacrylamide gel was prepared following Laemmli method [302]. The electrophoretic plate consists of two types of gel:

- *Stacking gel* at pH 6.8, which concentrates the proteins so that they are all aligned at the start of electrophoresis;
- *Running gel* at pH 8.8, in which the real protein separation occurs.

The plate size of 10×8cm was fixed in the Hoefer Mighty Small-If 250 Scientific Instruments machine (Amersham Biosciences). The electrophoresis was run for about 2 hours at 25mA.

2.3.7.3. Western blotting

After SDS-PAGE, proteins were transferred to a nitrocellulose membrane by application of an electric field, obtained supplying current at 350mA for 2 hours and 30 minutes. The buffer used for the transfer contained 25mM Tris,

192mM glycine, 20% methanol and 0.1% SDS and had a final pH of 8.0 (buffer A). After the transfer, the membrane was blocked overnight to prevent non-specific background binding of the primary and secondary antibodies. The blocking buffer consisted of 50mM Tris-HCl, pH 7.5, 150mM NaCl and 5% bovine serum albumin (BSA) (buffer B), important for nonspecific sites saturation. Membranes were then incubated for 2 hours and 30 minutes at RT with primary Abs diluted in 50mM Tris-HCl, pH 7.5, 150mM NaCl, 1% BSA (buffer C).

For our study, the following antibodies were used: polyclonal anti-LYN (Santa Cruz Biotechnology; Santa Cruz, CA, USA), anti-LYN-Tyr396 (Epitomics; Burlingame, CA, USA), anti-ERK (Cell Signaling Technology), anti-ERK-Thr202/Tyr204 (Cell Signaling Technology), anti-PARP (Cell Signaling Technology), and anti-β-actin (Sigma-Aldrich).

Three washes of 10 minutes each at RT were subsequently performed, using buffer C supplemented with 0.1% Tween. Membranes were then incubated for 1 hour with a secondary anti-IgG Ab, obtained against the animal species immunized for the primary Ab and conjugated with horseradish peroxidase (Amersham Biosciences), diluted in buffer C. After three additional washes, proteins were detected on the membranes using the enhanced ChemiLuminescence system (ECL) (Pierce; Waltham, MA, USA). The contact of the peroxidase and the Ag-Ab complex gives rise to an oxidation reaction with light emission that is captured by the imager machine (LAS500, GE Healthcare; Buckingamshire, UK). The densitometric analysis of the bands obtained was performed using the Image J program.

2.3.8 Apoptosis analysis by flow cytometry

Apoptosis of leukemic and normal B cells was assessed by staining with Annexin V-FITC (Apoptosis detection kit; Immunostep; Salamanca, Spain), according to manufacturer's instructions.

During the early stages of apoptosis the plasma membrane undergoes profound changes that indicate the status of apoptotic cells to macrophages, which ensure its elimination. In particular, phosphatidylserine (PS), a negatively charged aminophospholipid normally expressed only in the inner side of the plasma

membrane, is exposed on the outer surface. Annexin V is a protein that, in presence of high concentrations of Ca^{2+}, recognizes and binds selectively PS, making it useful for the identification of apoptotic cells that expose the phospholipid on their surface.

According to the experiments, after 3, 5 and 7 days of single culture or co-culture in direct or indirect (TW) contact with MSCs or HS-5 cells, B cells were harvested, washed, and incubated for 10 minutes in the dark and at RT with: 100µl of binding buffer (a Ca^{2+}-rich solution that optimizes the binding of Annexin V to the PS), 5µl of Annexin V-FITC, and 10µl of Propidium iodide (PI), provided by the kit (1µl/ml final concentration). After the incubation, 100µl of binding buffer were added and cell viability was analyzed by flow cytometry. For each sample, 20.000 events were acquired and the number of apoptotic cells was expressed as percentage of Annexin V positive cells in the total cells analyzed.

2.3.9 Chemotaxis assay

To assess the ability of the cells to respond to chemoattractant stimuli coming from the microenvironment, chemotaxis assay for CLL B cells was performed in presence of MSC-conditioned medium (MSC-CM) using 12-well Corning chemotaxis chamber (Corning Life Sciences; Acton, MA, USA).

To obtain MSC-CM, MSCs were cultured for 48h in complete RPMI-1640 at 37°C, 5% CO_2. $2.5x10^6$ cells were incubated in 0.5ml RPMI medium for 1 hour at 37°C before the assay with and without the kinase inhibitors. Cells were then transferred into the top chambers of transwell culture inserts of 3µm pore size, which were placed into wells containing complete RPMI medium or MSC-CM. Cells in the upper chamber were allowed to migrate for 3 hours at 37°C. Cells migrated in the lower chamber were then collected and counted at the flow cytometer for 60 seconds in triplicates. Depending on the number of cells counted and on the volume of cell suspension aspired by the machine we could define the number of cells migrated through the TW membrane.

2.3.10 Multiplex cytokine analysis

Cyotkines are typically measured by bioassays or immunoassays. The application of technologies based on the use of fluorescent beads has allowed the identification of multiple analytes in a single biological sample. In this study, the Bio-Plex ProTM Assays (Bio-Rad; Hercules, CA, USA) was used to allow the simultaneous quantification of 27 different cytokines/chemokines in media from single cultures of MSCs, CLL B cells, normal B cells, and from co-cultures of MSCs and leukemic lymphocytes. The tested cytokines were: IL-1β, IL-1ra, IL-2, IL-4, IL-5, IL-6, IL-7, IL-8 (CXCL18), IL-9, IL-10, IL-12 (p70), IL-13, IL-15, IL-17, IFN-γ, TNF-α, G-CSF, GM-CSF, Eotaxin (CCL11), MCP-1 (CCL2), MIP-1α (CCL3), MIP-1β (CCL4), Rantes (CCL5), CXCL10 (IP-10), PDGF, basic-FGF e VEGF. The Bio-Plex suspension array system is based on a flow cytometry principle that utilizes the Luminex xMAP detection technology and uses up to 100 different color-coded polystyrene microbeads (5.6μm diameter), each one conjugated with an antibody specific for different target molecules. The antibody-coupled beads will react with an unknown amount of cytokine, or with a standard solution that instead contains a known amount of cytokine. The cytokine is then recognized and bound by a biotinylated secondary antibody, which is added afterwards in the process (Figure 20). It follows that the antibodies form a sandwich around the cytokine, and the reaction mixture is then detected by addition of streptavidin-phycoerythrin (streptavidin-PE), which binds the biotinylated antibodies. Thus, the flow-based Bio-Plex suspension array system can identify and quantify each specific reaction based on bead color and fluorescence. The advantage of this technique over the other immunoassays is the ability to have a complete cytokine profile from each sample, reducing the preparation time and the amount of sample required (12.5μl of serum or 50μl of tissue culture sample), and increasing the throughput.

The cytokine quantification was carried out by the CRIBI (Centro Ricerche Interdipartimentale Biotecnologie Innovative) at the University of Padua. The samples were prepared as follows:

1) Culture media were centrifuged at 3000g for 10 minutes at 4°C, to precipitate debris that can compromise the quantification (by occlusion of the fluidic system);

2) The standard curve was obtained with serial dilution of the reagent supplied by the kit, according to the manufacturer's instructions;
3) 50µl per well of the microbead solution were loaded in a 96-well filter-plate, then two washes and vacuum filtering were performed;
4) 50 µl of standard or samples were loaded per well in the filter-plate and incubated for 30 minutes at room temperature (samples were loaded in duplicate);
5) Wells were then washed 3 times with 100µl washing buffer, removed each time by vacuum filtering;
6) 25µl of secondary antibody were added in each well and incubated at room temperature for 30 minutes (the antibody dilution was chosen according to the manufacturer's instructions);
7) Wells were washed 3 times with 100µl washing buffer as previously described;
8) After the last wash, 50µl of streptavidine-PE diluted as kit's instructions were added in each well and the plate was incubated for 10 minutes at room temperature;
9) Wells were then washed 3 times with 100µl washing buffer and filtered;
10) The beads in each well were resuspended in 125µl of Bio-Plex assay buffer and shaked for 30 seconds at 1100rpm immediately before reading the plate on the Bio-Plex system (Bio-Rad).

The data analysis was performed with the Bio-Plex Manager 5.0 software (Bio-Rad). The results were expressed as Median Fluorescence Intensity (MFI) as well as concentration (pg/ml) for each class of microbeads. All signals were normalized removing the fluorescence of the blank. Standard curves were calculated with a regression model at 5 parameters. Cytokine concentrations were obtained through interpolation of the standard curve fluorescence values, corrected considering the dilution factor, and expressed as pg/ml.

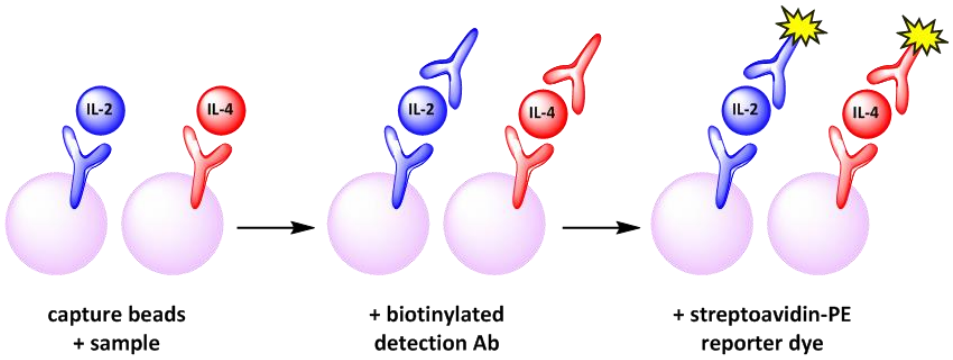

Figure 20. Bio-Plex functioning principle. Each microbead is conjugated with an anti-cytokine antibody. The complex Ag-Ab is detected by a secondary antibody conjugated with a fluorochrome. The micro-complexes are aspired and excited by 2 lasers: the first one recognizes the microbead and so the analyte identified by the primary antibody to which it is conjugated; the second laser quantifies the analyte, exciting the fluorochrome bound to the secondary antibody.

2.3.11 ELISA assay

The ELISA assay (Enzyme-Linked Immunoabsorbent Assay) is a technique designed for the quantification of analytes (usually peptides, cyto/chemokines and antibodies) present in a solution.

The Human CXCL10/IP-10 Quantikine ELISA kit (R&D Systems Europe Ltd.; Abingdon, UK) was used to quantify the chemokine CXCL10 in the culture medium of MSCs, CLL cells, normal B cells, and in the co-cultures of MSCs and CLL cells or MSCs and normal B cells, according to the manufacturer's instructions. Each sample was done in duplicate.

Before performing the assay, the reagents were properly prepared, as from the kit instructions. The Wash Buffer reagent for the test was obtained by dilution of 20ml Wash Buffer Concentrate in 500ml of deionized water. The Substrate Solution was prepared 15 minutes before use by mixing Color Reagents A and B, and it was kept in the dark. CXCL10 standard was reconstituted from the stock solution to a final concentration of 5,000pg/ml and was kept in gentle agitation for a least 15 minutes before use. Once ready, serial dilutions of the standard were prepared in 900µl Calibrator Diluent RD5K, from a higher concentration of 500pg/ml to a lower concentration (7.8pg/ml), to obtain the standard curve needed for the determination of CXCL10 concentration in the different samples. The dilution in Calibrator Diluent RD5K was 1:3 for the supernatants from MSC and CLL B cell single-cultures, 1:15 and 1:30 for the co-culture media. This dilution

allows the quantification of the chemokine in the range of values determined by the standard curve.

150µl of Assay Diluent RD1-56 were added in each well of a 96-well plate pre-coated with the capture antibody for CXCL10. Then, 100µl of samples, controls and Standards were added to the respective wells. The plate was incubated for 2 hours in the dark at room temperature to allow the binding of the capture antibody immobilized on the solid surface of the plate to the chemokine CXCL10, if present in the samples. After the incubation, the content of each well was removed by aspiration and the plate was washed three times with 400µl Wash Buffer, in order to wash away all the unbound reagent. Subsequently, 200µl of CXCL10 Coniugate were added to each well, and the plate was incubated at room temperature for 2 hours. The Coniugate solution contains the HRP-labelled detection antibody for CXCL10, which allows the detection of the amount of antigen bound to the capture antibody. The wells were then washed as previously described, 200µl of Substrate Solution were added to each well and let incubate in the dark for 30 minutes at room temperature. The Substrate Solution contains tetramethylbenzidine (TMB), substrate for the HRP, so that the more CXCL10 is present in the samples, the more reaction with the substrate will occur. During this reaction, blue coloration of the solution is developed in proportion to the amount of cytokine present in the sample. 50µl of Stop Solution were then added to the wells and the optical density was read at the wavelength of 450nm within the next 30 minutes. The standard curve was obtained plotting in a graph the absorbance mean of each standard sample versus the respective CXCL10 known concentration.

2.3.12 Migration assay of CLL cells beneath MSC layers (pseudoemperipolesis)

Pseudoemperipolesis is an *in vitro* phenomenon whereby CLL cells spontaneously migrate beneath marrow stromal cells layers, mimicking the migration and homing of leukemic cells that occurs in the tissues [186].

MSCs were seeded onto 12-well plates in complete RPMI medium up to confluence. CLL cells were suspended to a final concentration of $2x10^6$ cells/ml

in complete RPMI medium with or without 5μM Bafetinib or 5μM Ibrutinib, and were incubated for 1 hour at 37°C in 5% CO_2. After incubation, CLL cells were added to the MSC-coated wells and the plates were incubated at 37°C in 5% CO_2 overnight. Cells that had not migrated beneath stromal cells were removed by washing 3 times with medium. The MSC layer containing transmigrated CLL cells was collected after treatment with Accutase, used to gently remove the adherent cells. Staining with anti-CD19 APC was performed to discriminate CLL cells from MSCs, and the proportion of cells that undergone pseudoemperipolesis was analyzed by flow cytometer FACSCanto.

2.3.13 Statistical analysis

Statistical analysis was performed using Student's *t* test, paired Student's *t* test, Fisher's exact test and ANOVA test when appropriate. Data were expressed as mean ± standard deviation (SD) and were considered statistically significant when p values were ≤0.05.

2.4 Results

2.4.1 MSC isolation and expansion

In this study, 46 samples of marrow blood isolated from CLL patients were processed, and the BMMCs obtained were seeded at a density of 1,000 cells/cm^2. The initial adhesion of round-shaped cells to the flask surface was observed 48 hours after seeding. After 7 days, the suspension containing debris and non-adherent cells was replaced by fresh medium, in order to support the growth of the adherent cell fraction, which showed spindle-shape and fibroblast-like morphology. At day 14 of *in vitro* culture, foci containing highly proliferating cells were observed, while confluence was achieved after 30/40 days (Figure 21). All cultures maintained a homogeneous morphology and an undifferentiated status during *in vitro* passages.

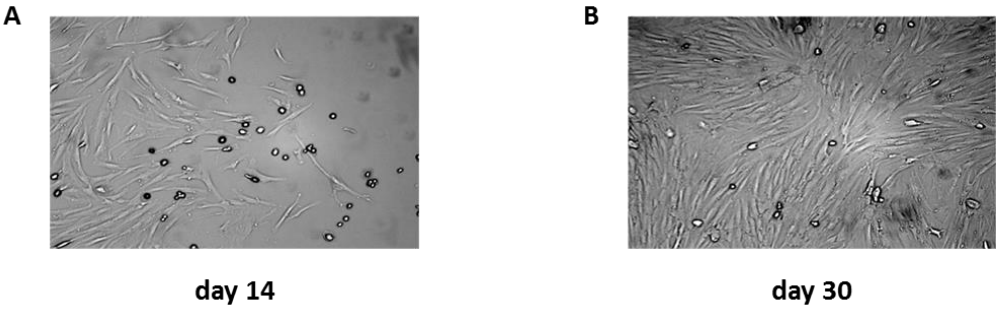

Figure 21. MSC expansion *in vitro*. After isolation from bone marrow aspirates, mononuclear cells were seeded in flasks, and cultures of MSCs were obtained by plastic adhesion. **A)** After about 14 days, cells grouped in *loci* with high proliferative capacity were observed. **B)** Confluence was achieved after 30 days of culture (10X magnification, Olympus BX60).

2.4.2 MSC phenotypic characterization

To assess the nature and the homogeneity of the expanded cell population, MSC immunophenotype was analyzed. Since there is no evidence of one marker specific for MSC identification, different markers were considered in order to characterize the population. MSCs showed positivity for CD105, CD73 and CD90, and negativity for hematopoietic antigens like CD14, CD34 and CD45, and for the endothelial marker CD31 (Figure 22). Thus, MSCs from CLL patients used in this study displayed a phenotypic profile similar to the one expected from MSCs of

normal subjects, confirming the selection of a homogeneous population of non-hematopoietic origin.

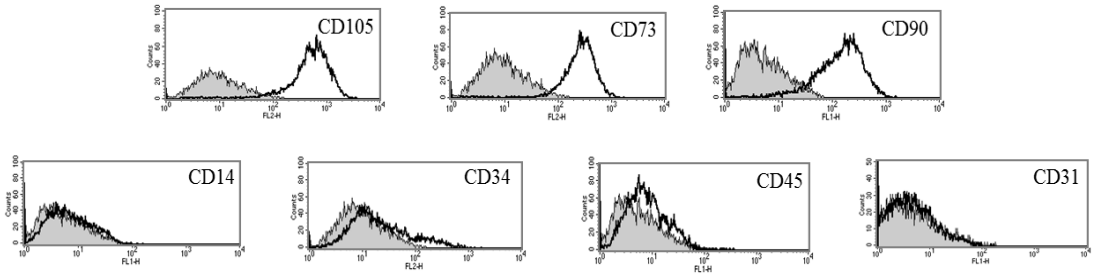

Figure 22. MSC phenotypic characterisation. Representative case of MSC immunophenotype analyzed by flow cytometry. In the upper line is shown the positivity for CD105, CD73 and CD90, in the bottom line the negativity for CD14, CD34, CD45 and CD31.

2.4.3 Effect of MSCs on CLL and normal B lymphocyte apoptosis

2.4.3.1 MSCs support CLL B cell survival *in vitro*

Since in the bone marrow the leukemic clone interacts with the mesenchymal population, we investigated the role played by MSCs on CLL cell survival. The effect of the stromal population was tested on B cells obtained from 30 CLL patients and from 11 healthy donors. Normal and pathological B cells were cultured alone or in contact with a confluent layer of MSCs or HS-5 stromal cells (20:1 ratio). Levels of apoptosis were evaluated at time zero and after 3, 5 and 7 days of culture by Annexin V staining, considering viable cells as the proportion of Annexin V negative events acquired by the flow cytometer. As shown in Figure 23, CLL B cells cultured in medium alone progressively underwent apoptosis *in vitro* (the percentage of viability after 7 days of culture was 13.3%±13.2%), confirming literature data [299]. The presence of a monolayer of MSCs isolated from CLL patients rescued malignant cells from apoptosis, as shown by the percentage of Annexin V negative cells (59.2%±17.1% after 7 days; $p<0.0001$).

In single-culture, normal B cells showed more rapid spontaneous apoptosis then CLL B lymphocytes; in fact, at day 3, viability levels were 19.6%±12.0% for normal B cells *vs* 48.9%±19.5% of CLL cells. At day 7 of culture, survival of normal B cells was 6.7%±4.3% in medium alone; the presence of MSCs in the culture system increased cell viability (34.9%±15.7%), and the recover from

apoptosis was significant (p<0.01) even if lower than the one found in the MSC/CLL B cell co-culture. These data suggest that MSCs exert a major protective effect on malignant B cells.

In addition, HS-5 stromal cells showed a significant protective effect on both CLL and normal B-lymphocytes, with viability levels of 45.9%±15.4% and 44.6±5.3% after 7 days of culture, respectively. However, MSCs displayed a higher protective effect with respect to the human stromal cell line HS-5 (59.2%±17.1% with MSCs *vs* 45.9%±15.4% with HS-5; p<0.01).

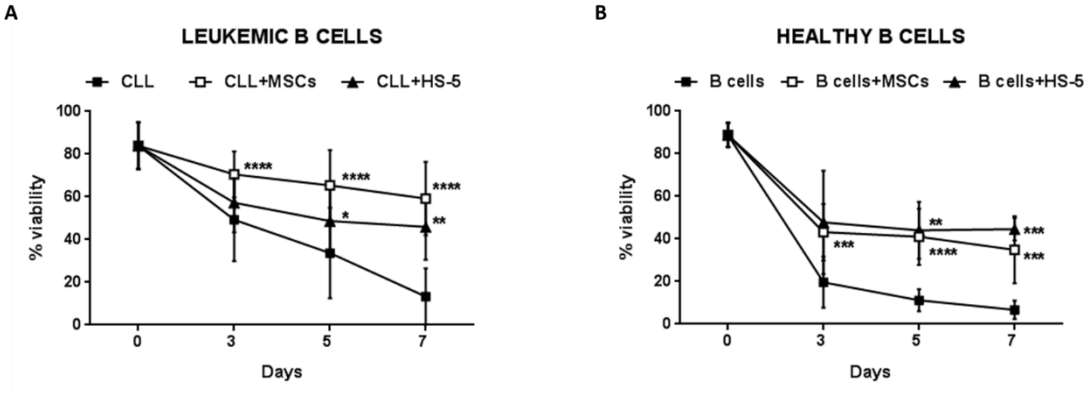

Figure 23. MSCs protect CLL and normal B cells from spontaneous apoptosis *in vitro*. A) Survival of CLL B cells cultured alone (n=30), with MSCs (n=30), or with HS-5 (n=16). **B)** Survival of B cells from healthy donors cultured alone (n=11), with MSCs (n=11), or with HS-5 (n=5). Viability was measured at day 0, 3, 5 and 7 of culture by Annexin V staining. Data are shown as mean ± standard deviation; paired Student's t test was used; *p<0.05, **p<0.01, ***p<0.001, ****p<0.0001.

2.4.3.2 Malignant clones show different responses to MSC pro-survival signals

The results obtained with the Annexin V technique were validated through western blot analysis of the protein PARP, in particular of its 89kDa cleaved form, which is an index of late apoptosis. As shown in Figure 24A, the increased survival rate of CLL B cells cultured in presence of MSCs was confirmed by the absence of the cleaved-PARP band, also after 7 days of culture. Conversely, normal B cells showed a band relative to the cleaved form of PARP both when alone and in co-culture condition, suggesting the presence of apoptotic cells and so a failed rescue from apoptosis (Figure 24B). In addition, in the western blot analysis of B cells co-cultured with HS-5 stromal cells, the presence of cleaved

PARP showed less ability of HS-5 rather than MSCs to protect from apoptosis (Figure 24C-D), confirming flow cytometry results, and suggesting a homogeneous response to pro-survival stimuli produced by HS-5 stromal cells.

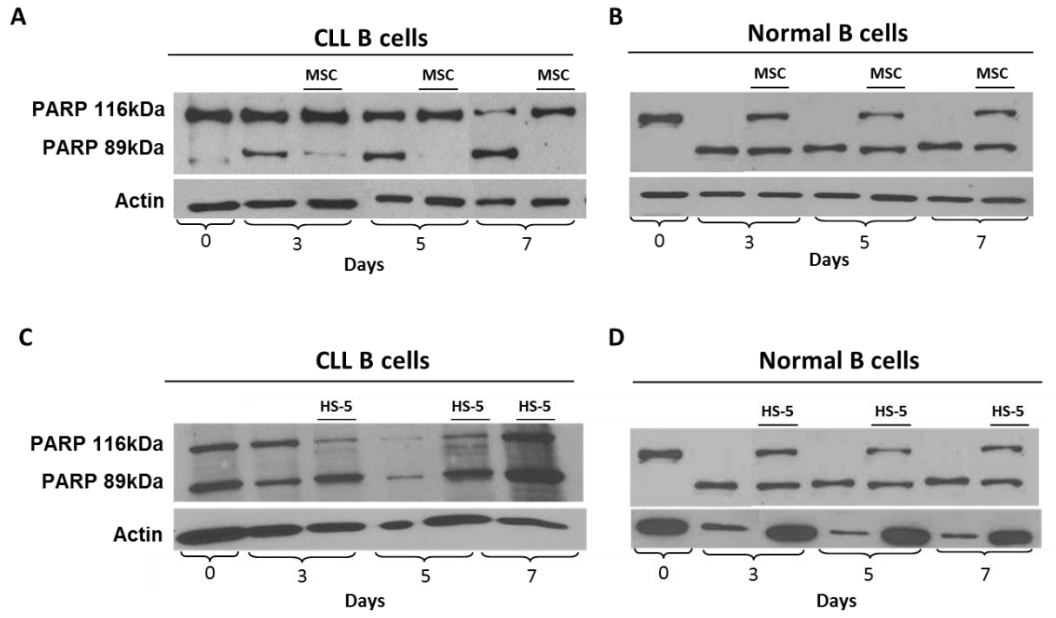

Figure 24. Analysis of lymphocytes viability *in vitro* by western blotting in presence of MSCs or HS-5 stromal cells. CLL B cells **(A)** and normal B cells **(B)** cultured alone and in presence of MSCs; CLL B cells **(C)** and normal B cells **(D)** cultured alone and in presence of stromal cells (HS-5). The figure reports a representative case for each condition. Actin was used as loading control.

However, in this study, an heterogeneous behavior of CLL clones was found during MSC/CLL B cell co-cultures; in particular, lymphocytes derived from different patients in presence of MSCs showed different responses in terms of viability *in vitro* (Figure 25A). For a better understanding of this behavior, PARP cleavage pattern of 27 CLL patient samples was evaluated after 7 days of culture with and without MSCs. Depending on the presence of the cleaved form of PARP, B lymphocytes of 15 patients showed apoptosis when cultured in medium alone, result that was reverted by the presence of MSCs (Figure 25B). This group of patients was defined as "dependent" from the microenvironment, because of the high rate of apoptosis in absence of stromal stimuli. The remaining 12 patients composed the group of the "independent" cases, for which the addition of MSCs to the culture system condition did not affect clone viability, as shown by the absence of cleaved PARP in both alone and co-culture condition (Figure 25C).

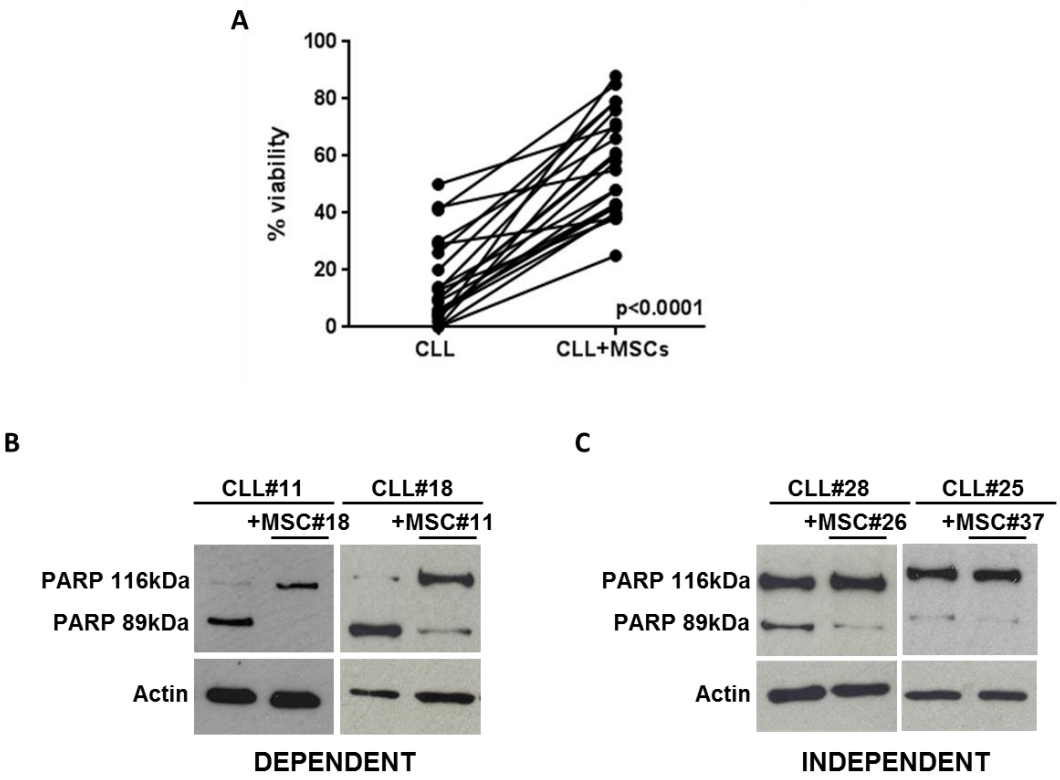

Figure 25. CLL B cell viability after 7 days of co-culture with MSCs. A) CLL B cell viability was assessed by flow cytometry using Annexin V staining. The data showed a high heterogeneity in response to MSC pro-survival stimuli. Student's paired *t* test was used. **B-C)** Representative cases of leukemic B cells obtained from CLL patients (CLL#) co-cultured with MSC (MSC#) analyzed by western blotting. **B)** CLL clones (*n*=15) showed the PARP cleavage after 7 days of single-culture, while full length protein was observed in co-culture with MSCs. These clones were classified as dependent from the microenvironment. **C)** CLL clones (*n*=12) showed the same full length PARP pattern after 7 days of culture alone and in presence of MSCs. This group of patients was classified as independent from the microenvironment.

Because of the allogeneic condition of co-culture experiments, clone viability was tested in presence of MSCs derived from different patients, in order to verify whether the behavior of neoplastic lymphocytes was due to intrinsic features of stromal cells. As shown in Figure 26A, no differences were observed using different MSCs for co-cultures with the same CLL clone; in fact, CLL B cells showed the same PARP pattern in all conditions. Conversely, different CLL clones exhibited different PARP cleavage pattern in presence of the same MSC line (Figure 26B). These data suggest that the heterogeneous behavior of CLL cells is not due to particular MSC features, but to intrinsic characteristics of the different clones.

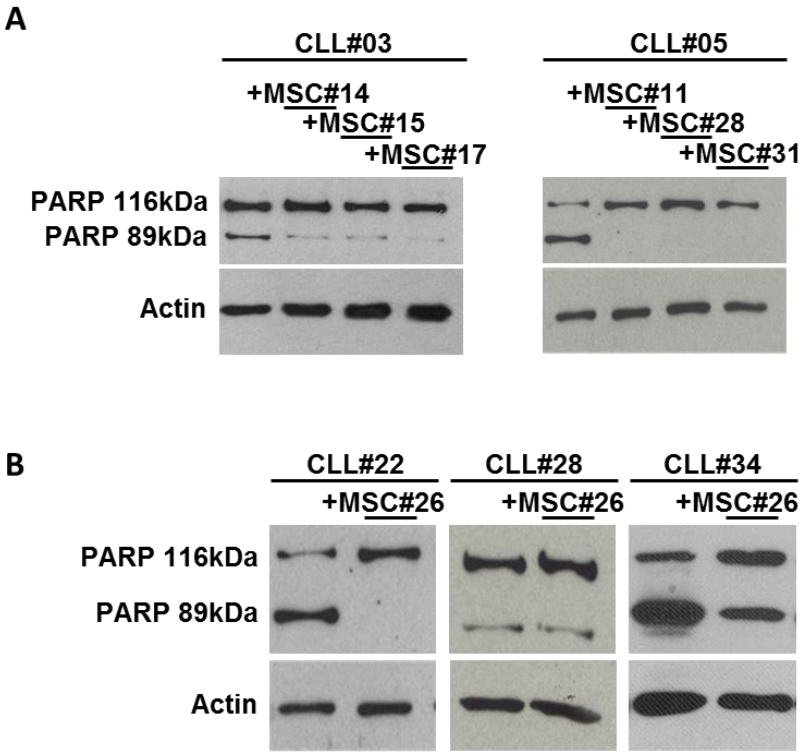

Figure 26. CLL B cell viability after 7 days of co-culture with MSCs depends on leukemic clone intrinsic features. CLL B cell viability was assessed by western blotting. **A)** Representative cases of CLL B cells (CLL#) co-cultured with MSCs (MSC#) derived from different patients showed that the clone behavior does not change using different MSC lines. **B)** Representative cases of CLL B cells (CLL#) co-cultured with the same MSC line (MSC#) demonstrated that CLL behavior depends on intrinsic features of neoplastic lymphocytes. Actin was used as loading control.

Finally, the different behavior of the dependent and independent group was correlated with the most common prognostic factors in CLL: IGHV mutational status, CD38 expression, ZAP70 expression, and genomic aberrations (del13q, del11q, del17p and trisomy 12). No significant correlation was observed between the two groups of patients for the different markers (Figure 27).

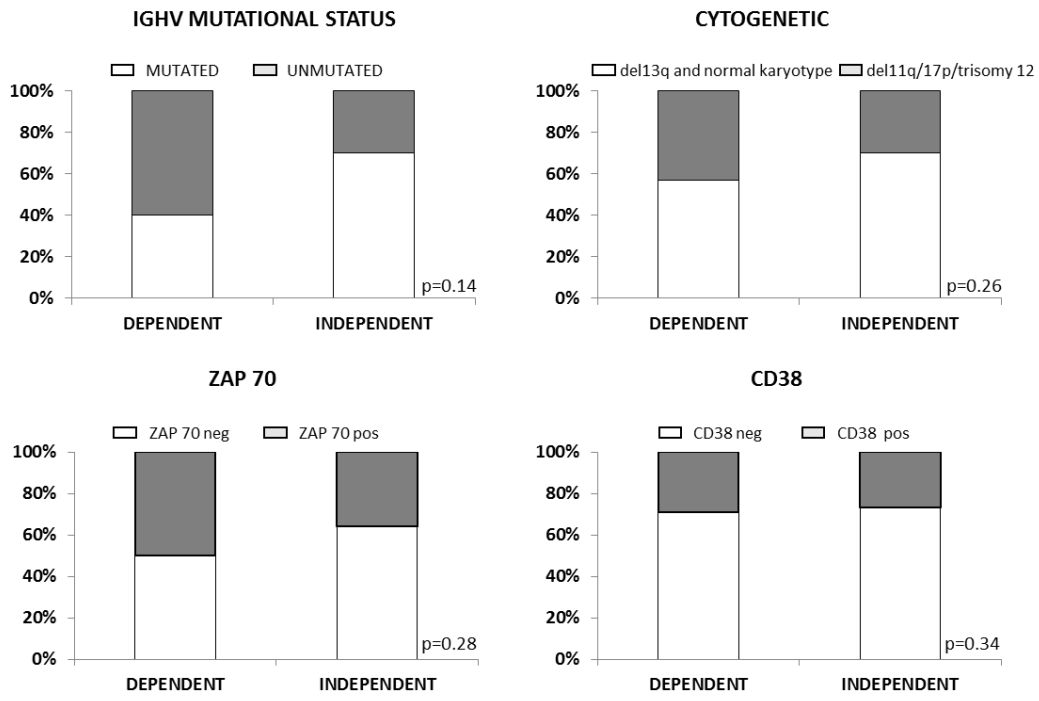

Figure 27. Correlation between PARP cleavage pattern and CLL prognostic markers. Data obtained from western blot analysis of PARP pattern in dependent and independent groups of patients were correlated to the CLL prognostic markers IGHV mutational status, cytogenetic aberrations, ZAP70 and CD38 expression. No correlation was found in any case. Fisher's exact test was used.

2.4.4 MSCs influence CLL lymphocyte behavior through release of soluble factors and cell-cell contact

In order to assess the role played by MSCs in prevention of CLL cell apoptosis through release of soluble factors and cell-cell contact, CLL B lymphocytes from 12 patients were cultured on a MSC layer in close contact or separated by a porous support (transwell system, TW). By the use of a polycarbonate membrane with 0.4 μm pores, the TW system permits the physical separation of the two cellular populations, still allowing the exchange of soluble factors between the compartments. After 7 days of culture, cell viability observed in the two conditions, direct cell-cell contact and TW system, was 61.5%±18.3% and 47.5%±7.8% (p=0.07), respectively (Figure 28). The not significant difference between the two conditions indicates that both cell-cell contact and soluble factor release by MSCs play a role in induction of the anti-apoptotic effect on neoplastic B cells.

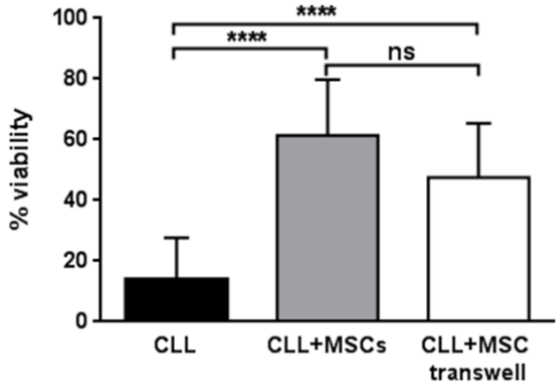

Figure 28. Effect of MSC direct contact and soluble factor release on CLL cell viability. Viability of CLL cells (*n*=12) cultured alone (CLL), with MSCs in direct contact (CLL+MSCs) or with MSCs separated by a 0.4μm TW system (CLL+MSC transwell) was assessed after 7 days of culture by flow cytometry using Annexin V staining. Data are presented as mean ± standard deviation. Student's paired *t* test was used; ****$p<0.0001$.

To further investigate the influence of MSCs on tumor lymphocyte behavior, CLL B cells were allowed to migrate in a 3μm TW system in presence of MSC medium alone or MSC-conditioned medium (MSC-CM). As shown in Figure 29, MSC-CM significantly increased CLL B cell migration through the TW membrane (651±543 migrated cells in medium alone *vs* 2,809±1,318 migrated cells in MSC-CM, $p<0.0001$). The data suggest that the soluble factors released by MSCs promote not only CLL cell survival, but also tumor cell migration.

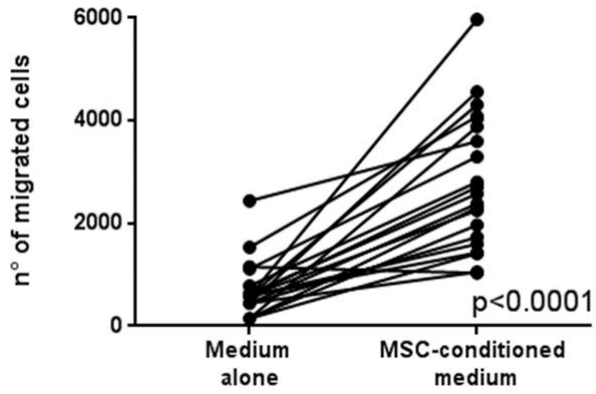

Figure 29. MSC-conditioned medium favors CLL cell migration. CLL B cells (*n*=21) were allowed to migrate through a 3μm pores TW system in medium alone or in MSC-conditioned medium for 3h. CLL cell migration in presence of MSC-CM resulted significantly increased than in medium alone. The number of migrated cells was analyzed by flow cytometry. Student's paired *t* test was used; ****$p<0.0001$.

2.4.5 CLL B cells modulate MSC cytokine secretion profile

In order to draw a profile of cytokines and chemokines that are released in the culture medium during CLL B cell and MSC co-culture, and to identify the soluble factors involved in the pro-survival effect exerted on CLL B cells, a multiplex cytokine analysis was performed using the Bio-Plex suspension array system. Cell suspensions obtained following culture of CLL B cells alone, MSCs alone and co-culture of the two cell populations were tested for the presence of a total of 27 cytokines/chemokines. The analysis of the secretoma of MSCs cultured alone showed elevate concentrations of IL-6, IL-8, G-CSF, GM-CSF, CCL2 and VEGF in the medium (Figure 30A). In the supernatants of CLL B cells cultured alone, the most highly secreted cytokines/chemokines were: IL-6, IL-8, CCL2, CCL4 and CCL5 (Figure 30B). MSC/CLL B cell co-culture induced an increase (expressed as Fold Induction, FI) of most of the tested cytokines/chemokines *in vitro*. In particular, the molecules IL-8, CCL4, CCL11 and CXCL10 resulted up-regulated after normalization of their concentrations on values obtained from both supernatants of MSCs cultured alone (IL-8 10.6 FI, CCL4 148.6 FI, CCL11 6.7 FI and CXCL10 49.7 FI, Figure 30C) and supernatants of CLL B cells alone (IL-8 5.8 FI, CCL4 1.8 FI, CCL11 6.9 FI and CXCL10 4,411 FI, Figure 30D).

To further characterize the role of the four most up-regulated molecules in the co-culture experiments, the levels of cytokine release were also tested on normal B cells. Interestingly, IL-8, CCL4 and CCL11 reached similar levels in co-cultures of MSC/leukemic B cells and MSC/normal B cells *in vitro* (Figure 31A). Conversely, CXCL10 was up-regulated only in co-cultures between MSCs and tumor B cells (Figure 31B). To confirm Bio-Plex results, ELISA assay for the chemokine CXCL10 was performed on supernatants obtained from MSCs, CLL B cells, normal B cells and co-cultures of MSCs and the two lymphocytic populations after 7 days of culture (Figure 31C). The data indicate that the co-culture of CLL B cells and MSCs induces the production of higher amounts of CXCL10 than the co-culture with normal B cells (247.5±240 *vs* 1.5±2 pg/ml; $p<0.01$), suggesting an involvement of this chemokine in the CLL pathological process.

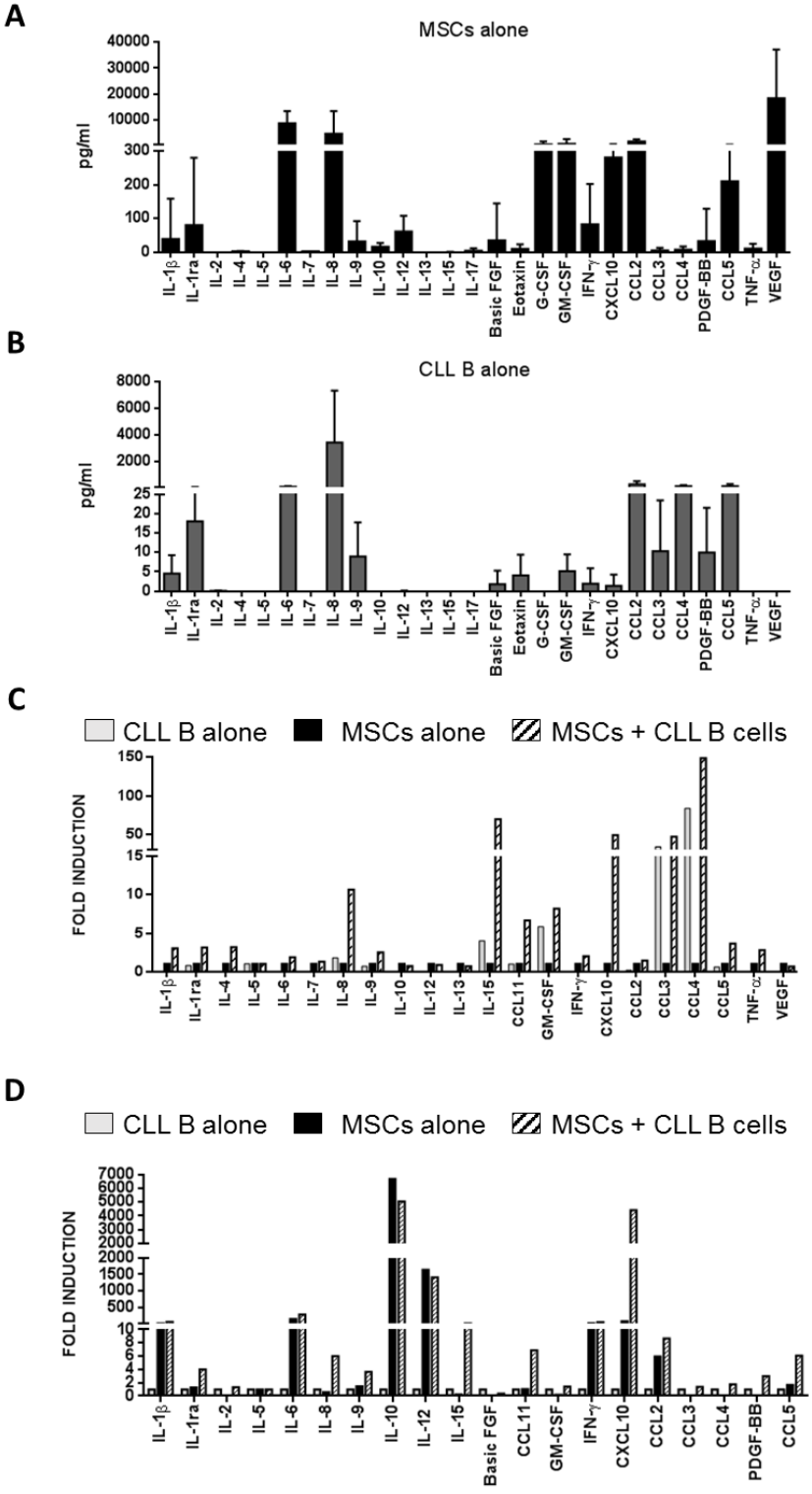

Figure 30. Cytokine/chemokine secretion profile of MSCs and CLL B cells. MSCs **(A)** and CLL B cells **(B)** were cultured in medium alone for 7 days and the levels of released soluble factors were assessed by Bio-Plex (n=11). Data are presented as mean ± standard deviation of the concentration in pg/ml. **(C-D)** MSCs and CLL B cells (n=4) were cultured in direct contact in complete media for 7 days. The cytokine/chemokine levels quantified in the co-culture system were normalized on the levels observed in the MSCs alone **(C)** and CLL B cells alone **(D)** culture media. Data are expressed as fold induction.

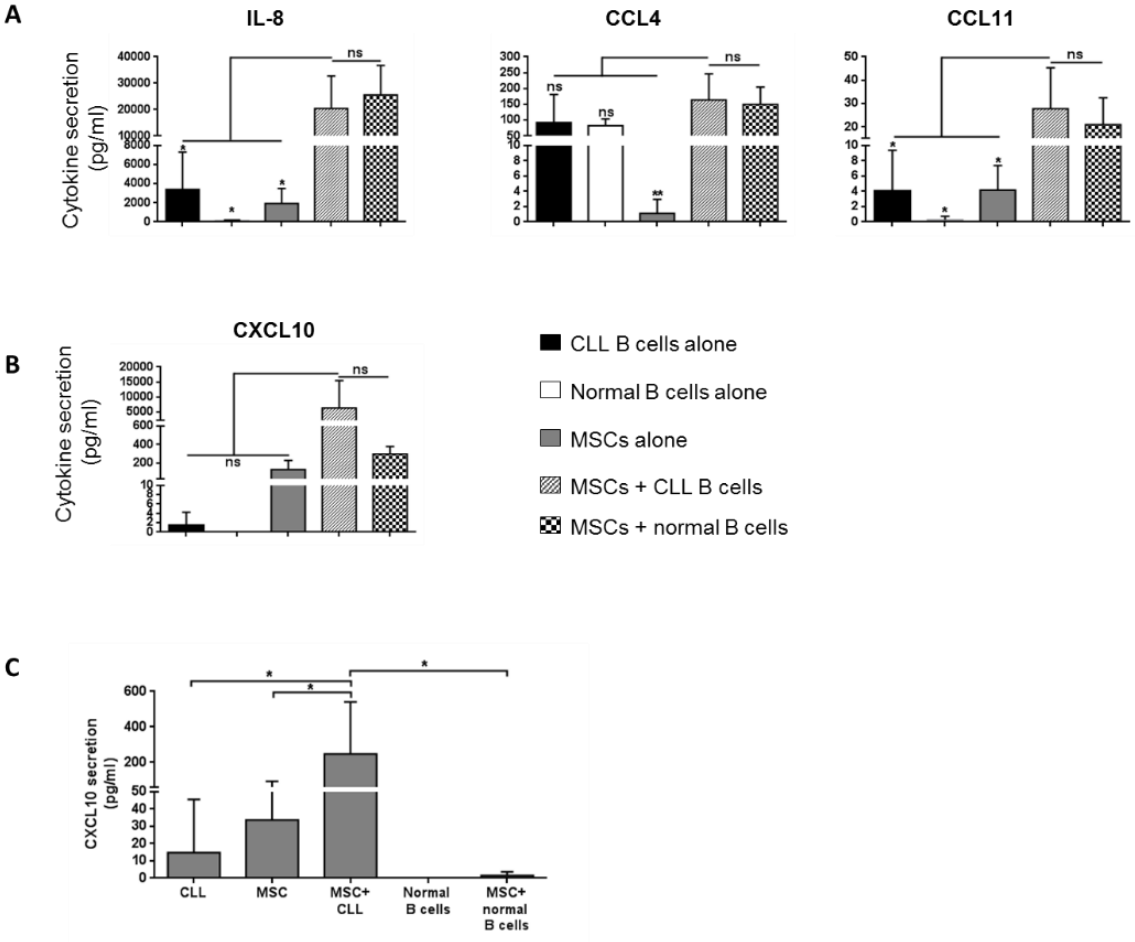

Figure 31. Modulation of soluble factor release in different *in vitro* culture conditions. A-B) Quantification of supernatants obtained from MSC, CLL B cell and normal B cell culture alone, and from co-cultures of MSCs and CLL B cells or normal B cells. IL-8, CCL4 and CCL11 concentrations were similar in the two co-culture conditions (MSC + CLL B cells and MSCs + normal B cells), and higher than in the single-cultures examined (MSC, CLL and normal B cells; *p<0.05, **p<0.01) **(A)**. CXCL10 production was increased only in the co-cultures of MSCs and CLL B cells **(B)**. **C)** B cells from CLL patients (n=7) and healthy donors (n=3) were cultured with and without MSCs for 7 days (n=7) and quantification of CXCL10 chemokine concentration in culture supernatants was performed by ELISA assay. ANOVA test was used; *p<0.05.

Moreover, to assess how MSC soluble factors could influence CLL lymphocyte production of cytokines and chemokines, the Bio-Plex analysis was performed on supernatants obtained from cultures of CLL B cells with MSC-conditioned medium (MSC-CM). As shown in Figure 32, MSC-CM induced an increase in the production of different molecules, such as IL-8 (27.4 FI), CCL4 (149 FI), CXCL10 (40 FI) and CCL5 (9.9 FI). These data suggest that, also in the case of secretoma modulation, both cell-cell contact and soluble factor release play an important role in influencing tumor cell behavior.

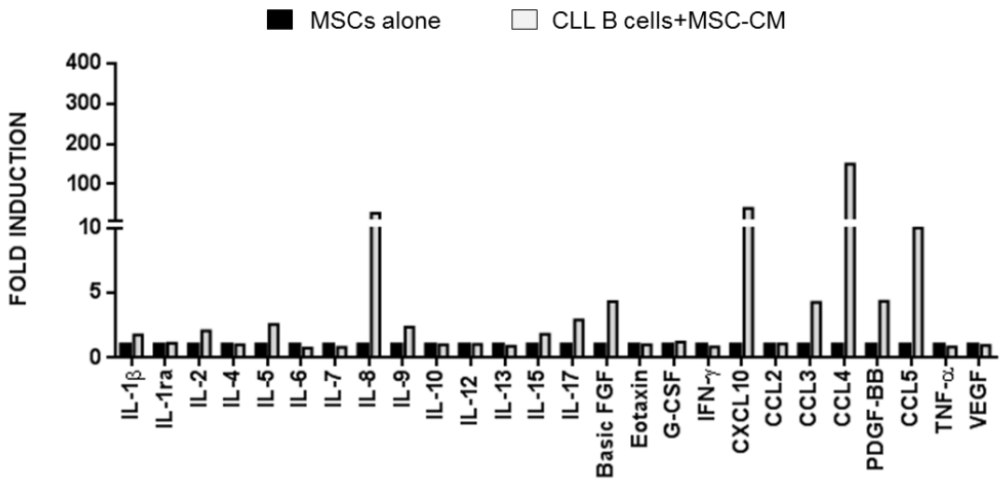

Figure 32. Cytokine/chemokine secretion in presence of CLL B cells and MSC-conditioned medium. B lymphocytes from 7 CLL patients were cultured for 7 days in medium previously conditioned by MSCs (MSC-CM); levels of cytokines/chemokines present in the culture supernatants were quantified by Bio-Plex. Concentrations of molecules present in the co-culture medium were normalized on levels of the respective molecules detected in MSC single-cultures.

2.4.6 MSCs protect CLL B cells from *in vivo* treatment with Fludarabine and Cyclophosphamide

The data reported above demonstrate that MSCs have the great potential to increase cell survival and maintain CLL cells viable after several days of culture *in vitro*. The disposability of drugs and treatments which are known to induce cell death in leukemic cells have increased the interest in studying the influence of the factors that can still favor the survival of neoplastic clones, like MSCs. In order to verify the ability of stromal cells to overcome external pro-apoptotic stimuli, the effect of MSCs on CLL lymphocytes treated with Fludarabine (FLU) and Cyclophosphamide (Cy) containing regime therapy was tested. It has been previously demonstrated in literature that MSCs exert a protective effect on CLL B cells treated *in vitro* with Fludarabine, Cyclophosphamide, Bendamustine, Prednisone and Hydrocortisone [303]. In this study, MSC anti-apoptotic effect was tested in a co-culture system with cells obtained from CLL patients before and after *in vivo* treatment with FLU-Cy containing therapy, and compared with the survival rate of CLL cells cultured in medium alone. After 3, 5 and 7 days, tumor lymphocyte survival was significantly increased in the co-culture condition both before and after FLU-Cy treatment (Figure 33). Cell viability, measured by Annexin V staining, was 55.2%±18.2% with MSCs *vs* 9.4%±13.6% without

MSCs (p<0.0001) before FLU-Cy treatment, and 34.2%±2.6% with MSCs *vs* 13.1%±16.7% without MSCs (p<0.0001) after *in vivo* therapy.

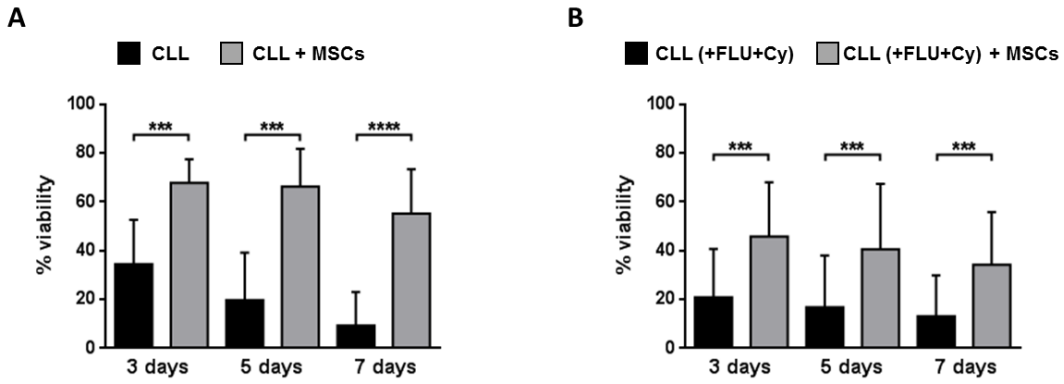

Figure 33. MSCs protect CLL B cells from *in vivo* treatment with Fludarabine/Cyclophosphamide containing regime. CLL B cells were collected before **(A)** and at day 3 of *in vivo* treatment **(B)**, according to the Fludarabine/Cyclophosphamide protocol, and cultured for 3, 5 and 7 days in medium alone or in presence of MSCs (n=10). Viability was measured at day 3, 5 and 7 of culture by flow cytometry using Annexin V staining. Both before and after treatment, CLL cell survival was significantly increased by co-culture with MSCs compared to the single-culture condition. FLU, Fludarabine. Cy, Cyclophosphamide. Data are presented as mean ± standard deviation. Student's paired t test was used; ***p<0.001, ****p<0.0001.

In order to better define MSC role in protection from apoptosis, we also tested the effect of *in vitro* administration of the same compound that is used in *in vivo* therapy. Leukemic cells from 8 CLL untreated patients were collected and pre-treated with 20μM Fludarabine and 5μM Cyclophosphamide for 3 or 12 hours before being cultured with and without MSCs for 7 days. Cell viability was measured at day 3, 5 and 7 of culture; as shown in Figure 34 A-B, CLL B cell viability was significantly increased in the co-culture condition (27%±20% with MSCs *vs* 3.6%±3.4% without MSCs after 3 hour pre-treatment and 7 day culture, p<0.05; 25.1%±20.3% with MSCs *vs* 0.86%±0.69% without MSCs after 12 hour pre-treatment and 7 day culture, p<0.05). In addition, the same protective effect was observed when MSCs and CLL B cells were co-cultured with MSCs in presence of 20μM Fludarabine and 5μM Cyclophosphamide for 7 days without pre-treatment (Figure 34C), compared to the viability of CLL B cells cultured alone with FLU-Cy (tumor B cell viability after 7 days was 9.8%±4.5% with

MSCs *vs* 1.8%±1.3% without MSCs, $p<0.01$). The data indicate that MSCs can effectively protect CLL B cells from apoptosis after *in vivo* and *in vitro* treatment with Fludarabine and Cyclophosphamide.

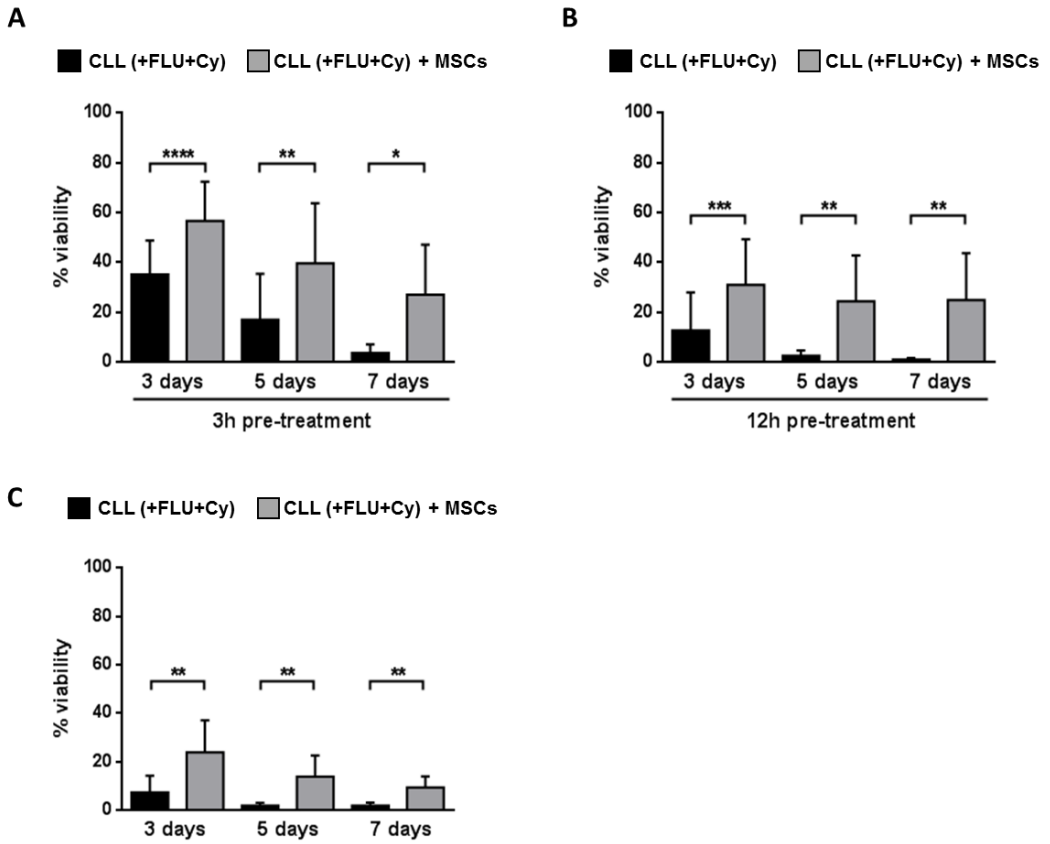

Figure 34. MSCs protect CLL B cells from *in vitro* Fludarabine/Cyclophosphamide treatment. CLL B cells (n=8) were pre-treated with FLU-Cy for 3 hours **(A)** or 12 hours **(B)**, or directly treated without pre-treatment **(C)**, before being cultured for 7 days with and without MSCs. Viability was measured after 3, 5 and 7 days by flow cytometry using Annexin V staining. In all the conditions analyzed, MSCs protected CLL cells from apoptosis, significantly increasing tumor cell survival. Data are presented as mean ± standard deviation. Student's paired t test was used; *$p<0.05$, **$p<0.01$, ***$p<0.001$, ****$p<0.0001$.

2.4.7 MSCs do not protect neoplastic cells from apoptosis induced by *in vitro* administration of kinase inhibitors

This study and previous literature data have demonstrate that MSCs can protect CLL B cells from anti-apoptotic drugs and conventional chemotherapy [292, 303]. Recently, new generation inhibitors have been developed to target key components of signaling pathways in leukemic clones. In order to determine whether these kinase inhibitors could overcome the protective effect of stromal cells, CLL lymphocytes were co-cultured with MSCs in presence of Ibrutinib

(BTK inhibitor) or Bafetinib (Bcr-Abl/LYN inhibitor) for 3, 5 and 7 days *in vitro*. As shown in Figure 35A, viability of treated CLL cells was significantly decreased (at day 7, 85.7%±4.1% in absence of kinase inhibitors, 53.9%±17.2%, $p<0.001$, with Bafetinib, and 37.7%±14.7%, $p<0.0001$, with Ibrutinib), despite MSC co-culture. To confirm these results, western blot analysis of the cleaved form of PARP (89kDa fragment) was performed from total lysates of CLL cells alone and co-cultured with MSCs in presence or absence of kinase inhibitors. PARP pattern analysis showed that leukemic lymphocytes underwent apoptosis, in particular after 7 days of culture with inhibitors, although MSCs were present in the system (Figure 35B, row a). These data suggest that Ibrutinib and Bafetinib can overcome the protective effect exerted by MSCs on CLL B cells *in vitro*.

To better understand the molecular implications of the use of kinase inhibitors, western blot analysis of LYN and ERK proteins was performed on CLL cells cultured alone or with MSCs. Bafetinib and Ibrutinib treatment completely turned-off LYN phosphorylation at the active site Y396, in both alone and co-culture condition (Figure 35B, row b). As well, ERK phosphorylation was severely decreased after drug treatment with respect to the untreated controls (Figure 35B, row d). This set of experiments suggests that kinase inhibitors are able to impair signaling pathways in leukemic cells, exerting their cytotoxic effect even in presence of MSCs.

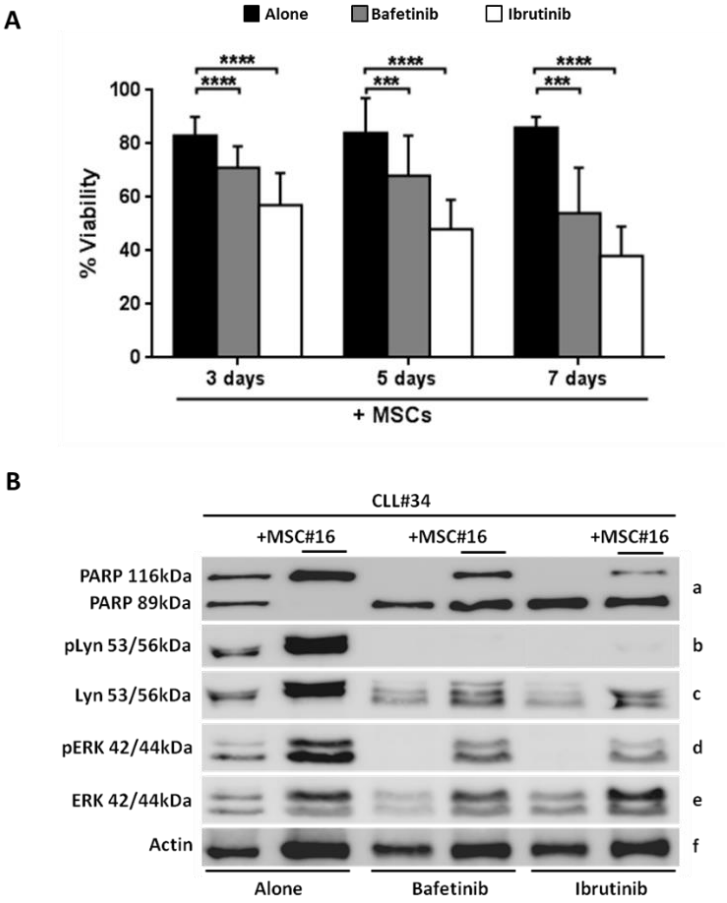

Figure 35. BCR-signaling inhibitors overcome MSC protective effect and induce apoptosis in CLL B cells. CLL lymphocytes were cultured with MSCs in presence of Bafetinib and Ibrutinib. **A)** CLL B cells and MSCs (n=12) were cultured alone, with 5μM Bafetinib or 5μM Ibrutinib for 3, 5 and 7 days. Cell viability was measured by flow cytometry using Annexin V staining. Data are presented as mean ± standard deviation. Student's paired t test was used; ***p<0.001, ****p<0.0001. **B)** Representative case of signaling inhibition in CLL cells treated *in vitro* with Bafetinib or Ibrutinib. Cell lysates of CLL cells (n=10) cultured in medium alone or with MSCs and treated with 5μM Bafetinib or 5μM Ibrutinib for 7 days were analyzed by western blotting for the proteins PARP, pLYN (Y396), LYN, pERK (T202/Y204) and ERK. Actin was used as loading control.

2.4.8 Effects of Bafetinib and Ibrutinib administration on CLL cell migration

2.4.8.1 Bafetinib and Ibrutinib treatment does not inhibit stromal cells-induced migration of tumor lymphocytes

Since the molecules targeted by the kinase inhibitors are involved in different intracellular pathways, and in particular they play a role in migration [190], the effects of Ibrutinib and Bafetinib *in vitro* administration were tested on CLL cell migration and chemokine receptor expression. As shown in Figure 36, pre-treatment of leukemic lymphocytes with Bafetinib and Ibrutinib did not

inhibit CLL cell chemotaxis towards MSC-CM, and the number of migrated cells measured was significantly higher compared to basal migration (8,850±7,920 untreated CLL cells in RPMI media *vs* 20,391±6,184 untreated cells in MSC-CM, 19,517±7,931 cells treated with Bafetinib in MSC-CM, 18,772±10,094 cells treated with Ibrutinib in MSC-CM; $p<0.01$).

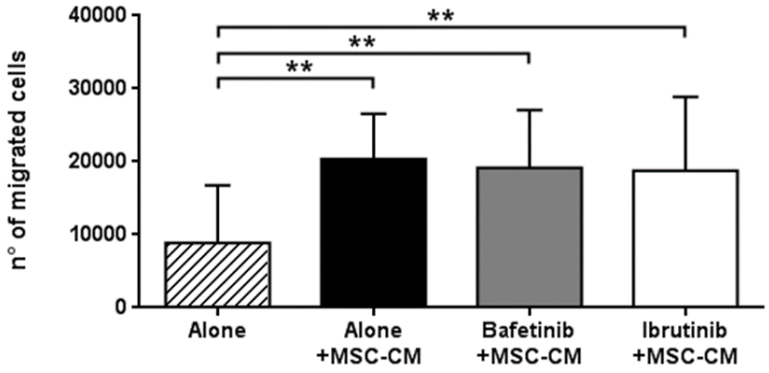

Figure 36. Kinase inhibitors do not affect CLL B cell migration towards MSC-CM. CLL B cells (n=10) alone or pre-treated with 5μM Bafetinib or 5μM Ibrutinib were allowed to migrate through a TW polycarbonate membrane (3μm pore size) for 3 hours, in presence of RPMI medium alone or MSC-CM. The conditioned medium significantly enhanced CLL B cell migration with respect to medium alone (basal migration), even in presence of kinase inhibitors. Data are presented as mean of the number of migrated cells ± standard deviation. Student's paired *t* test was used; **$p<0.01$.

Cell trafficking and homing is mediated by chemokine receptors present on cell surface, which interact with specific ligands released in the microenvironment [304]. The ligand binding induces internalization of the receptor and consequent activation of intracellular pathways that lead to migration. It has been demonstrated that CLL cells express high levels of CXCR4, CCR7, CXCR5 and CXCR3 receptors, which bind the chemokines CXCL12/SDF-1α, CCL19/21, CXCL13 and CXCL10/IP-10, respectively [200, 305]. Thus, to further determine the possible effect of kinase inhibitor treatment on lymphocyte migration *in vitro*, tumor B cells were cultured alone or with MSCs, and the chemokine receptor expression on cell surface was determined by flow cytometry. The data collected from the analysis of 11 CLL samples (summarized in Table IV) showed different responses to Bafetinib and Ibrutinib treatment in terms of receptor expression (Figure 37). In particular, CXCR4 resulted increased by treatment with Bafetinib and Ibrutinib, while CCR7 was reduced by Bafetinib; at

the same time, CXCR5 was affected only by Ibrutinib, and the two kinase inhibitors did not show a significant influence on CXCR3 expression. These results suggest that kinase inhibitors can target and disrupt the cross-talk between CLL cells and MSCs.

Table IV. Expression levels of chemokine receptors on CLL cells.

	no MSCs			with MSCs		
	Alone (MFI)	**+Bafetinib (MFI)[a]**	**+Ibrutinib (MFI)[a]**	**Alone (MFI)**	**+Bafetinib (MFI)[a]**	**+Ibrutinib (MFI)[a]**
CXCR4	19,880±4,858	28,568±5,563 *p*<0.01	24,442±6,105 ns	8,561±5,513	18,009±7,154 *p*<0.0001	13,776±6,374 *p*<0.0001
CCR7	5,085±1,308	3,475±988 *p*<0.05	4,498±890 *p*<0.05	5,229±1,237	3,845±609 *p*<0.001	4,904±1,040 ns
CXCR5	1,697±590	1,712±600 ns	1,245±402 *p*<0.01	1,623±507	1,621±466 Ns	1,269±353 *p*<0.05
CXCR3	3,969±2,635	2,379±1,721 ns	2,366±1,704 ns	4,405±2,601	3,053±2,374 ns	2,841±1,994 ns

Values were assessed by flow cytometry after 48h incubation with/without Bafetinib or Ibrutinib, in presence/absence of MSCs. Data are presented as mean ± standard deviation of MFI.
MFI, mean fluorescence intensity. Ns, not significant.
[a] *p* values are calculated compared to the alone condition.

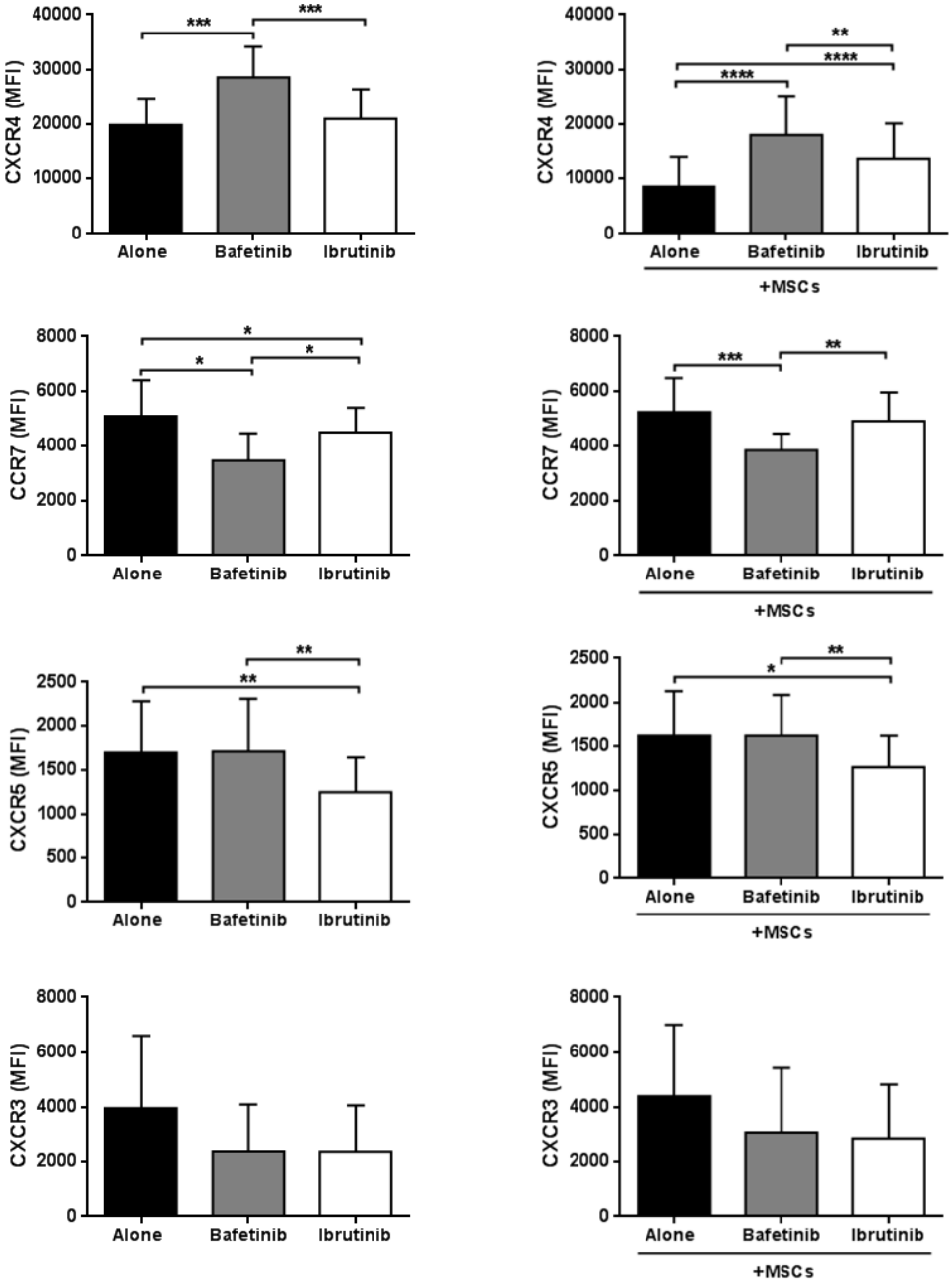

Figure 37. Bafetinib and Ibrutinib effect on CLL chemokine receptor expression. CLL B cells (n=11) were cultured alone or with MSCs in presence/absence of Bafetinib (5μM) or Ibrutinib (5μM) for 48h. The expression level of the receptors CXCR4, CCR7, CXCR5 and CXCR3 was assessed by flow cytometry Bafetinib increased CXCR4 expression in both culture conditions, while Ibrutinib only in presence of MSCs. CCR7, CXCR5 and CXCR3 showed a response to treatment similar between the two culture conditions, suggesting that the kinase inhibitors might effectively disrupt the cross-talk between CLL cells and MSCs. Data are presented as mean ± standard deviation of MFI for each receptor. Student's paired t test was used; *p<0.05, **p<0.01, ***p<0.001, ****p<0.0001.

2.4.8.2 Bafetinib and Ibrutinib impair CLL B cell pseudoemperipolesis in a CD49d-dependent way

It has been observed that, in co-culture with marrow stroma cells, CLL B cells have the ability to spontaneously migrate beneath stromal layers *in vitro* (pseudoemperipolesis) [186]. In order to better characterize the effect of the kinase inhibitors on leukemic cell migration, CLL lymphocytes were co-cultured with MSCs, and pseudoemperipolesis capacity was evaluated in presence of Bafetinib and Ibrutinib. As shown in Figure 38A by phase-contrast photomicrographs, a marked reduction of neoplastic cell adhesion to and migration beneath MSC layers was observed after Bafetinib and Ibrutinib treatment, with respect to the untreated control. Moreover, the fraction of CLL B cells adherent to the stromal layer, measured by flow cytometry, resulted significantly decreased in presence of both kinase inhibitors; the percentage of adherent tumor cells was 7.7%±3.8% in the alone condition, 2.5%±3.0% with Bafetinib ($p<0.01$), and 3.3%±2.4% with Ibrutinib ($p<0.05$) (Figure 38B).

CD49d is a membrane integrin that has been shown to play an important role in CLL cell adhesion, in particular it allows the homing of leukemic cells in protective niches, thus favoring their survival [306]. Due to its critical role, CD49d levels on CLL B cell surface were determined after treatment with kinase inhibitors (Figure 39). While only Ibrutinib decreased CD49d levels in CLL cells cultured in medium alone (MFI ratio 0.88±0.07), both Bafetinib and Ibrutinib down-modulated CD49d expression on CLL lymphocytes co-cultured with MSCs (MFI ratio was 0.87±0.12 with Bafetinib, $p<0.05$, and 0.89±0.05 with Ibrutinib treatment, $p<0.01$). Overall, these data suggest that Bafetinib and Ibrutinib can affect CLL cell pseudoemperipolesis, reducing lymphocyte adhesion and migratory capacity.

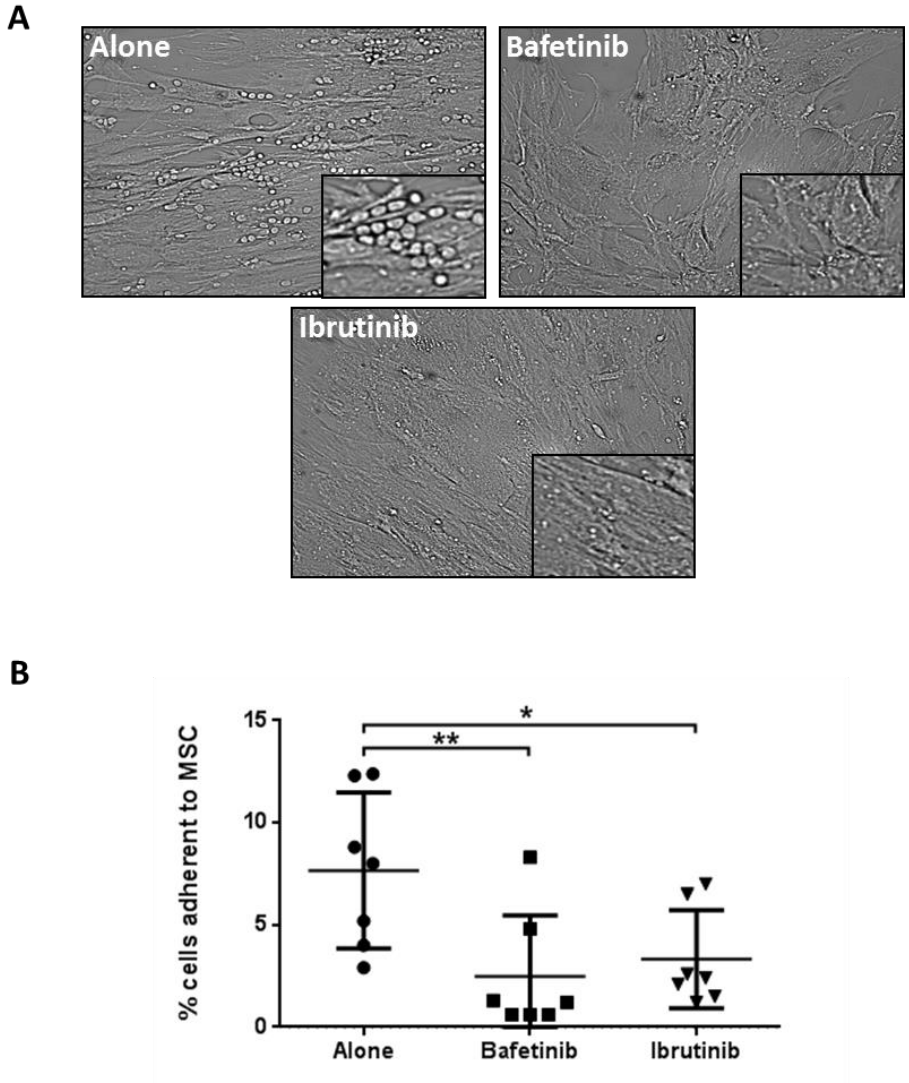

Figure 38. Bafetinib and Ibrutinib inhibit CLL cell pseudoemperipolesis and adhesion to MSCs *in vitro*. CLL B cells (n=7) pre-treated for 1h with Bafetinib (5μM) or Ibrutinib (5μM) were seeded on a confluent layer of MSCs and were allowed to migrate overnight beneath the layer. After incubation, the non-adherent fraction of CLL cells was washed off and adherent cells were analyzed by microscopy and flow cytometry. **A)** Representative phase-contrast photomicrographs of untreated CLL B cells (alone) that had migrated beneath the stromal layer (pseudoemperipolesis) and, in comparison, reduced pseudoemperipolesis of leukemic cells treated with Bafetinib or Ibrutinib (20X magnification, Olympus 1X81). **B)** The percentage of CLL cells that firmly adhered to MSCs after overnight pseudoemperipolesis was reduced when cells were pre-treated with kinase inhibitors, with respect to the control. Data are presented as mean ± standard deviation of the percentage of migrated CLL cells from 7 different patients. Student's paired t test was used; *p<0.05, **p<0.01.

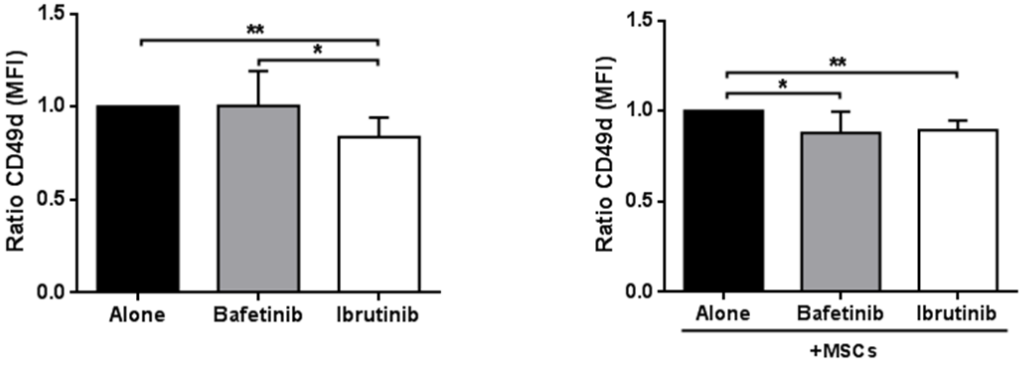

Figure 39. Kinase inhibitors reduce CD49d expression on CLL B cells *in vitro*. CLL B cells (*n*=7) pre-treated for 1h with Bafetinib (5μM) or Ibrutinib (5μM) were cultured alone or in presence of MSCs for 24h. The expression levels of CD49d decreased after drug treatment, in comparison to the untreated control, even in presence of MSCs, as assessed by flow cytometry. Data are presented as mean ± standard deviation of CD49d MFI. Student's paired *t* test was used; **p*<0.05, ***p*<0.01.

2.5 Discussion

CLL is a lymphoproliferative disorder characterized by the accumulation of mature B lymphocytes in peripheral blood, bone marrow and lymphoid organs [1]. This phenomenon is due to apoptotic defects coming from intrinsic features of the neoplastic clone, like the dis-regulation of BCR signaling and the overexpression of anti-apoptotic proteins (such as Bcl-2 and MCL-1), and from the interaction with microenvironmental elements, in particular marrow stromal cells. In literature, in fact, it has been reported that, when co-cultured *in vitro*, MSCs isolated from marrow blood of CLL patients are able to support leukemic B cell survival, and that there is an active cross-talk between the two populations [292].

Since the malignant clone is inclined to infiltrate bone marrow and lymphoid organs in patients affected by CLL, and mesenchymal stromal cells are essential elements of the marrow stroma and can be functionally altered in some haematological diseases [307], the focus of this study has been the analysis of cross-talk modulation of CLL B cells and MSCs [308]. In this thesis, mesenchymal stromal cells obtained from 46 CLL marrow aspirates were characterized and used to mimic the *in vivo* tumor microenvironment. MSCs from CLL patients displayed phenotype similar to stromal cells isolated from healthy subjects, indicating that the characteristics of normal MSCs are maintained in CLL.

Previous studies have tried to elucidate the role of stromal cells in CLL B cell survival, and it has been shown that marrow stromal cells can inhibit apoptosis of cultured CLL and acute lymphocytic leukemia cells (B-ALL) *in vitro* [299, 309]. In these reports, the co-culture system was represented by marrow cells, but it included fibroblasts, macrophages and fat cells. In the present study, instead, the data reported derived from co-cultures with a well-defined mesenchymal stromal population. The presence of MSCs in the *in vitro* co-culture with CLL B cells significantly increased leukemic clone survival, compared to the culture of CLL lymphocytes in medium alone; in fact, our results show that CLL B cells cultured *in vitro* without supportive stroma rapidly undergo apoptosis, confirming literature data [299]. However, we found a great variability in CLL

cell response to MSC co-culture in terms of survival: in average, almost 60% of viability was observed after 7 days of culture, but the fraction of living cells ranged from 40% to 76%. A possible explanation of this phenomenon relies on the extreme heterogeneity that characterizes CLL. Despite tumor cells display typical phenotype and cytogenetic abnormalities, the disease turns out to present different clinical courses, suggesting the involvement of intrinsic clone-dependent features that might affect the response to extracellular stimuli and cell behaviour. Moreover, the rescue from apoptosis exerted by MSCs on lymphocytes from healthy donors was not as significant as for CLL cells, suggesting that tumor clones possess characteristics and ability to respond better to environmental pro-survival stimuli.

The analysis of PARP protein cleavage pattern performed by western blotting confirmed the above reported data: CLL B cells cultured in presence of MSCs showed significantly increased viability in comparison to leukemic cells in medium alone and to normal B cells. In this context, variability in the neoplastic response to pro-survival stimuli was observed, allowing the distinction of tumor clones into two groups, dependent and independent from the microenvironment. In the first group were counted all CLL samples that, after 7 days of culture, showed increased viability only in presence of MSCs, suggesting a strong dependence from the external pro-survival stimuli provided by stromal cells. Conversely, CLL clones that displayed similar PARP pattern and high viability both in presence and absence of stromal support were defined as independent from the microenvironment, and were thought to be more likely responsible of aggressive disease. However, no significant correlation was found with any of the most known CLL prognostic factors (IGHV mutational status, CD38 expression, ZAP70 expression and cytogenetic aberrations), suggesting that the different degree of dependency from microenvironmental signals might influence other aspects of the disease. Moreover, we observed that different clones behaved differently in presence of the same MSC line, while the co-culture of the same CLL clone with MSC obtained from different patients did not influence tumor cell survival. Overall, the data presented are suggesting that the responses to the microenvironment are not due to a variable behavior of MSCs, but to intrinsic

features of CLL cells that make clones differently inclined to survive in presence of external stimuli.

The nature of MSC/CLL B cell interaction is still under investigation. The pro-survival effect of MSCs on CLL cells can be mediated by soluble factors and cell-cell contact. *In vitro* studies have demonstrated that the binding of stromal cells to β_1 and β_2 integrins expressed by B cells increases neoplastic lymphocyte viability [299], while the production of SDF-1α/CXCL12, and the consequent binding of the specific receptor CXCR4 expressed on B cell surface, can inhibit apoptosis and favor migration of CLL cells [191]. In this thesis, experiments where CLL lymphocytes were co-cultured with MSCs in direct contact or separated by a porous membrane, which allowed only the exchange of soluble factors, demonstrated that both the cell-cell contact and the release of soluble mediators by MSCs are able to support CLL cell viability. In general, from our and literature results, we can assert that an important role is played by soluble molecules, but the pro-survival effect is certainly potentiated by the close contact of leukemic cells with MSCs, which seems to be also responsible of resistance to drug-induced apoptosis [292, 308].

The simultaneous analysis of a complex panel of cytokines/chemokines through the Bio-Plex array system has allowed a better understanding of the secretion profile of MSCs, CLL B cells and normal B cells. Survival factors able to counteract CLL cell apoptosis have already been reported in literature [310, 311], while the humoral/cellular factors involved in the pro-survival effect *in vivo* had not yet been identified. Ding and colleagues have previously demonstrated that the co-culture condition can increase the production by MSCs of pro-angiogenic factors, while it can increase the expression of CD38, and induce the activation of CD25, CD69, CD70 and CD71 on CLL B cells, with an overall positive effect on disease progression [292]. The analysis performed on supernatants of MSC/CLL B cell co-cultures revealed that neoplastic lymphocytes are able to modulate stromal cell secretion profile, stimulating the production of factors with pro-survival activity. Among all the cytokines/chemokines tested, the most up-regulated resulted to be IL-8, CCL4, CCL11 and CXCL10. The involvement of IL-8 and CCL4 in CLL survival had already been reported in literature [304, 312], and the data showed in this thesis confirm and extend the

observations on CCL11 and CXCL10. In particular, since CCL11 resulted increased also in normal B cell co-cultures, the most interesting results were obtained from the analysis of CXCL10. CXCL10, chemokine that binds the receptor CXCR3 expressed on B cell surface, was exclusively produced when MSCs were co-cultured with malignant B cells but not with lymphocytes isolated from healthy donors, indicating a potential role of this chemokine in disease progression. The basal production of CXCL10 was instead low in supernatants of CLL cell and MSC single-cultures. Since CXCR3 has been reported to be overexpressed on CLL cells [200], the data collected in this study point out the importance of the interconnection between chemokine receptor signaling and extracellular stimuli in cell fate.

Furthermore, the involvement of MSCs in drug-induced apoptosis has been studied. The reported results show that MSCs are able to rescue CLL B cells from apoptosis induced by Fludarabine (FLU) and Cyclophosphamide (Cy) *in vivo* and *in vitro*, indicating the importance of stromal microenvironment in lymphocyte protection from the *in vivo* administration of chemotherapy.

In the last few years, different new therapeutic agents have been developed. In particular, BCR-signaling inhibitors have been designed to target specific kinases that are key mediators of intracellular pathways in CLL. The presence of microenvironmental elements, such as MSCs, might interfere with the biological effects of the drug, and this could lead to the identification of patients that might or might not benefit from these new treatments aimed to arrest the cross-talk of leukemic cells with the supportive microenvironment. Hence, in this thesis the effects of Bafetinib and Ibrutinib treatment were tested in the MSC/CLL B cell co-culture context. Both Bafetinib (BCR-ABL inhibitor) and Ibrutinib (BTK inhibitor) induced apoptosis in CLL cells when cultured on the MSC layer, through a mechanism that involves the inhibition of LYN and ERK, key molecules in the BCR- and chemokine receptor-signaling pathways, as well as relevant proteins in CLL pathogenesis. However, in contrast with these findings, migration of CLL cells treated *in vitro* with Bafetinib or Ibrutinib toward MSC-conditioned medium did not seem to be affected by the drugs. Since the migration process is initiated and mediated by the binding of chemokine receptors on B cell surface, the expression of CXCR4, CCR7, CXCR5 and CXCR3 was investigated

after kinase inhibitor *in vitro* treatment, in presence/absence of MSCs. CXCR5 and CXCR3 expression was decreased by Ibrutinib. Of particular interest, CCR7 expression (this receptor is involved in the lymphocyte entry in the lymph node) resulted significantly decreased after Bafetinib treatment, while CXCR4 (involved in cell trafficking in lymphoid organs) was up-regulated by both Ibrutinib and Bafetinib, in presence of MSCs. Thus, our results show that the *in vitro* treatments exert different effects on chemokine receptor expression, and suggest that further investigations will be required to better understand the mechanisms beneath this modulation.

The activity of the kinase inhibitors was also tested on the adhesion properties of CLL cells. In literature, it has been demonstrated that CLL B cells can spontaneously migrate beneath stromal cell layers *in vitro* [186]; this phenomenon is called pseudoemperipolesis, term used to describe symbiotic complexes of leukemia cells and stromal components *in vitro*. In our study, the treatment of CLL cells with Ibrutinib or Bafetinib inhibited pseudoemperipolesis toward the mesenchymal stromal layer in a CD49d-dependent way; in fact, a significant reduction of CD49d level on CLL cells was found after kinase inhibitor administration. Taken together, these results suggest that both Bafetinib and Ibrutinib are effectively able not only to overcome the protective effect exerted by MSCs on apoptosis, but also to block the cross-talk between CLL lymphocytes and MSCs, acting on chemokine receptor modulation and disruption of cell-cell interactions.

In conclusion, this study has demonstrated that MSC co-cultures represent a reproducible *in vitro* system, with functional similarities to the *in vivo* bone marrow conditions. We can assert that MSCs obtained from bone marrow of CLL patients, albeit functionally and phenotypically similar to the respective normal counterpart, play an active role in favoring neoplastic B cell survival. The different responses of CLL cells to microenvironmental stimuli reflect the general heterogeneity of the disease. However, the malignant clone can in turn modulate the MSC cytokine secretion profile, shaping the microenvironment to its own advantage. Moreover, this study has proved that, in presence of BCR-signaling inhibitors, MSCs do not protect tumor B cells from drug-induced apoptosis, and CLL cells lose their ability to interact with the stromal support. In addition, for the

first time, it has been demonstrated that the blocking of MSC/CLL B cell cross-talk exerted by Bafetinib is quite similar to that of Ibrutinib.

The understanding of the relations between neoplastic cells and microenvironmental elements aims to identify new therapeutic strategies to make tumor cells more sensible to apoptosis, and thus improving patient response to therapy. To date, treatments that interrupt the neoplastic/microenvironmental cell cross-talk are already used in clinical practice (such as Lenalidomide and CXCR4 antagonists). The results reported in this study on the role of MSCs and their effect on neoplastic B lymphocytes open a new scenario to better identify the most effective drugs targeting the pro-survival cross-talk between CLL B cells and marrow stroma elements.

ABSTRACT – Chapter 3

Surface IgM (sIgM) signaling is key to CLL behavior and is a therapeutic target of BTK-inhibitor Ibrutinib. SIgM levels and signaling capacity are variable in CLL and high sIgM levels and signaling correlate with aggressive disease. The BTK inhibitor Ibrutinib affects CXCR4-mediated migration and induces a rapid redistribution of CLL cells into the blood. We investigated expression and function of sIgM and other phenotypic changes in the circulating leukemic cells at an early phase (week 1) of Ibrutinib therapy, when treatment discontinuation associates with very short survival, in 12 patients with CLL. Pre-therapy, sIgM-induced intracellular calcium (iCa^{2+}) was high, consistent with features of progressive CLL. Following 1 week of therapy, lack of IgM-mediated BTK activation *in vitro* confirmed suppression of BTK *in vivo*. Strikingly, expression of sIgM increased (P=0.001), with little change in other receptors including sIgD. SIgM increase was accompanied by full N-glycan maturation of sIgM heavy-chain, indicative of recovery from antigen engagement. The sIgM levels correlated with increased sIgM-mediated SYK phosphorylation (P=0.03). Variably reduced sIgM-mediated iCa^{2+} mobilization and ERK1/2 activation was evident downstream to BTK. SYK activation correlated with the residual downstream activity. CXCR4-mediated signaling was also significantly reduced (P=0.007). The very short survival upon Ibrutinib suspension typically follows rapid re-colonization of tissue sites and proliferation by CLL cells. Our data reveal IgM maturation and enhanced signal inducibility upstream of BTK in the circulating CLL cells. BTK-inhibition appears to prevent antigen encounter, while favoring recovery and maturation of functional sIgM which may be dangerous if Ibrutinib is withdrawn early.

Chapter 3 – IgM expression and signaling during Ibrutinib therapy

3.1 Introduction

3.1.1 Bruton's Tyrosine Kinase (BTK)

Bruton's tyrosine kinase (BTK) was identified in 1993 as a non-receptor protein tyrosine kinase defective in the inherited immunodeficiency disease X-linked agammaglobulinemia (XLA) [313, 314]. In affected individuals, XLA leads to the absence of B lymphocytes in peripheral circulation and decreased levels of serum immunoglobulins as a consequence of severe impairment of B cell development and differentiation arrest.

BTK belongs to the TEC family of non-receptor kinases. The defining feature of this family is the PH domain at the N terminus, which comes along with three other structural domains: the SH3 (Src homology 3) domain, the SH2 domain and the kinase (SH1) domain. The PH domain is essential for the protein membrane localization, and is followed by the proline-rich TEC homology (TH) domain, which contains a zinc-finger motif that has been shown to be important for activity and stabilization of the protein [315, 316].

BTK is expressed in most cells of the hematopoietic system, mostly in B cells, myeloid cells and platelets, whereas T and plasma cells present undetectable levels of the protein [317, 318]. BTK is part of a wide variety of signaling pathways linked to surface molecules and, in addition, it activates many downstream pathways, which lead to cell development, survival, migration and homing.

BTK in BCR signaling

Upon antigen binding to the BCR, both LYN and SYK can activate BTK by trans-phosphorylation in position Y551, situated in the activation loop, allowing the subsequent auto-phosphorylation of BTK at Y223 in the SH3 domain (Section 1.2.1) [131]. The fully activated protein can interact and phosphorylate the direct downstream target PLCγ2 in positions Y753 and Y759, which are essential for the lipase activity of PLCγ2 [319]. Moreover, BTK activation

promotes iCa^{2+} mobilization and the activation of NF-kB, PI3K and MAPK pathways mediated by AKT and ERK [320, 321]. BTK is a cytoplasmic protein, and it is only transiently recruited to the plasma membrane, when its PH domain binds to the phosphatidylinositol-3,4,5-trisphosphate (PIP_3) generated by PI3K [322].

The placement of BTK in the BCR-signaling pathway is consistent with the defective signal transduction observed in BCR-stimulated BTK-deficient mouse B cells, which show arrest of the cell cycle, high susceptibility to apoptosis and limited induction of activation marker on cell surface [323, 324]. On the contrary, BTK overexpression in B cells has been shown to induce spontaneous formation of germinal centers and increase in plasma cell numbers, as a result of hyper-responsive BCR signaling and increased NF-κB activation [325].

BTK in CXCR4 signaling

BTK directly interacts with CXCR4-linked G proteins, binding to the subunits Gα and Gβγ through the PH and TH domains (Figure 40) [326, 327]. The ligand of CXCR4, CXCL12, is able to induce the phosphorylation of BTK at Y551 [328] and at Y223, allowing full activation of the kinase [190]. The subsequent calcium mobilization and the activation of downstream molecules such as PLCγ2, PKC and ERK are important events in chemokine-controlled B cell trafficking and tissue homing [186, 190, 329]. It has been shown that in BTK-deficient B cells migration and adhesion, and so *in vivo* tissue homing, are impaired [190], confirming the essential role of the kinase in chemokine-mediated homing and adhesion of B cells.

CXCR4 could be the key for CLL cell migration and recirculation between peripheral blood and tissues. While in the periphery, B cells seem to increase CXCR4 surface expression in order to be able to enter the tissue niches, in response to the chemoattractant CXCL12, and escape apoptosis [330]. The ligand engagement causes the internalization of the receptor, and activated cells egress from the lymphoid tissue back to the periphery.

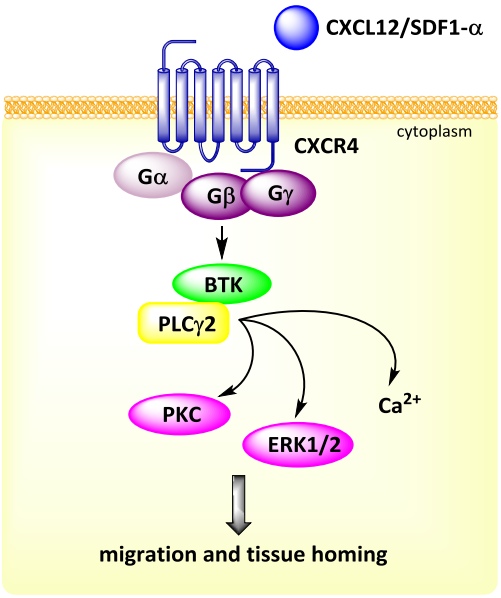

Figure 40. CXCR4 signaling pathway. Schematic representation of BTK involvement in CXCR4 signaling pathway. Upon CXCL12 binding to CXCR4, the G-proteins coupled to the receptor phosphorylate and activate BTK by direct interaction via the PH domain of the kinase. The fully activated BTK can then promote the transduction of the downstream signaling that leads to migration and tissue homing of B cells.

3.1.2 Bruton's Tyrosine Kinase inhibitor Ibrutinib

Ibrutinib (PCI-32765) is an orally active agent, potent inhibitor of BTK, which binds covalently and irreversibly to the cysteine-481 of the enzyme, thus occupying the protein active site [74, 76]. Therefore, Ibrutinib is potentially able to inhibit BCR signaling, which is the most activated pathway in CLL cells isolated from lymph nodes [331]. BTK expression is restricted to hematopoietic cells, in particular to those of the B-lineage, but Ibrutinib is able not only to block the signaling downstream of the antigen receptor in B cells, but also to target BTK homologous proteins like ITK, which is present in T lymphocytes [332]. Moreover, BTK is expressed in macrophages and it has been recently shown that Ibrutinib can affect their function, exerting an immunomodulatory effect on the monocyte/macrophage population in CLL [333].

Ibrutinib is administered once daily and is well tolerated because of its short half-life, rapid absorption and elimination. A phase 1 study showed mild toxicity and clinical antitumor activity in patients with relapsed or refractory CLL/SLL [76]. In addition, modest toxicity was observed during long-term

Ibrutinib therapy; the most commonly reported adverse effects were diarrhea, fatigue and upper respiratory tract infection [77].

Despite the rapid clearance, occupancy studies have shown that the BTK active site remains occupied by Ibrutinib for at least 24 hours in patients, and that the occupancy of the target correlates with the impairment of BCR signaling and *in vivo* efficacy of the treatment [74, 76].

Clinical response

A recent study of three-year follow up of single-agent Ibrutinib on treatment-naive or relapsed/refractory CLL patients has demonstrated durable responses to therapy and diminished toxicity over time (84% ORR in previously-untreated patients, 90% ORR in relapsed/refractory CLL) across the different risk groups [334]. Another recent study compared Ibrutinib and Chlorambucil therapy outcome on previously-untreated CLL or SLL patients [335]. With respect to Chlorambucil, Ibrutinib significantly increased progression-free and overall survival. Progression-free survival at 18 months was 89% with Ibrutinib in both unmutated and mutated IGHV subgroups *vs* 47% and 51% with Chlorambucil respectively; the overall survival rate at 24 months was 98% with Ibrutinib *vs* 85% with Chlorambucil. Moreover, an improvement in the hematological variables was observed and Ibrutinib toxicity was modest in the majority of the patients. Notably, a positive effect of the treatment was observed also in the high-risk patient subgroups, similarly to the findings reported for patients on Ibrutinib therapy with relapsed disease [336]. In this context, Ibrutinib has proved to be an effective option for patients with 17p deletion involving the *TP53* gene, which usually have an aggressive disease and reduced life expectancy. The fact that these patients carrying del17p responded to Ibrutinib therapy as well as patients without the mutation, and the evidence that the progression-free survival rate achieved on Ibrutinib was longer than that with other treatments [77, 336-338], has allowed the approval of Ibrutinib for high-risk treatment-naive patients and as primary therapy for patients with del17p [339]. Moreover, Ibrutinib has been approved for patients with relapsed/refractory CLL who have received one or more previous treatments.

Discontinuation of Ibrutinib due to disease progression, transformation to an aggressive lymphoma, stem cell transplantation or other reasons has been associated with poor survival [340]. Despite the high response rates on Ibrutinib, some patients can progress early during therapy and have a poor outcome. However, treatment discontinuation for disease progression or transformation seems to be more frequent in patients with del17p and unmutated IGHV.

Tumor response - Lymphocytosis

Treatment-induced lymphocytosis has become a hallmark of Ibrutinib therapy, and it has been recognized as a class effect during the clinical use of several BCR inhibitors [79, 88, 341]. Ibrutinib-induced lymphocytosis develops quickly, within hours, however its entity is variable between patients. Notably, cases with unmutated IGHV have been reported to have a lower rise of ALC (absolute lymphocyte count) and a more rapid normalization of the lymphocyte counts rather than mutated IGHV patients [77, 79]. A clinical phenomenon that has been associated with the lymphocytosis is the notable reduction in lymph node and spleen size that occurs in patients during the first phases of Ibrutinib treatment. The concomitant rise in ALC and reduction of lymphadenopathy suggests that the treatment-induced lymphocytosis is not a sign of disease progression but an evidence of tumor cell redistribution from the tissue to the peripheral blood [76, 77, 79, 342]. The continued treatment with Ibrutinib leads to the resolution of the lymphocytosis [77].

Resistance to Ibrutinib therapy

CLL cells can develop resistance to Ibrutinib, probably as the result of continuous pressure by the drug on the target. The possible mechanisms of resistance could be related to acquisition of a primary mutation on the *BTK* gene, which is usually not mutated in CLL; the C481S mutation would prevent the irreversible binding of the drug to the target site [343]. Moreover, acquired gain-of-function mutations on the *PLCγ2* gene can also confer resistance to Ibrutinib by constitutive activation of the lipase, thus bypassing BTK blockade and propagating the BCR signal even in the presence of the drug. These hypermorphic mutations, in particular R665W, have been associated with augmented and persistent BCR signaling downstream of BTK in DT40 cells and CLL patients

[344]. The *in vitro* analysis of transfected DT40 cells with the *PLCγ2* mutated gene showed persistent phosphorylation capacity of ERK, while the study conducted on Ibrutinib patients who carried the mutation revealed in addition increased intracellular calcium mobilization compared to non-resistant cases. Somatic PLCγ2 aberrations were acquired only after long-term Ibrutinib therapy, thus supporting the idea that they can evolve under the constant pressure exerted by the treatment, avoiding the impairment of important survival pathways. Despite the small proportion of patients in which these kind of mutations appear, it seems that clones with high-risk features, such as genomic instability and complex karyotype could be more prone to relapse [343]. The mechanisms of Ibrutinib resistance in patients who do not present mutations on BTK or PLCγ2 could involve mutations in different genes that can provide other alternative survival pathways.

3.1.2.1 Ibrutinib *in vitro* effect on CLL cells

The effect of Ibrutinib treatment *in vitro* has been extensively studied. Ibrutinib has been shown to have a cytotoxic effect on CLL lymphocytes *in vitro*, inducing cell apoptosis in a dose- and time-dependent manner [321]. However, the variability observed could suggest that not only BTK expression levels but also the interaction of the clone with the microenvironment could play a role in cell response. Notably, in the same study, no cytotoxic effect was observed in T cells, which lack BTK protein.

PCI-32765 activity is demonstrated by the decreased basal phosphorylation of BTK at Y223 reported in cell lines and in primary CLL cells [74, 321]. However, the phosphorylation at Y551, mediated by LYN and SYK, is not influenced by the treatment [328]. Ibrutinib is able to antagonize the BCR-dependent signaling downstream of BTK. The pathways mediated by ERK and AKT have been shown to be inhibited by Ibrutinib treatment *in vitro*, with a decrease in both basal and anti-IgM induced phosphoprotein levels [139, 321]. In addition, the treatment of CLL cells with PCI-32765 reduces NF-κB signaling by interfering with the DNA binding to consensus sites after CD40L treatment [321].

Ibrutinib affects also the chemokine- and integrin-mediated pathways that involve BTK, thus having consequences on cell migration and adhesion.

Preclinical studies have demonstrated that this compound inhibits CLL cell survival and proliferation as well as CXCL12-mediated migration and adhesion [139, 328]. This reduction in cell responsivity to CXCL12 is accompanied by an impairment in the signaling downstream of CXCR4, in particular by the decrease of CXCL12-induced ERK phosphorylation. Moreover, the capacity of Namalawa cells (Burkitt lymphoma-derived cell line) to adhere to fibronectin and vascular cell adhesion molecule-1 (VCAM-1) was significantly reduced after *in vitro* incubation with PCI-32765 [328].

The effect of Ibrutinib is also evident on the secretion profile of B and T cells. Ibrutinib has been shown to inhibit the production of the cytokines IL-6, IL-10 and TNF-α in T cells [321], and it blocks the secretion of the cytokines CCL3 and CCL4 by CLL cells [139].

Finally, as also previously reported in this thesis (Section 2.4.6), Ibrutinib treatment *in vitro* is able to overcome the protective effect that the microenvironment usually exerts on CLL B cells; in fact, both co-cultures with mesenchymal stromal cells or nurse like cells could not rescue the tumor lymphocytes from apoptosis [139, 321, 345].

3.1.2.2 Cellular responses during Ibrutinib therapy

Ibrutinib inhibits CLL cell proliferation and activation *in vivo* [346]. In particular, a study conducted by Cheng and colleagues has shown that while apoptosis is observed only occasionally in the CLL cells of patients after 28 days of therapy, the inhibitory effect on CLL proliferation by Ibrutinib is clear [347]. The analysis of CLL cells resident in LN and BM showed a marked downregulation of the expression of the activation markers CD69 and CD86, together with the reduction of the proliferation marker Ki67, suggesting that Ibrutinib effectively affects tumor proliferation also for cells in the tissue microenvironment [346].

However, the consequences of Ibrutinib therapy on CLL intracellular signaling have not been completely elucidated. The inhibition of basal BTK phosphorylation at Y223 has been reported in the literature, and together with occupancy assays it demonstrates that the therapy is effectively targeting the kinase [74, 347, 348]. The blockade of BTK leads to the inhibition of the direct

downstream target PLCγ2, which occurs both in the early phases and in the later time points of Ibrutinib therapy [346-348]. However, the effect of Ibrutinib on other downstream pathways is difficult to establish. After 28 days of therapy, the basal levels of pERK and pAKT seem to be decreased by Ibrutinib [347], while in another study it has been reported that basal phosphorylation of ERK and AKT are increased in tumor cells of patients that experienced prolonged lymphocytosis at 6 and 9 months of therapy [348]. Moreover, the NF-κB pathway in both tissue-resident and circulating CLL cells is inhibited after 28 days of Ibrutinib therapy [346].

Ibrutinib targets *in vivo* BTK-mediated pathways involved in migration and adhesion. A study on Ibrutinib treated mice has shown that BTK is important for the retention of CLL cells in the lymphoid tissues; the treatment caused the redistribution of cells into the peripheral blood, suggesting that the blockade of BTK activity influences this phenomenon [342]. Moreover, both short and long-term treatment inhibit the signaling downstream of CXCR4, as demonstrated by reduced calcium mobilization. In addition, Ibrutinib inhibits CLL migration towards different chemoattractants, but with evident interpatient variability [349]. Adhesion to fibronectin and stromal cells is also inhibited by Ibrutinib, with concomitant slight reduction of the expression of the adhesion markers CD29, CD44 and CD49d. However, due to the high variability of the responses, it can be hypothesized that the proportion of circulating cells mobilized by Ibrutinib may comprehend the fraction of cells more inhibited by the treatment, while the tissues would retain cells that are less affected by therapy.

3.2 Aim of the study

SIgM levels and signaling capacity are key to CLL behavior, survival and proliferation; they vary between the two subsets of CLL, being generally higher in U-CLL than in M-CLL, and are associated with disease progression. For this reason, different kinases involved in the BCR pathway have been therapeutically targeted by specific BCR-associated kinase inhibitors. Ibrutinib is a potent BTK inhibitor, which binds irreversibly at Cys481 of the protein active site, thus suppressing BTK full activation. Ibrutinib has been shown to affect also CXCR4-mediated cell migration, inducing a rapid redistribution of CLL cells into the blood.

In this study, the effect of Ibrutinib therapy on sIgM expression and function has been evaluated. In order to investigate that, we:

- isolated B cells from CLL patients prior to (pre-) and after one week of Ibrutinib therapy;
- evaluated the changings in the levels of sIgM and other surface markers on CLL cells during Ibrutinib by flow cytometry;
- determined the maturational status of the sIgM after one week of therapy by analysis of the glycosylation pattern of the sIgs;
- analyzed the signaling capacity of CLL cells from patients on Ibrutinib following BCR and CXCR4 stimulation.

3.3 Materials and Methods

3.3.1 Patients

In this study, PBMCs were obtained from 12 previously treated, relapsed CLL patients prior to (pre-) and at one week following the initiation of a single-arm Ibrutinib treatment. Although all patients had relapsed from prior treatments, none of them had received any chemotherapy or steroids for the 6 months prior to Ibrutinib commencement. Following pre-Ibrutinib sample collection, all patients received 420 mg Ibrutinib once daily each morning and blood collection at week 1 was performed no later than 2 hours from the daily Ibrutinib administration. Clinical characteristics of patients enrolled for the study are listed in Table V.

3.3.2 Isolation and storage of PBMCs

PBMCs were isolated from peripheral blood of 12 CLL patients. A sample of heparinized venous blood was processed by density gradient centrifugation. 20ml of whole blood were layered on Lymphoprep (Axis-shield; Dundee, UK) and the tubes were spun at 2,100rpm for 20 minutes with the brake off and at room temperature. The PBMC layer at the interface was then collected and washed in complete RPMI medium by centrifugation at 1,500rpm for 10 minutes. Once discarded the supernatant, the pellet was resuspended in an adequate amount of RPMI medium and cells were counted in the Neubauer chamber.

After a 10 minutes centrifugation at 1,500rpm, PBMCs were resuspended in freezing medium composed by decomplemented fetal calf serum (FCS) plus 10% dimethyl sulfoxide (DMSO; Sigma-Aldrich) at the concentration of $5x10^7$ cells/ml. Cells were aliquoted into cryovials (1ml per tube) and placed at -80°C overnight, then transferred to liquid nitrogen for long-term storage.

Table V. Characteristics of the patients included in the study.

Symbol	Sample	IgM MFI[b]	IgM iCa^{2+} (%)[b,d]	IgD MFI[b]	IgD iCa^{2+} (%)[b,d]	IGHV	% homol.[a]	CD38 (%)[b]	CXCR4 MFI[b]	CD49d (%)[b]	ZAP70 (%)[c]	FISH	NOTCH1	SF3B1	Prior lines
▼	222	81	37.8	17	51.3	3-72	96.26	76	258	54	4	Del(13q)	nk	nk	2 (Chl, R-CVP)
◎	343	212	69.6	17	73.3	3-48	98.26	32	110	84	2	FISH neg	wt	wt	2 (FC, O)
△	346	97	36.6	32	76	3-49	100	52	311	31	NK	Del(13q)/Del (11q)	wt	wt	2 (FCR, R-CVP)
⊡	409	100	27.9	38	46.6	1-69	100	48	264	70	16	+12/Del(17p)	wt	nk	3 (FC, Chl, BR)
▲	489	20	1	28	86.2	4-30-4	91.03	33	169	19	2	Del(13q)	wt	wt	1 (Chl)
■	495	131	77.3	7	37	3-21	97.37	40	125	77	2	Del(13q)	wt	wt	1 (Chl)
▽	531	52	15.7	10	37.9	4-39	100	29	213	20	15	Del(17p)	wt	wt	3 (Chl, FC, BR)
⬡	551	221	55.6	83	74.1	3-33	100	99	67	30	21	Del(11q)	wt	wt	9 (Chl, Chl, Chl, Chl, R-CVP, Chl, R, O, Splenectomy)
◆	558	24	16.8	6	43.2	4-31	97.59	34	117	21	4	Del(13q)	wt	wt	1 (Chl)
○	632	107	51.3	18	58.1	2-26	100	79	298	32	52	Del(11q)	wt	mut	1 (Chl)
□	644	59	24.9	17	29.1	4-39	100	50	273	20	55	Del(11q)	wt	wt	6 (Chl, CHOP, FC, BMT, FC, BR)
●	727	35	26.7	42	80.8	3-72	93.88	47	255	22	0	Del(17p)	wt	nk	0

MFI, Mean Fluorescence Intensity. IGHV, immunoglobulin heavy chain variable genes. FISH, fluorescence in situ hybridization. nk, not known. wt, wild type. mut, mutated. Chl, Chlorambucil. FC(R), fludarabine, cyclophosphamide (rituximab). O, ofatumumab. R-CVP, rituximab, cyclophosphamide, vincristine, prednisone. BR, bendamustine, rituximab. CHOP, cyclophosphamide, doxorubicin, vincristine, prednisone. BMT, bone marrow transplantation

a mutational status expressed as percentage of homology in respect to the closest germline sequence. U, unmutated IGHV (>98% homology to germline). M, mutated IGHV (<98% homology to germline).

b values assessed by flow cytometric analysis pre-therapy

c ZAP70 values were obtained by flow cytometric analysis at time of diagnosis

d percentage of iCa2+ release after anti-IgM or anti-IgD stimulation was corrected on the percentage of CD19+CD5+ cells pre-therapy

Each symbol identifies one individual patient and has been maintained throughout the study. Open symbols represent U-CLL, closed symbols represent M-CLL.

3.3.3 BCR and CXCR4 *in vitro* stimulation and Immunoblotting

Prior to each assay, PBMCs were thawed, washed by 5 minutes spin at 1,500rpm, and allowed to recover for 1 hour at 37°C in complete RPMI1640 medium. Recovered PBMCs ($1x10^7$/ml) were plated on a 12-well plate and stimulated with polyclonal goat F(ab')2 anti-human IgM or soluble polyclonal control (20µg/ml; Southern Biotech; Birmingham, USA) at 37°C for 10 minutes, or with 200ng/ml CXCL12 (Miltenyi Biotec; Bisley, UK)) at 37°C for 5 minutes.

For immunoblotting, cells were washed twice in ice-cold PBS and incubated for 30 minutes on ice in RIPA buffer (150mM NaCl, 1% NP-40, 0.5% sodium deoxycholate, 0.1% sodium-dodecyl-sulphate (SDS), 50 mM tris(hydroxymethyl)aminomethane hydrochloride (Tris-HCl), pH 8.0), containing 1X protease inhibitor and phosphatase inhibitor cocktail 2 and 3 (Sigma-Aldrich). Protein concentration was determined using the Pierce BCA Protein Assay Kit (Thermo Scientific). Equivalent protein amounts were boiled for 5 minutes in Red Loading buffer and dithiothreitol (DTT; Cell Signaling), separated by SDS 10% polyacrylamide gel electrophoresis (SDS-PAGE) and transferred to nitrocellulose membranes (GE Healthcare). After blocking with 5% BSA in Tris-buffered saline, the membranes were probed with the required primary antibody and subsequently stained with horseradish peroxidase-conjugated secondary antibodies (Dako, Agilent Technologies; Santa Clara, CA, USA). Following enhancement by chemiluminescence reagents (Pierce ECL and SuperSignal West Femto, Thermo Scientific), proteins were visualized using the ChemiDoc-It imaging system (UVP). The following antibodies were used: anti-phosphoBTK (Tyr223), anti-BTK, anti-phosphoSYK (Tyr525/526), anti-SYK, anti-phosphoERK1/2 (Thr202/Tyr204), anti-ERK1/2 (Cell Signaling) and anti-GAPDH (Ambion, Applied Biosystems; Waltham, MA, USA). Band optical density (OD) was quantified using ImageJ and normalized to GAPDH. "Basal" and "induced" phosphoprotein levels were defined as [test phosphoprotein OD/test total protein OD] in the absence and in the presence of stimulation by anti-IgM or CXCL12 *in vitro*, respectively. "Inducibility" was defined as the ratio of induced/basal phosphoprotein levels at each time point.

3.3.4 Immunophenotypic analysis of the CLL population

PBMCs ($5x10^6$ cells/ml) were washed by 5 minutes spin at 1,500rpm, re-suspended in fluorescence-activated cell sorting (FACS) buffer (1% bovine serum albumin (BSA), 4mM ethylenediaminetetraacetic acid (EDTA), and 0.15 mM NaN3 in phosphate-buffered saline (PBS)) and stained for markers ($5x10^5$ cells/100µl) on ice for 30 minutes protected from light. The following antibodies, and corresponding isotype controls, were used: peridinin-chlorophyll-protein complex/CY5.5 conjugate (PerCP/Cy5.5)-conjugated anti-CD5 (UCHT2), Pacific Blue-conjugated anti-CD19 (HIB19), allophycocyanin (APC)-conjugated anti-CXCR4 (12G5), fluorescein isothiocyanate (FITC)-conjugated anti-IgD (IA6-2), FITC anti-CD49d (9F10) and FITC anti-CD38 (HB-7; Biolegend). Following incubation, cells were washed, re-suspended in FACS buffer and $1x10^4$ lymphocytes were acquired on a FACSCanto (BD Biosciences). Analysis and determination of expression (mean fluorescence intensity (MFI)) by CD19+CD5+ CLL cells were performed with FlowJo software.

3.3.5 Biotinylation and glycosylation assay of cell surface IgM

In order to determine the glycosylation pattern of sIgs on CLL cells, cell-surface proteins were biotinylated and isolated using the Cell Surface Protein Isolation kit (Pierce).

Recovered CLL cells were layered on Lymphoprep and centrifuged for 10 minutes at 2,100rpm with the brake off, in order to remove dead cells. The PBMC layer was collected and resuspended in 3ml of cold PBS1X, and the number of cells in the suspension were counted using the Neubauer chamber. $25x10^6$ cells were washed in 2ml of cold PBS1X by centrifugation for 5 minutes at 1,500rpm and the pellet was incubated in PBS with 0.5mg/ml sulfo-NHS-SS-biotin at 4°C. After 30 minutes the reaction was terminated using the Quencing solution. After a 10 minute centrifugation at 2,000rpm at 4°C, the pellet was washed twice in PBS1X (2,000rpm for 5 minutes centrifugation). Cells were then resuspended in 250µl of Lysis buffer supplemented with 1:100 protease inhibitor cocktail (Sigma-Aldrich) and lysed by sonication. The suspension was centrifuged at 10,000rpm for 5 minutes at 4°C, and the supernatant was mixed with NeutrAvidin Agarose

and incubated for 60 minutes at room temperature. The NeutrAvidin Agarose was then washed three times in Wash Buffer supplemented with protease inhibitor (1:100; Sigma-Aldrich). The glycosylation pattern was determined by digestion with endoglycosidase H (EndoH; New England Biolabs; Hitchin, UK) which cleaves mannosylated glycans characteristic of the immature Ig form, or peptide:N-glycosidase F (PNGase; New England Biolabs), which cleaves all N-glycans (Figure 41). At the last wash step, the NeutrAvidin Agarose was divided into three tubes, one for the analysis of the total surface proteins, one for EndoH digestion and one for the PNGase digestion. Total surface proteins were treated with 50mM DTT (Pierce) and Red Loading Buffer (Cell Signaling), and boiled at 95°C for 5 minutes. Before enzymatic digestion, EndoH and PNGase tubes were treated with Denaturating Buffer (New England Biolabs) and boiled for 5 minutes at 95°C. For EndoH digestion, the NeutrAvidin Agarose was treated with G3 Reaction Buffer and the EndoH enzyme (New England Biolabs). The last tube was treated with G2 Reaction Buffer, NP-40 and the PNGase enzyme (New England Biolabs). Samples were incubated at 37°C for 3 hours, then treated with Red Loading Buffer and 50mM DTT and boiled at 95°C for 5 minutes. Biotinylated proteins were analyzed by immunoblotting using the primary antibody anti-μ (Jackson ImmunoResearch Laboratories; West Grove, PA, USA).

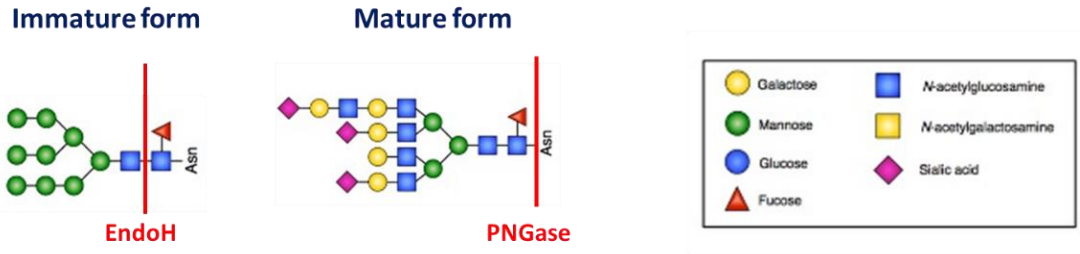

Figure 41. EndoH and PNGase cleavage. Mannosylated glycans, indicative of the immature form of the Igs, can be recognized and cleaved by digestion with the glycosidase EndoH. Conversely, complex glycans that are present on the mature form of the sIgs are cleaved only by PNGase. Modified from Lyons J. et al, Front Pediatr, 2015 [350].

3.3.6 Intracellular calcium mobilization

Signaling capacity of CLL cells prior to and after one week of Ibrutinib therapy was measured as percentage intracellular Ca^{2+} mobilization following

stimulation. PBMCs at 10^7 cells/ml were incubated with 4μM Fluo3-AM (Invitrogen) and 0.02% (vol/vol) Pluronic F-127 (Sigma-Aldrich) for 30 minutes at 37°C. Cells were than washed and resuspended at $5x10^6$ cells/ml at room temperature, warmed at 37°C for 5 minutes prior to acquisition for 35 seconds to obtain the background fluorescence (i.e. of unstimulated cells). Following, 20μg/ml goat $F(ab')_2$ anti-human IgM (Southern Biotech) were added to the tube and data were acquired for a further 5 minutes. Treatment with 1μM ionomycin (Sigma-Aldrich), which elicited robust calcium fluxes in all samples, was used to confirm viability of samples and to exclude negative artefacts. FACSCanto was used for data acquisition, FlowJo software was used for analysis of signaling profiles.

To calculate the percentage of cells that exhibited increased fluorescence following addition of anti-IgM, a background fluorescence threshold (T) was established for each sample at fluorescence intensity of the 85^{th} percentile of unstimulated cells; this level allows the separation of background and anti-immunoglobulin stimulated fluorescence. Then, the peak percentage of cells that showed an increase in fluorescence intensity above T following anti-IgM treatment was calculated. The percentage of cells responding was corrected taking into account the percentage of tumor population in each sample [25].

3.3.7 Statistical analysis

Continuous variables were compared by Wilcoxon-signed rank or Mann-Whitney non-parametric tests, as appropriate. For statistical correlation between two variables, the non-parametric Spearman's rank test was used. All statistical tests were 2-sided. Statistical significance was defined as P-value <0.05. Analyses were performed with GraphPad Prism 6 software (La Jolla, CA).

3.4.1 Lymphocyte count kinetics and pre-therapy characteristics of Ibrutinib treated patients

Analysis of the published real-world series of 315 CLL patients treated with Ibrutinib in the UK compassionate use scheme, including the patients involved in this study [351], documented that, although numbers are small, suspension of Ibrutinib within a month of therapy associated with extremely short overall survival (Figure 42). We focused on events at week 1 in 12 patients (7 U-CLL, 5 M-CLL of which one used IGHV3-21, Table V, Section 3.3.1). Week 1 was chosen as an early time point when blood lymphocyte counts were increasing in all patients (fold increase range from pre-therapy 1.4-3.5, mean 2.1), although the peak Ibrutinib-induced lymphocyte count was reached at variable times (Table VI).

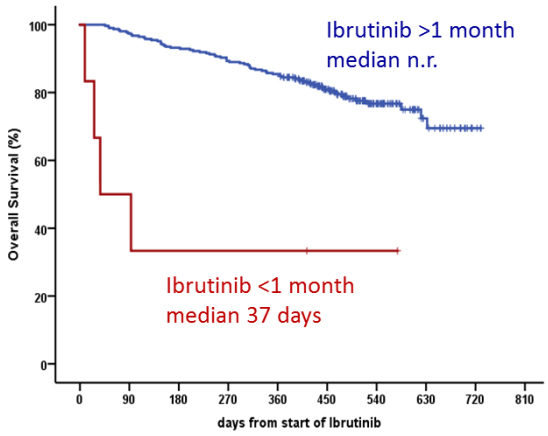

Ibrutinib duration	Total	Events	Median survival (days)	S.E.	P
not stopped in <1 month	309	67	n.r.	-	
stopped in <1 month	6	4	37	41	<0.001
Overall	315	71			

Figure 42. Overall survival of patients who stop Ibrutinib therapy early. Kaplan-Meier curves of overall survival in 315 patients with CLL who received therapy in the named patient scheme (NPS) of Ibrutinib in the UK and Ireland [351]. Blue line: patients who have not stopped Ibrutinib in the first month of therapy. Red line: patients who have stopped Ibrutinib within the first month from therapy commencement. Median overall survival in days from suspension of Ibrutinib is indicated by each line. n.r. median overall survival not reached. Total: total number of patients per group. Events: number of deaths. P: probability.

SIgM levels and signaling capacity (measured by iCa^{2+} mobilization assay) prior to therapy commencement were variable (MFI range 20-221, mean 95; and IgM iCa^{2+} % range 1-77, mean 37). The high mean levels were representative of an aggressive cohort with features of progressive CLL, including the M-CLL cases, as compared to a general CLL population at presentation [158]. CXCR4 was expressed in all cases (MFI range 67-311, mean 205).

Table VI. Lymphocyte count kinetics of the patients included in the study.

Sample	Ly pre-therapy ($x10^3$/µl)	CD19+CD5+ cells pre-therapy (%)	Ly week 1 ($x10^3$/µl)	CD19+CD5+ cells week1 (%)	Ly peak ($x10^3$/µl)	Ly peak time (week)
222	88.2	94.7	155.5	96.6	157.9	2
343	43.7	84.1	150.6	88.3	200.2	4
346	49.9	91.8	104.7	95.5	192.8	10
409	52.6	90.4	75.8	93.1	79.7	4
489	69.4	94.4	115.8	95.6	245.1	14
495	50.2	95.5	128	95.9	128	1
531	108.2	98.5	206.5	98.8	206.5	1
551	120.8	92.4	210.3	97.1	659	6
558	53	96.4	95.1	95.2	223.8	8
632	51.7	97.7	168.9	96.7	228.5	5
644	87.1	95.6	169.4	95.3	177.2	3
727	126.6	97.7	183.3	95.7	423.3	8

3.4.2 BTK auto-phosphorylation capacity following anti-IgM stimulation is completely inhibited in patients on Ibrutinib

BTK auto-phosphorylation at site Y223 was measured to determine BTK activation status prior to and on Ibrutinib therapy. Basal BTK activity was significantly down regulated at week 1 (Figure 43A). Following stimulation with anti-IgM, BTK activity levels increased significantly prior to Ibrutinib commencement, whereas it did not increase on therapy (Figure 43B). These results confirmed that Ibrutinib significantly reduced basal BTK activity [347, 348], and documented complete inhibition of IgM-mediated BTK induction capacity at week 1 in each individual patient.

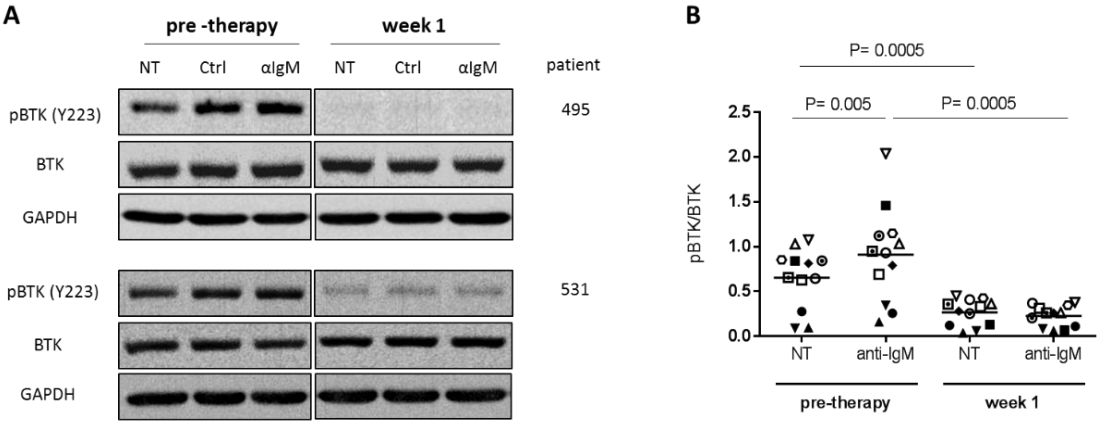

Figure 43. BTK activity is reduced following anti-IgM stimulation of CLL cells from patients on Ibrutinib. PBMCs taken pre- and at week 1 of Ibrutinib therapy were stimulated with polyclonal control (Ctrl), anti-IgM F(ab')$_2$ (αIgM) or left untreated (NT). **(A)** Immunoblots of two cases (495 and 531) showing expression of phosphorylated BTK and of total BTK. GAPDH was used as loading control. **(B)** BTK phosphorylation of each sample was measured as the ratio between pBTK optical density and total BTK optical density (pBTK/BTK). The statistical significance of difference was analyzed using the Wilcoxon-signed rank test. Horizontal lines indicate mean values.

3.4.3 IgM expression increases on CLL cells during Ibrutinib therapy

The expression of molecules involved in BCR signaling (IgM, IgD, CD19) or migration and adhesion (CXCR4, CD38, CD49d) was determined on the circulating CLL cells prior to and during Ibrutinib therapy. A significant increment of sIgM levels was observed on the tumor cells of 11/12 patients (P=0.001), whilst expression of the other markers remained constant or slightly decreased (Figure 44A-B). In one patient, sIgM levels remained similar to those determined prior to Ibrutinib (M-CLL 489, Table V), with very low sIgM levels and signaling capacity from before treatment commencement and failed sIgM expression recovery. The other 4 M-CLL cases (including the IGHV3-21 M-CLL) had an increment similar to U-CLL, documenting no substantial differences between these U-CLL and M-CLL cases.

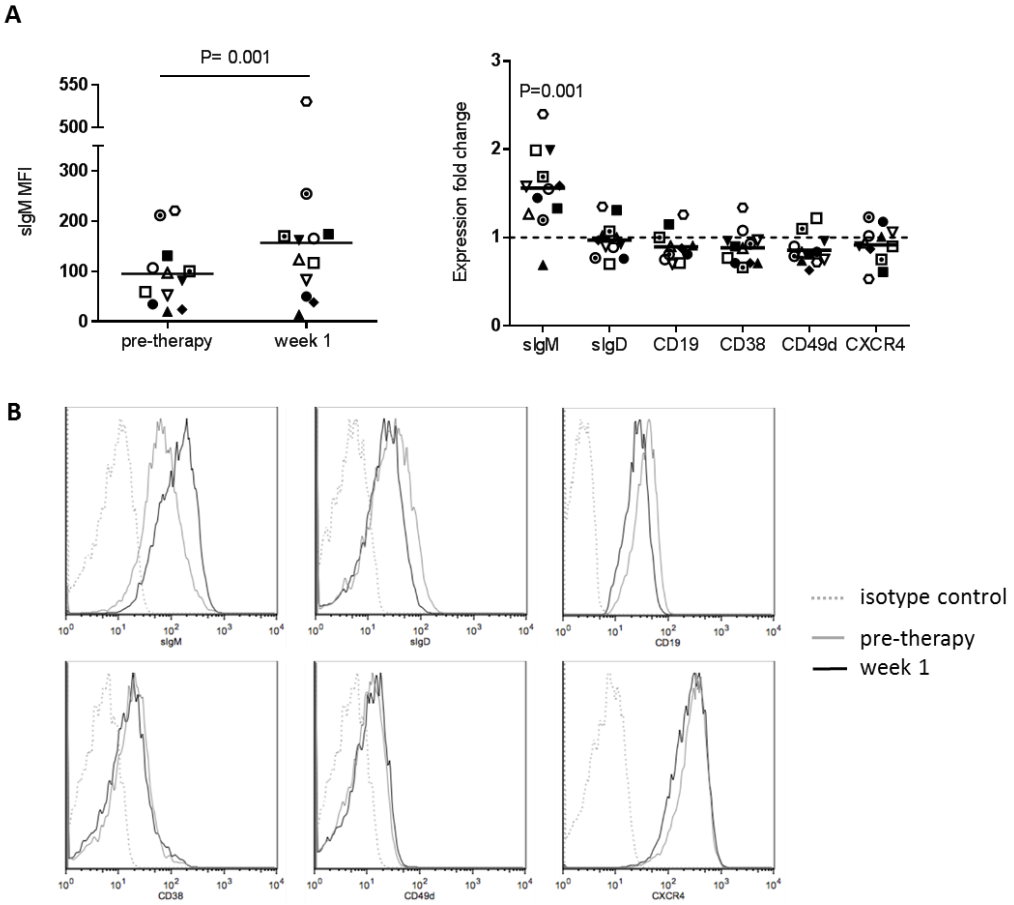

Figure 44. Surface IgM expression is increased on CLL cells at week 1 of Ibrutinib therapy. **(A)** PBMCs taken prior to and at week 1 of Ibrutinib therapy were analyzed for cell surface marker expression. Left panel shows surface IgM (sIgM) mean fluorescence intensity (MFI) following subtraction of isotype control MFI. Right panel shows fold change for the expression of each marker compared with pre-therapy. Pre-therapy values were normalized to one (dashed line). The statistical significance of difference was analyzed using the Wilcoxon-signed rank test. Horizontal lines indicate mean values. **(B)** An example (case 644) of the flow cytometric plots. Full grey line indicates expression at pre-therapy, full black line indicates expression at week 1 of therapy, dashed grey line indicates isotype control.

SIgM levels were then determined in the circulating CLL cells recently egressed from tissue sites ($CXCR4^{dim}CD5^{hi}$) and in those that had been persisting in the circulation ($CXCR4^{bright}CD5^{low}$) [330]. At week 1, both the $CXCR4^{dim}CD5^{hi}$ and the $CXCR4^{bright}CD5^{low}$ absolute cell counts increased in the peripheral blood. On average, the relative proportion of the tissue egressed fraction was higher (mean percentage, 33% pre-therapy, 39% week 1) while the $CXCR4^{bright}CD5^{low}$ fraction lower (mean percentage, 28% pre-therapy, 23% week 1; Figure 45A-B), although the differences were not significant. However, the

sIgM increase was significant and similar in both the CXCR4^{dim}CD5^{hi} cells and the CXCR4^{bright}CD5^{low} cells (median fold increase 1.4 in both fractions; Figure 45C). These data indicated that sIgM increased in all fractions and suggested that the increase was not simply a reflection of the redistribution of subpopulations with different sIgM levels [352].

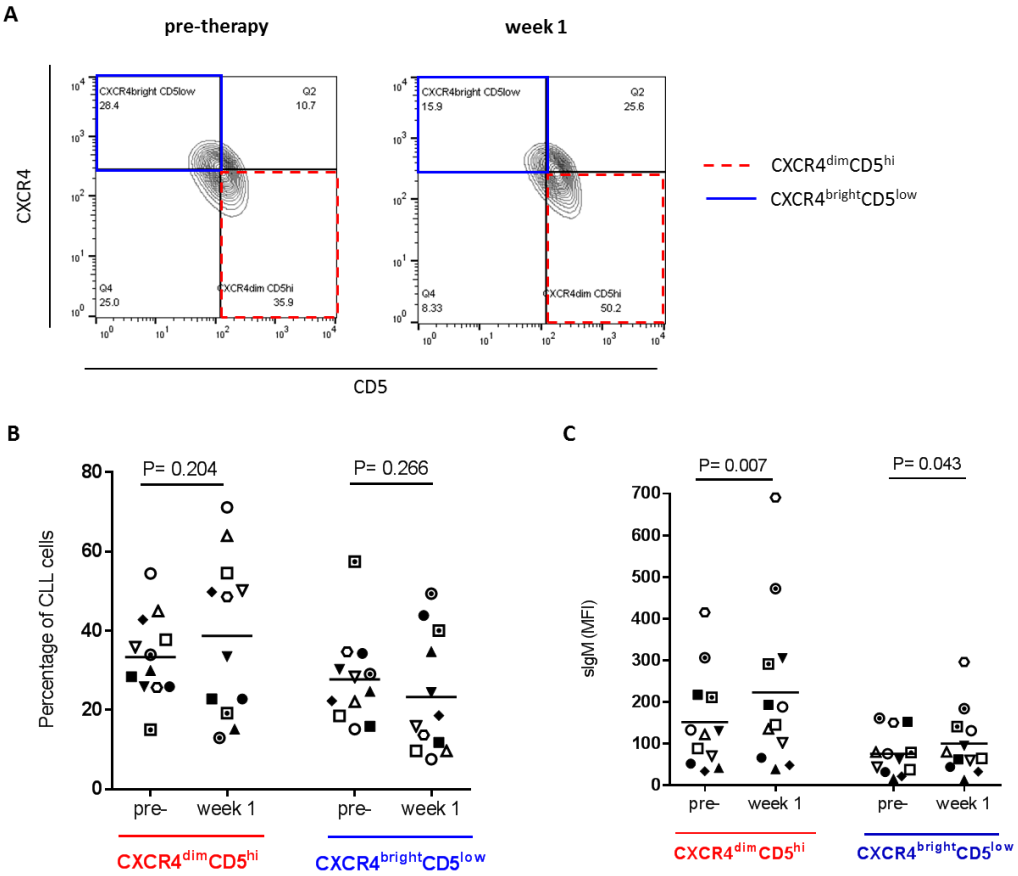

Figure 45. Both CXCR4^{dim}CD5^{hi} and CXCR4^{bright}CD5^{low} fractions increase sIgM expression on Ibrutinib therapy. PBMCs were taken prior to and at week 1 of Ibrutinib therapy. **(A)** Representative plot (case 531) showing the gating strategy to identify the CXCR4^{dim}CD5^{hi} and CXCR4^{bright}CD5^{low} fractions. **(B)** The percentage of CLL cells expressing CXCR4^{dim}CD5^{hi} and CXCR4^{bright}CD5^{low} in all 12 CLL patients. The statistical significance of difference was analyzed using the Wilcoxon-signed rank test. **(C)** The expression of sIgM by the CXCR4^{dim}CD5^{hi} and CXCR4^{bright}CD5^{low} fractions in all 12 CLL patients. The statistical significance of difference was analyzed using the Wilcoxon-signed rank test. Horizontal lines indicate mean values.

3.4.4 Increased sIgM expression is associated with mature fully N-glycosylated μ-chains.

Assessment of the N-glycosylation status of the sIgM μ-chains was used to investigate if the increased sIgM levels were associated with sIgM maturation, since it has been shown that in circulating CLL cells IgM μ-chains can exist in both immature (oligomannosylated) or mature (with complex sugars) form [353]. Samples from 3 Ibrutinib-treated patients were chosen, 2 which had increased sIgM levels on ibrutinib (551 and 343) and the single patient which had maintained similarly very low sIgM levels on therapy (case 489; Figure 46). The ratio of mature to immature glycoforms increased in both the patients with increased sIgM, while it did not change in the patient that did not increase sIgM levels. In fact, the sample that had the greatest increase in sIgM expression (551) also had the greatest increase in the expression of the mature glycoform. These data support the hypothesis that recovery of expression of mature sIgM in CLL cells is the result of the failure of Ibrutinib-treated cells to re-engage with antigen in tissue sites [25, 353].

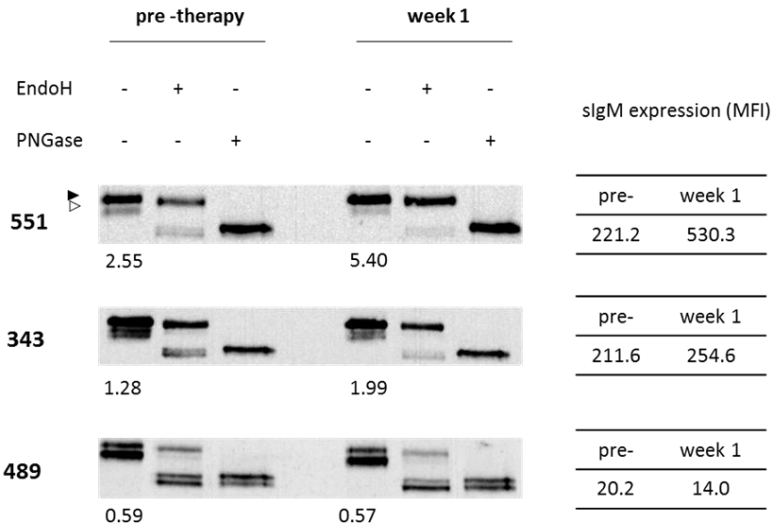

Figure 46. Increase of sIgM expression is associated with μ-chain mature glycosylation pattern. Purified surface proteins of 3 patients on Ibrutinib therapy were treated with EndoH, PNGase or untreated, and analyzed by immunoblotting. The ratio of expression of the two glycoforms of the μ-chain (mature/immature) is shown for each sample. Filled arrow represents the mature glycoform, open arrow represents the immature glycoform.

3.4.5 Increased sIgM expression correlates with increased inducibility of SYK phosphorylation

The induced phosphorylation of SYK, which is upstream of BTK, was measured to determine if the elevated levels of sIgM on the CLL cells were functional during Ibrutinib therapy. As shown in Figure 47A-B, the basal levels of SYK phosphorylation were significantly reduced during treatment, while the ability of anti-IgM to induce SYK phosphorylation was maintained following Ibrutinib commencement.

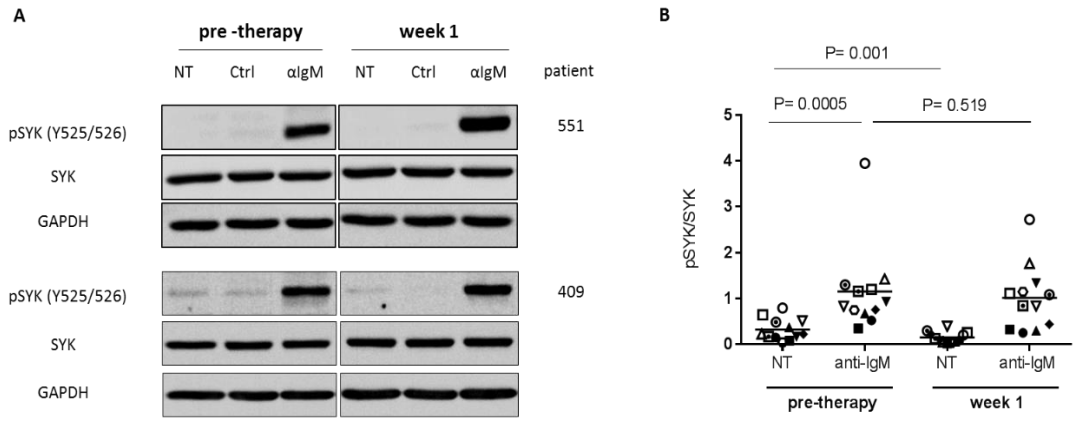

Figure 47. SYK activity is maintained following anti-IgM stimulation in CLL cells from patients on Ibrutinib. PBMCs taken prior to and at week 1 of Ibrutinib therapy were stimulated with polyclonal control (Ctrl), anti-IgM $F(ab')_{2f}$ (αIgM) or left untreated (NT). **(A)** Immunoblots of two cases (551 and 409) showing expression of pSYK and of total SYK. GAPDH was used as loading control. **(B)** SYK phosphorylation for all 12 CLL samples. The statistical significance of difference was analyzed using the Wilcoxon-signed rank test. Horizontal lines indicate mean values.

By defining "inducibility" as the ratio of induced/basal phosphoprotein levels at each time point, we found that, since pSYK basal level was decreased at week 1, IgM mediated SYK inducibility appeared greater than pre-therapy (P=0.012; Figure 48A). This inducibility correlated both with overall sIgM levels at week 1 (r=0.64, P=0.03; Figure 48B) and with the differential increase of sIgM levels (Figure 48C). These results demonstrated the maintained capacity of anti-IgM to induce SYK activity during Ibrutinib therapy, and that the changes of sIgM levels influence SYK activation.

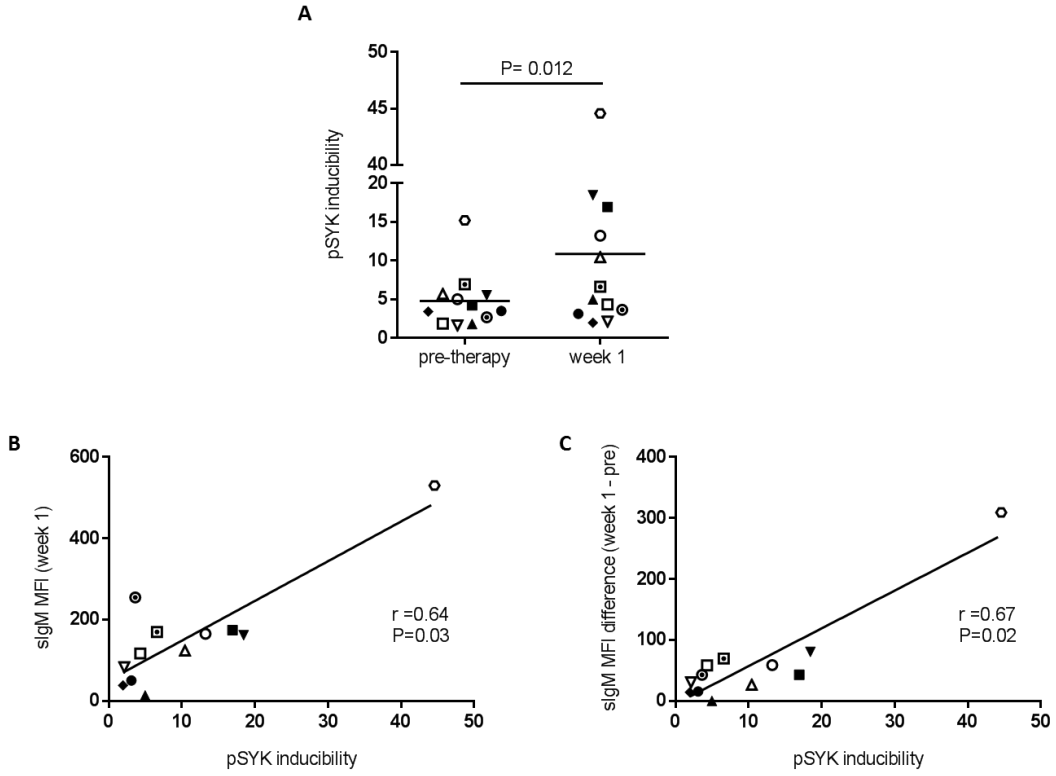

Figure 48. IgM mediated SYK inducibility is increased after one week of Ibrutinib therapy and correlates with changes in sIgM levels. (A) Inducibility of pSYK was calculated as the ratio between anti-IgM induced pSYK/SYK and NT pSYK/SYK pre-therapy and at week 1 in each CLL sample. Horizontal lines indicate mean values. The statistical significance of difference was analyzed using the Wilcoxon-signed rank test. **(B)** Correlation between anti-IgM pSYK inducibility and the expression of sIgM at week 1 of Ibrutinib therapy determined by flow cytometry. Linear regression and Spearman correlation are shown. **(C)** Correlation between anti-IgM pSYK inducibility at week 1 of therapy and the differential expression of sIgM determined by flow cytometry. Inducibility of pSYK was calculated as the ratio between anti-IgM induced pSYK/SYK and NT pSYK/SYK at week 1 in each CLL sample. Linear regression and Spearman correlation are shown.

3.4.6 Anti-IgM-mediated SYK induction associates with the residual signaling capacity downstream of BTK

In order to further investigate the consequences of Ibrutinib on the BCR-mediated pathways, the signaling capacity downstream of BTK was measured by assessment of iCa^{2+} mobilization and by ERK1/2 activity following sIgM stimulation.

Anti-IgM-mediated iCa^{2+} mobilization capacity was significantly reduced but not abolished during Ibrutinib therapy (P=0.016) with a mean reduction from 37% (range 1-77%) to 23% (1-44%) (Figure 49A-B). However, by using the 23%

mean value to discriminate patients with residual low and high signaling capacity at week 1, we found that residual low iCa^{2+} signalers had lower SYK induction than residual high signalers (P=0.009; Figure 49C). These data revealed an association between the ability of anti-IgM to induce SYK phosphorylation and to induce iCa^{2+} mobilization in CLL cells of patients on Ibrutinib.

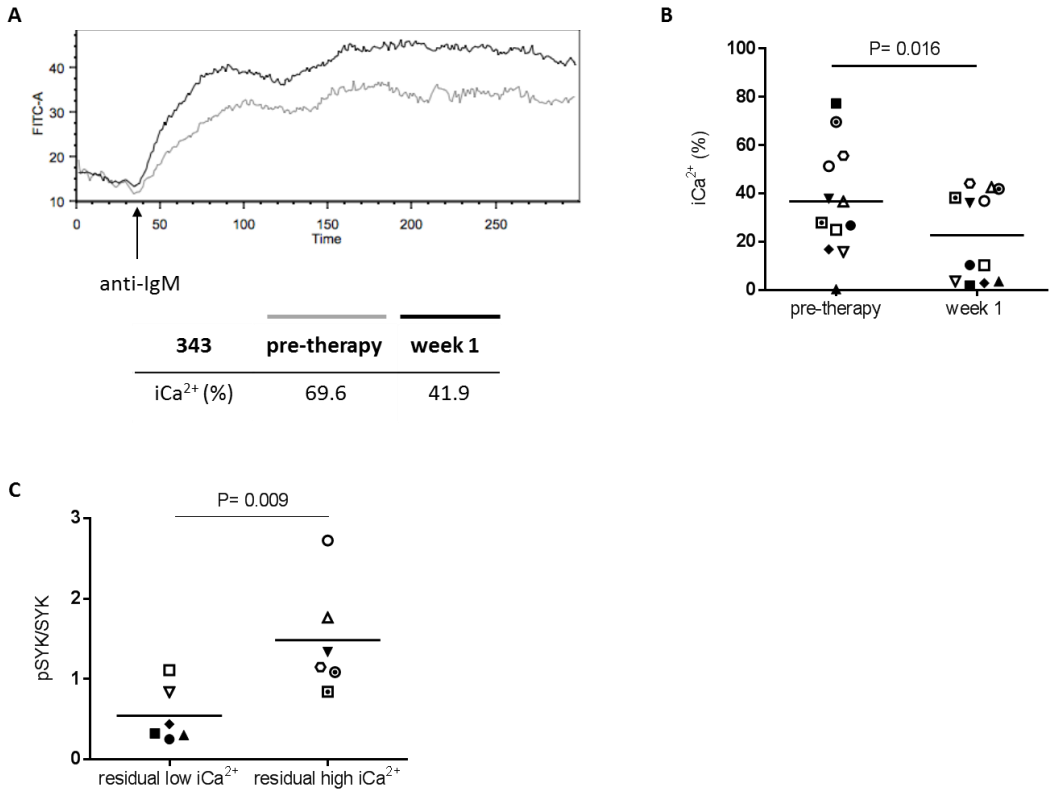

Figure 49. Anti-IgM induced intracellular Ca^{2+} mobilization is reduced during Ibrutinib therapy. PBMCs taken prior to and at week 1 of Ibrutinib therapy were stimulated with anti-IgM $F(ab')_2$ antibody, and intracellular iCa^{2+} (iCa^{2+} %) mobilization was measured by flow cytometry. **(A)** Intracellular iCa^{2+} of case 343 is represented as an example of the flow cytometric plots. Full grey line indicates pre-therapy, full black line indicates week 1 of therapy. The arrow indicates stimulation with anti-IgM $F(ab')_2$ polyclonal antibody. **(B)** Anti-IgM intracellular iCa^{2+} signaling capacity for all 12 CLL samples. The statistical significance of difference was analyzed using the Wilcoxon-signed rank test. **(C)** The mean iCa^{2+} % value was used to divide CLL samples at week 1 of Ibrutinib therapy into residual high signalers (>23% iCa^{2+} %) and residual low signalers (<23% iCa^{2+} %), and the two groups were associated with anti-IgM induced SYK phosphorylation at week 1 (pSYK/SYK). SYK phosphorylation was measured as the ratio between pSYK and total SYK optical density (pSYK/SYK). The statistical significance of difference was analyzed using the Mann-Whitney test. Horizontal lines indicate mean values.

At week 1, the basal levels of ERK1/2 phosphorylation were reduced and less variable than pre-therapy, and the mean anti-IgM induced ERK1/2

phosphorylation was significantly reduced (Figure 50A-B). However, the residual ERK1/2 phosphorylation capacity was variable between individual cases and higher than pre-therapy in one patient. As per iCa^{2+}, we used the mean value of anti-IgM induced ERK1/2 phosphorylation to discriminate patients with residual low and high signaling capacity at week 1; we found that residual low signalers had lower induction of SYK phosphorylation than residual high signalers (P=0.048; Figure 50C).

These data reveal that, while activation of BTK appears inhibited, sIgM stimulation can induce residual downstream activity that correlates with the induced SYK phosphorylation during Ibrutinib.

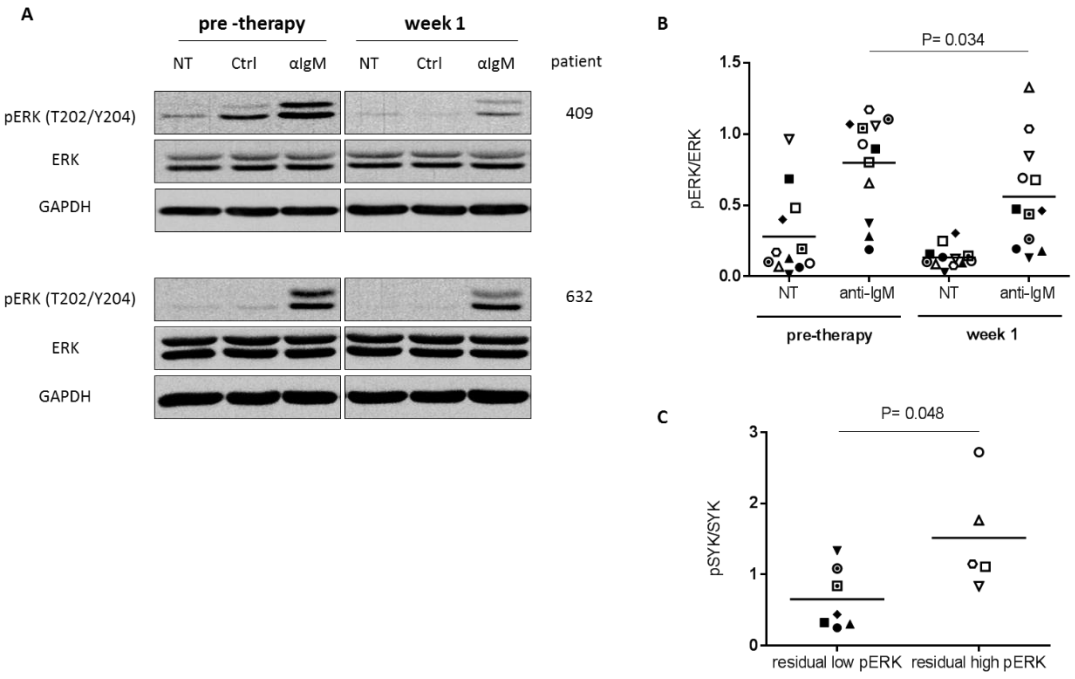

Figure 50. Anti-IgM induced phosphorylation of ERK is reduced at week 1 of Ibrutinib therapy. PBMCs taken prior to and at week 1 of Ibrutinib therapy were stimulated with polyclonal control (Ctrl), anti-IgM $F(ab')_2$ (αIgM) or left untreated (NT). **(A)** Immunoblots of two cases (409 and 632) showing expression of phosphorylated and total ERK1/2 protein. GAPDH was used as loading control. **(B)** ERK1/2 phosphorylation of each sample was measured as the ratio between pERK and total ERK optical density (pERK/ERK) for each condition. The statistical significance of difference was analyzed using the Wilcoxon-signed rank test. **(C)** CLL samples were divided by their anti-IgM signaling capacity at week 1 of Ibrutinib therapy (pERK/ERK). Residual high signalers (pERK/ERK>0.56) and residual low signalers (pERK/ERK<0.56) associated with anti-IgM induced SYK phosphorylation at week 1. The statistical significance of difference was analyzed using the Mann-Whitney test. Horizontal lines indicate mean values.

3.4.7 CXCL12-mediated signaling through CXCR4 is inhibited in the circulating CLL cells of patients o Ibrutinib

In order to investigate the direct effect of BTK inhibition on CXCR4-mediated signaling in patients, CXCL12-induced ERK phosphorylation was measured *in vitro* by immunoblotting. CXCR4-mediated capacity to induce ERK was evident in CLL cells prior to treatment commencement (Figure 51A-B). However, on average, CXCR4-mediated ERK1/2 phosphorylation capacity was significantly decreased in the circulating CLL cells at week 1 of treatment. These data indicate that CXCR4 signaling capacity is inhibited in patients in the early phases of Ibrutinib therapy.

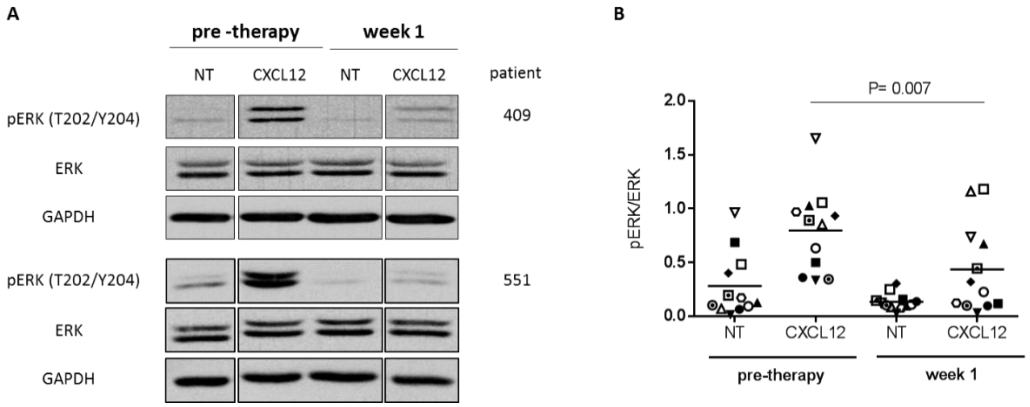

Figure 51. CXCR4 signaling is reduced in CLL cells from patients on Ibrutinib. PBMCs taken prior to and at week 1 of Ibrutinib therapy were stimulated with CXCL12 or left untreated (NT). **(A)** Immunoblots of two cases (409 and 551) showing expression of phosphorylated and total ERK. GAPDH was used as loading control. **(B)** ERK phosphorylation of each sample was measured as the ratio between pERK and total ERK optical density (pERK/ERK) for each condition. The statistical significance of difference was analyzed using the Wilcoxon-signed rank test. Horizontal lines indicate mean values.

3.5 Discussion

In CLL the role of the BCR has been proven to have a great influence on tumor cell behavior, and sIgM levels and signaling capacity have been associated with disease progression [158]. Thus, BCR-mediated signaling inside the cells has become an attractive target for therapy, and it has led to the development of inhibitors that are specific for the main kinases involved in the pathway.

The BTK inhibitor Ibrutinib has given encouraging results for CLL treatment, and it has been approved for clinical use by the US FDA. The ability of Ibrutinib treatment to target and block BTK activity has been demonstrated by *in vitro* studies, which additionally reported the inhibition of the pathways downstream of the kinase [74, 321]. However, the functional consequences on the intracellular signaling in response to sIgM stimulation during Ibrutinib treatment *in vivo* are not completely elucidated.

In this study, we investigated the status of sIgM on tumor cells from CLL patients prior to and at week one of Ibrutinib therapy, in order to determine the consequences of the treatment on the BCR in terms of surface expression and signaling capacity. Week 1 of treatment was chosen as an early time point of therapy in which all the patients experienced the classical increment in peripheral lymphocytosis seen during Ibrutinib administration [79]. Ibrutinib, in fact, is known to prevent the return of circulating CLL cells to tissue sites, while their egress will continue during treatment. At week 1 of therapy, the circulating cells will include two fractions, identified as $CXCR4^{dim}CD5^{hi}$ recent emigrants, and $CXCR4^{bright}CD5^{low}$ earlier emigrants respectively [330]. However, the proportions are difficult to estimate and the phenotype is likely to change overtime [352]. Our results demonstrate that sIgM expression is higher in the recently egressed CLL cells, however we observe that both fractions have increased their relative sIgM levels on therapy, suggesting that the reversible downregulation of sIgM due to antigen noted *in vitro* is a feature of both recent and earlier emigrant CLL cells circulating in the peripheral blood [25]. Direct evidence of the re-expression of IgM in the absence of antigen was obtained by studying the Ig maturational status by N-glycosylation pattern analysis. N-glycosylation consists of adding glycans to

a specific acceptor motif present on the proteins. The process starts in the endoplasmic reticulum (ER), where oligomannoses are added to the Asn of the target sequence (Asn-X-Ser/Thr motif, where X is any amino acid except Pro); while passing through the Golgi network, more complex glycans are added to the existing chain, making the protein mature and ready to be exposed on the membrane [354]. An *in vitro* study has previously demonstrated that the sIg μ-chains of CLL cells exist in two forms: a mature form, characterized by the presence of complex glycans on the Ig (resembling the condition observed in normal B cells), and a more immature form, characterized by the presence of oligomannoses on the μ-chains [353]. In our study, we find that the recovered sIgM expressed the fully N-glycosylated form in the Ibrutinib-treated cases, supporting the concept that CLL cells released from the tissue are kept away from antigen exposure, favoring the maturation of the sIgM.

After one week of therapy, basal BTK phosphorylation is significantly inhibited, as expected, but also the ability of the cells to phosphorylate BTK after a strong anti-IgM stimulus is suppressed. However, we find that the signaling upstream of BTK is still active, and the BCR-mediated stimulus can induce SYK phosphorylation and residual downstream activity. Since SYK lies upstream of BTK, it is not surprising that its activation occurs at week one of Ibrutinib therapy. Conversely, the residual anti-IgM induced phosphorylation of ERK and the intracellular calcium mobilization observed in the patients involved in the study indicate the presence of a potential pathway that can operate even in the presence of the drug. Previous studies have reported that in a BTK-deficient cell line, anti-IgM induced tyrosine phosphorylation of PLCγ2 is significantly reduced. This leads to the loss of both BCR-coupled phosphatidylinositol hydrolysis and iCa^{2+} mobilization, and any residual iCa^{2+} signaling would imply incomplete inhibition of BTK [355]. However, the possibility that BTK is not completely suppressed in the Ibrutinib patients involved in the study seems unlikely, because of the observed inhibition of BTK induction even after a strong stimulation through the BCR. Moreover, BTK occupancy assays have shown that the irreversible complete BTK occupation occurs after less than 4 hours from the first dose [77, 346]. Residual iCa^{2+} mobilization has been observed in BTK-deficient XLA B

cells [356], and BTK knock out in B cells has documented that iCa^{2+} mobilization requires BTK only partially [135], while pathways proposed to bypass BTK at least in part require SYK [357], and signal either through AKT or PKCδ [358].

Previous *in vitro* and murine studies have reported that CXCR4 signaling is inhibited by Ibrutinib [139, 328, 342]. Our results confirm these findings, indicating that the CXCR4-mediated pathway is inhibited also during *in vivo* treatment. The direct consequence of the inhibition could be that CLL cells during therapy may be held in circulation *in limbo* [348]. In the absence of survival signals coming from the tissue, where lymphocytes encounter antigen and are stimulated, CLL cells kept in the periphery will eventually die [359].

Future studies may be directed to the *in vivo* analysis of therapy combination. Treatment with Venetoclax, a BH3-mimetic that targets BCL-2 (section 1.1.5), has already been proposed in addition to Ibrutinib, in order to exploit the cytotoxic effect of Venetoclax on CLL cells that have been kept in the periphery, so away from the supportive tissue microenvironment, by Ibrutinib.

In conclusion, our data indicate that the circulating CLL cells of patients on Ibrutinib express higher levels of functional sIgM. Our data reveal enhanced signal inducibility upstream of BTK, which correlates with sIgM levels. While BTK inhibition appears to prevent access to tissue via CXCR4 inhibition, the data may point to a dangerous condition in which CLL cells can become super-responsive if therapy is stopped too early and cells re-encounter antigen in tissue sites.

REFERENCES

1. Caligaris-Cappio, F. and T.J. Hamblin, *B-cell chronic lymphocytic leukemia: a bird of a different feather.* J Clin Oncol, 1999. **17**(1): p. 399-408.
2. Dores, G.M., et al., *Chronic lymphocytic leukaemia and small lymphocytic lymphoma: overview of the descriptive epidemiology.* Br J Haematol, 2007. **139**(5): p. 809-19.
3. Siegel, R., et al., *Cancer statistics, 2011: the impact of eliminating socioeconomic and racial disparities on premature cancer deaths.* CA Cancer J Clin, 2011. **61**(4): p. 212-36.
4. Landgren, O., et al., *Acquired immune-related and inflammatory conditions and subsequent chronic lymphocytic leukaemia.* Br J Haematol, 2007. **139**(5): p. 791-8.
5. Wiernik, P.H., et al., *Anticipation in familial chronic lymphocytic leukaemia.* Br J Haematol, 2001. **113**(2): p. 407-14.
6. Barcellini, W., et al., *Relationship between autoimmune phenomena and disease stage and therapy in B-cell chronic lymphocytic leukemia.* Haematologica, 2006. **91**(12): p. 1689-92.
7. Binet, J.L., et al., *Perspectives on the use of new diagnostic tools in the treatment of chronic lymphocytic leukemia.* Blood, 2006. **107**(3): p. 859-61.
8. Landgren, O., et al., *Risk of second malignant neoplasms among lymphoma patients with a family history of cancer.* Int J Cancer, 2007. **120**(5): p. 1099-102.
9. Hallek, M., et al., *Guidelines for the diagnosis and treatment of chronic lymphocytic leukemia: a report from the International Workshop on Chronic Lymphocytic Leukemia updating the National Cancer Institute-Working Group 1996 guidelines.* Blood, 2008. **111**(12): p. 5446-56.
10. Nowakowski, G.S., et al., *Percentage of smudge cells on routine blood smear predicts survival in chronic lymphocytic leukemia.* J Clin Oncol, 2009. **27**(11): p. 1844-9.
11. Marti, G.E., et al., *Diagnostic criteria for monoclonal B-cell lymphocytosis.* Br J Haematol, 2005. **130**(3): p. 325-32.
12. Rawstron, A.C., et al., *Monoclonal B-cell lymphocytosis and chronic lymphocytic leukemia.* N Engl J Med, 2008. **359**(6): p. 575-83.
13. Moreau, E.J., et al., *Improvement of the chronic lymphocytic leukemia scoring system with the monoclonal antibody SN8 (CD79b).* Am J Clin Pathol, 1997. **108**(4): p. 378-82.
14. Rai, K.R., et al., *Clinical staging of chronic lymphocytic leukemia.* Blood, 1975. **46**(2): p. 219-34.
15. Binet, J.L., et al., *A new prognostic classification of chronic lymphocytic leukemia derived from a multivariate survival analysis.* Cancer, 1981. **48**(1): p. 198-206.
16. Hallek, M., *Chronic lymphocytic leukemia: 2015 Update on diagnosis, risk stratification, and treatment.* Am J Hematol, 2015. **90**(5): p. 446-60.
17. Melo, J.V., D. Catovsky, and D.A. Galton, *Chronic lymphocytic leukemia and prolymphocytic leukemia: a clinicopathological reappraisal.* Blood Cells, 1987. **12**(2): p. 339-53.
18. Hallek, M., et al., *Elevated serum thymidine kinase levels identify a subgroup at high risk of disease progression in early, nonsmoldering chronic lymphocytic leukemia.* Blood, 1999. **93**(5): p. 1732-7.
19. Sarfati, M., et al., *Prognostic importance of serum soluble CD23 level in chronic lymphocytic leukemia.* Blood, 1996. **88**(11): p. 4259-64.

20. Damle, R.N., et al., *Ig V gene mutation status and CD38 expression as novel prognostic indicators in chronic lymphocytic leukemia.* Blood, 1999. **94**(6): p. 1840-7.
21. Hamblin, T.J., et al., *Unmutated Ig V(H) genes are associated with a more aggressive form of chronic lymphocytic leukemia.* Blood, 1999. **94**(6): p. 1848-54.
22. Ibrahim, S., et al., *CD38 expression as an important prognostic factor in B-cell chronic lymphocytic leukemia.* Blood, 2001. **98**(1): p. 181-6.
23. Ghia, P. and F. Caligaris-Cappio, *The indispensable role of microenvironment in the natural history of low-grade B-cell neoplasms.* Adv Cancer Res, 2000. **79**: p. 157-73.
24. Schweighoffer, E., et al., *Unexpected requirement for ZAP-70 in pre-B cell development and allelic exclusion.* Immunity, 2003. **18**(4): p. 523-33.
25. Mockridge, C.I., et al., *Reversible anergy of sIgM-mediated signaling in the two subsets of CLL defined by VH-gene mutational status.* Blood, 2007. **109**(10): p. 4424-31.
26. Chen, L., et al., *Expression of ZAP-70 is associated with increased B-cell receptor signaling in chronic lymphocytic leukemia.* Blood, 2002. **100**(13): p. 4609-14.
27. Wiestner, A., et al., *ZAP-70 expression identifies a chronic lymphocytic leukemia subtype with unmutated immunoglobulin genes, inferior clinical outcome, and distinct gene expression profile.* Blood, 2003. **101**(12): p. 4944-51.
28. Poulain, S., et al., *Is ZAP-70 expression stable over time in B chronic lymphocytic leukaemia?* Leuk Lymphoma, 2007. **48**(6): p. 1219-21.
29. Degheidy, H.A., et al., *Methodological comparison of two anti-ZAP-70 antibodies.* Cytometry B Clin Cytom, 2011. **80**(5): p. 300-8.
30. Calin, G.A., et al., *Frequent deletions and down-regulation of micro- RNA genes miR15 and miR16 at 13q14 in chronic lymphocytic leukemia.* Proc Natl Acad Sci U S A, 2002. **99**(24): p. 15524-9.
31. Zenz, T., et al., *From pathogenesis to treatment of chronic lymphocytic leukaemia.* Nat Rev Cancer, 2010. **10**(1): p. 37-50.
32. Seiffert, M., et al., *Exploiting biological diversity and genomic aberrations in chronic lymphocytic leukemia.* Leuk Lymphoma, 2012. **53**(6): p. 1023-31.
33. Krober, A., et al., *V(H) mutation status, CD38 expression level, genomic aberrations, and survival in chronic lymphocytic leukemia.* Blood, 2002. **100**(4): p. 1410-6.
34. Oscier, D.G., et al., *Multivariate analysis of prognostic factors in CLL: clinical stage, IGVH gene mutational status, and loss or mutation of the p53 gene are independent prognostic factors.* Blood, 2002. **100**(4): p. 1177-84.
35. Dohner, H., et al., *Genomic aberrations and survival in chronic lymphocytic leukemia.* N Engl J Med, 2000. **343**(26): p. 1910-6.
36. Harley, C.B., A.B. Futcher, and C.W. Greider, *Telomeres shorten during ageing of human fibroblasts.* Nature, 1990. **345**(6274): p. 458-60.
37. Blackburn, E.H., C.W. Greider, and J.W. Szostak, *Telomeres and telomerase: the path from maize, Tetrahymena and yeast to human cancer and aging.* Nat Med, 2006. **12**(10): p. 1133-8.
38. Terrin, L., et al., *Telomerase expression in B-cell chronic lymphocytic leukemia predicts survival and delineates subgroups of patients with the same igVH mutation status and different outcome.* Leukemia, 2007. **21**(5): p. 965-72.
39. Tchirkov, A., et al., *hTERT expression and prognosis in B-chronic lymphocytic leukemia.* Ann Oncol, 2004. **15**(10): p. 1476-80.

40. Rampazzo, E., et al., *Telomere length and telomerase levels delineate subgroups of B-cell chronic lymphocytic leukemia with different biological characteristics and clinical outcomes.* Haematologica, 2012. **97**(1): p. 56-63.
41. Ward, B.P., G.J. Tsongalis, and P. Kaur, *MicroRNAs in chronic lymphocytic leukemia.* Exp Mol Pathol, 2011. **90**(2): p. 173-8.
42. Kluiver, J.L. and C.Z. Chen, *MicroRNAs regulate B-cell receptor signaling-induced apoptosis.* Genes Immun, 2012. **13**(3): p. 239-44.
43. Ferracin, M., et al., *MicroRNAs involvement in fludarabine refractory chronic lymphocytic leukemia.* Mol Cancer, 2010. **9**: p. 123.
44. Calin, G.A., et al., *MicroRNA profiling reveals distinct signatures in B cell chronic lymphocytic leukemias.* Proc Natl Acad Sci U S A, 2004. **101**(32): p. 11755-60.
45. Rai, K.R., et al., *Fludarabine compared with chlorambucil as primary therapy for chronic lymphocytic leukemia.* N Engl J Med, 2000. **343**(24): p. 1750-7.
46. Dillman, R.O., R. Mick, and O.R. McIntyre, *Pentostatin in chronic lymphocytic leukemia: a phase II trial of Cancer and Leukemia group B.* J Clin Oncol, 1989. **7**(4): p. 433-8.
47. Robak, T., et al., *Cladribine with prednisone versus chlorambucil with prednisone as first-line therapy in chronic lymphocytic leukemia: report of a prospective, randomized, multicenter trial.* Blood, 2000. **96**(8): p. 2723-9.
48. Yamauchi, T., et al., *DNA repair initiated in chronic lymphocytic leukemia lymphocytes by 4-hydroperoxycyclophosphamide is inhibited by fludarabine and clofarabine.* Clin Cancer Res, 2001. **7**(11): p. 3580-9.
49. Bellosillo, B., et al., *In vitro evaluation of fludarabine in combination with cyclophosphamide and/or mitoxantrone in B-cell chronic lymphocytic leukemia.* Blood, 1999. **94**(8): p. 2836-43.
50. Flinn, I.W., et al., *Phase III trial of fludarabine plus cyclophosphamide compared with fludarabine for patients with previously untreated chronic lymphocytic leukemia: US Intergroup Trial E2997.* J Clin Oncol, 2007. **25**(7): p. 793-8.
51. Knauf, W.U., et al., *Phase III randomized study of bendamustine compared with chlorambucil in previously untreated patients with chronic lymphocytic leukemia.* J Clin Oncol, 2009. **27**(26): p. 4378-84.
52. Fischer, K., et al., *Bendamustine in combination with rituximab for previously untreated patients with chronic lymphocytic leukemia: a multicenter phase II trial of the German Chronic Lymphocytic Leukemia Study Group.* J Clin Oncol, 2012. **30**(26): p. 3209-16.
53. Alas, S., C. Emmanouilides, and B. Bonavida, *Inhibition of interleukin 10 by rituximab results in down-regulation of bcl-2 and sensitization of B-cell non-Hodgkin's lymphoma to apoptosis.* Clin Cancer Res, 2001. **7**(3): p. 709-23.
54. Wierda, W., et al., *Chemoimmunotherapy with fludarabine, cyclophosphamide, and rituximab for relapsed and refractory chronic lymphocytic leukemia.* J Clin Oncol, 2005. **23**(18): p. 4070-8.
55. Tam, C.S., et al., *Long-term results of the fludarabine, cyclophosphamide, and rituximab regimen as initial therapy of chronic lymphocytic leukemia.* Blood, 2008. **112**(4): p. 975-80.
56. Hallek, M., et al., *Addition of rituximab to fludarabine and cyclophosphamide in patients with chronic lymphocytic leukaemia: a randomised, open-label, phase 3 trial.* Lancet, 2010. **376**(9747): p. 1164-74.

57. Stilgenbauer, S. and H. Dohner, *Campath-1H-induced complete remission of chronic lymphocytic leukemia despite p53 gene mutation and resistance to chemotherapy.* N Engl J Med, 2002. **347**(6): p. 452-3.
58. Dreger, P. and E. Montserrat, *Autologous and allogeneic stem cell transplantation for chronic lymphocytic leukemia.* Leukemia, 2002. **16**(6): p. 985-92.
59. O'Brien, S., et al., *Randomized phase III trial of fludarabine plus cyclophosphamide with or without oblimersen sodium (Bcl-2 antisense) in patients with relapsed or refractory chronic lymphocytic leukemia.* J Clin Oncol, 2007. **25**(9): p. 1114-20.
60. Thomas, A., et al., *Bcl-2 and bax expression and chlorambucil-induced apoptosis in the T-cells and leukaemic B-cells of untreated B-cell chronic lymphocytic leukaemia patients.* Leuk Res, 2000. **24**(10): p. 813-21.
61. Pepper, C., et al., *Mcl-1 expression has in vitro and in vivo significance in chronic lymphocytic leukemia and is associated with other poor prognostic markers.* Blood, 2008. **112**(9): p. 3807-17.
62. Hussain, S.R., et al., *Mcl-1 is a relevant therapeutic target in acute and chronic lymphoid malignancies: down-regulation enhances rituximab-mediated apoptosis and complement-dependent cytotoxicity.* Clin Cancer Res, 2007. **13**(7): p. 2144-50.
63. Roberts, A.W., et al., *Substantial susceptibility of chronic lymphocytic leukemia to BCL2 inhibition: results of a phase I study of navitoclax in patients with relapsed or refractory disease.* J Clin Oncol, 2012. **30**(5): p. 488-96.
64. Seymour, J., *ABT-199 for chronic lymphocytic leukemia.* Clin Adv Hematol Oncol, 2014. **12**(10): p. 698-700.
65. Konopleva, M., et al., *Mechanisms of apoptosis sensitivity and resistance to the BH3 mimetic ABT-737 in acute myeloid leukemia.* Cancer Cell, 2006. **10**(5): p. 375-88.
66. Lee, E.F., et al., *Crystal structure of ABT-737 complexed with Bcl-xL: implications for selectivity of antagonists of the Bcl-2 family.* Cell Death Differ, 2007. **14**(9): p. 1711-3.
67. Mazumder, S., et al., *Mcl-1 Phosphorylation defines ABT-737 resistance that can be overcome by increased NOXA expression in leukemic B cells.* Cancer Res, 2012. **72**(12): p. 3069-79.
68. Chanan-Khan, A.A. and B.D. Cheson, *Lenalidomide for the treatment of B-cell malignancies.* J Clin Oncol, 2008. **26**(9): p. 1544-52.
69. Burger, J.A. and A. Peled, *CXCR4 antagonists: targeting the microenvironment in leukemia and other cancers.* Leukemia, 2009. **23**(1): p. 43-52.
70. Jones, J.A. and J.C. Byrd, *How will B-cell-receptor-targeted therapies change future CLL therapy?* Blood, 2014. **123**(10): p. 1455-60.
71. Chanan-Khan, A., et al., *Clinical efficacy of lenalidomide in patients with relapsed or refractory chronic lymphocytic leukemia: results of a phase II study.* J Clin Oncol, 2006. **24**(34): p. 5343-9.
72. Badoux, X.C., et al., *Phase II study of lenalidomide and rituximab as salvage therapy for patients with relapsed or refractory chronic lymphocytic leukemia.* J Clin Oncol, 2013. **31**(5): p. 584-91.
73. Sher, T., et al., *Efficacy of lenalidomide in patients with chronic lymphocytic leukemia with high-risk cytogenetics.* Leuk Lymphoma, 2010. **51**(1): p. 85-8.

74. Honigberg, L.A., et al., *The Bruton tyrosine kinase inhibitor PCI-32765 blocks B-cell activation and is efficacious in models of autoimmune disease and B-cell malignancy.* Proc Natl Acad Sci U S A, 2010. **107**(29): p. 13075-80.
75. Burger, J.A. and J.J. Buggy, *Bruton tyrosine kinase inhibitor ibrutinib (PCI-32765).* Leuk Lymphoma, 2013. **54**(11): p. 2385-91.
76. Advani, R.H., et al., *Bruton tyrosine kinase inhibitor ibrutinib (PCI-32765) has significant activity in patients with relapsed/refractory B-cell malignancies.* J Clin Oncol, 2013. **31**(1): p. 88-94.
77. Byrd, J.C., et al., *Targeting BTK with ibrutinib in relapsed chronic lymphocytic leukemia.* N Engl J Med, 2013. **369**(1): p. 32-42.
78. Wang, M.L., et al., *Targeting BTK with ibrutinib in relapsed or refractory mantle-cell lymphoma.* N Engl J Med, 2013. **369**(6): p. 507-16.
79. Herman, S.E., et al., *Ibrutinib-induced lymphocytosis in patients with chronic lymphocytic leukemia: correlative analyses from a phase II study.* Leukemia, 2014. **28**(11): p. 2188-96.
80. Burger, J.A., et al., *Safety and activity of ibrutinib plus rituximab for patients with high-risk chronic lymphocytic leukaemia: a single-arm, phase 2 study.* Lancet Oncol, 2014. **15**(10): p. 1090-9.
81. Srinivasan, L., et al., *PI3 kinase signals BCR-dependent mature B cell survival.* Cell, 2009. **139**(3): p. 573-86.
82. Okkenhaug, K. and B. Vanhaesebroeck, *PI3K in lymphocyte development, differentiation and activation.* Nat Rev Immunol, 2003. **3**(4): p. 317-30.
83. Lannutti, B.J., et al., *CAL-101, a p110delta selective phosphatidylinositol-3-kinase inhibitor for the treatment of B-cell malignancies, inhibits PI3K signaling and cellular viability.* Blood, 2011. **117**(2): p. 591-4.
84. Jou, S.T., et al., *Essential, nonredundant role for the phosphoinositide 3-kinase p110delta in signaling by the B-cell receptor complex.* Mol Cell Biol, 2002. **22**(24): p. 8580-91.
85. Herman, S.E., et al., *Phosphatidylinositol 3-kinase-delta inhibitor CAL-101 shows promising preclinical activity in chronic lymphocytic leukemia by antagonizing intrinsic and extrinsic cellular survival signals.* Blood, 2010. **116**(12): p. 2078-88.
86. Ikeda, H., et al., *PI3K/p110{delta} is a novel therapeutic target in multiple myeloma.* Blood, 2010. **116**(9): p. 1460-8.
87. Hoellenriegel, J., et al., *The phosphoinositide 3'-kinase delta inhibitor, CAL-101, inhibits B-cell receptor signaling and chemokine networks in chronic lymphocytic leukemia.* Blood, 2011. **118**(13): p. 3603-12.
88. Brown, J.R., et al., *Idelalisib, an inhibitor of phosphatidylinositol 3-kinase p110delta, for relapsed/refractory chronic lymphocytic leukemia.* Blood, 2014. **123**(22): p. 3390-7.
89. Furman, R.R., et al., *Idelalisib and rituximab in relapsed chronic lymphocytic leukemia.* N Engl J Med, 2014. **370**(11): p. 997-1007.
90. Bantscheff, M., et al., *Quantitative chemical proteomics reveals mechanisms of action of clinical ABL kinase inhibitors.* Nat Biotechnol, 2007. **25**(9): p. 1035-44.
91. Hantschel, O., et al., *The Btk tyrosine kinase is a major target of the Bcr-Abl inhibitor dasatinib.* Proc Natl Acad Sci U S A, 2007. **104**(33): p. 13283-8.
92. Williams, N.K., et al., *Crystal structures of the Lyn protein tyrosine kinase domain in its Apo- and inhibitor-bound state.* J Biol Chem, 2009. **284**(1): p. 284-91.

93. Hallaert, D.Y., et al., *c-Abl kinase inhibitors overcome CD40-mediated drug resistance in CLL: implications for therapeutic targeting of chemoresistant niches.* Blood, 2008. **112**(13): p. 5141-9.
94. Amrein, P.C., et al., *Phase II study of dasatinib in relapsed or refractory chronic lymphocytic leukemia.* Clin Cancer Res, 2011. **17**(9): p. 2977-86.
95. Kater, A.P., et al., *Dasatinib in combination with fludarabine in patients with refractory chronic lymphocytic leukemia: a multicenter phase 2 study.* Leuk Res, 2014. **38**(1): p. 34-41.
96. Santos, F.P., et al., *Bafetinib, a dual Bcr-Abl/Lyn tyrosine kinase inhibitor for the potential treatment of leukemia.* Curr Opin Investig Drugs, 2010. **11**(12): p. 1450-65.
97. Contri, A., et al., *Chronic lymphocytic leukemia B cells contain anomalous Lyn tyrosine kinase, a putative contribution to defective apoptosis.* J Clin Invest, 2005. **115**(2): p. 369-78.
98. Kadia, T., et al., *A Pilot Phase II Study of the Lyn Kinase Inhibitor Bafetinib in Patients with Relapsed or Refractory B Cell Chronic Lymphocytic Leukemia.* Blood, 2011. **118**(21): p. 1232-1233.
99. Packard, T.A. and J.C. Cambier, *B lymphocyte antigen receptor signaling: initiation, amplification, and regulation.* F1000Prime Rep, 2013. **5**: p. 40.
100. Dighiero, G., *CLL biology and prognosis.* Hematology Am Soc Hematol Educ Program, 2005: p. 278-84.
101. Litman, G.W., et al., *Phylogenetic diversification of immunoglobulin genes and the antibody repertoire.* Mol Biol Evol, 1993. **10**(1): p. 60-72.
102. Kirkham, P.M. and H.W. Schroeder, Jr., *Antibody structure and the evolution of immunoglobulin V gene segments.* Semin Immunol, 1994. **6**(6): p. 347-60.
103. Tonegawa, S., *Somatic generation of antibody diversity.* Nature, 1983. **302**(5909): p. 575-81.
104. Dreyer, W.J. and J.C. Bennett, *The molecular basis of antibody formation: a paradox.* Proc Natl Acad Sci U S A, 1965. **54**(3): p. 864-9.
105. Grawunder, U., R.B. West, and M.R. Lieber, *Antigen receptor gene rearrangement.* Curr Opin Immunol, 1998. **10**(2): p. 172-80.
106. Early, P., et al., *An immunoglobulin heavy chain variable region gene is generated from three segments of DNA: VH, D and JH.* Cell, 1980. **19**(4): p. 981-92.
107. Cook, G.P. and I.M. Tomlinson, *The human immunoglobulin VH repertoire.* Immunol Today, 1995. **16**(5): p. 237-42.
108. Wiestner, A., *The role of B-cell receptor inhibitors in the treatment of patients with chronic lymphocytic leukemia.* Haematologica, 2015. **100**(12): p. 1495-507.
109. Pavri, R., et al., *Activation-induced cytidine deaminase targets DNA at sites of RNA polymerase II stalling by interaction with Spt5.* Cell, 2010. **143**(1): p. 122-33.
110. Muramatsu, M., et al., *Class switch recombination and hypermutation require activation-induced cytidine deaminase (AID), a potential RNA editing enzyme.* Cell, 2000. **102**(5): p. 553-63.
111. Zotos, D. and D.M. Tarlinton, *Determining germinal centre B cell fate.* Trends Immunol, 2012. **33**(6): p. 281-8.
112. Schroeder, H.W., Jr. and G. Dighiero, *The pathogenesis of chronic lymphocytic leukemia: analysis of the antibody repertoire.* Immunol Today, 1994. **15**(6): p. 288-94.

113. Stevenson, F.K., F. Forconi, and G. Packham, *The meaning and relevance of B-cell receptor structure and function in chronic lymphocytic leukemia.* Semin Hematol, 2014. **51**(3): p. 158-67.
114. Packham, G., et al., *The outcome of B-cell receptor signaling in chronic lymphocytic leukemia: proliferation or anergy.* Haematologica, 2014. **99**(7): p. 1138-48.
115. Klein, U., et al., *Gene expression profiling of B cell chronic lymphocytic leukemia reveals a homogeneous phenotype related to memory B cells.* J Exp Med, 2001. **194**(11): p. 1625-38.
116. Reth, M. and J. Wienands, *Initiation and processing of signals from the B cell antigen receptor.* Annu Rev Immunol, 1997. **15**: p. 453-79.
117. Cambier, J.C., *New nomenclature for the Reth motif (or ARH1/TAM/ARAM/YXXL).* Immunol Today, 1995. **16**(2): p. 110.
118. Saijo, K., et al., *Essential role of Src-family protein tyrosine kinases in NF-kappaB activation during B cell development.* Nat Immunol, 2003. **4**(3): p. 274-9.
119. Johnson, S.A., et al., *Phosphorylated immunoreceptor signaling motifs (ITAMs) exhibit unique abilities to bind and activate Lyn and Syk tyrosine kinases.* J Immunol, 1995. **155**(10): p. 4596-603.
120. Rowley, R.B., et al., *Syk protein-tyrosine kinase is regulated by tyrosine-phosphorylated Ig alpha/Ig beta immunoreceptor tyrosine activation motif binding and autophosphorylation.* J Biol Chem, 1995. **270**(19): p. 11590-4.
121. Reichlin, A., et al., *B cell development is arrested at the immature B cell stage in mice carrying a mutation in the cytoplasmic domain of immunoglobulin beta.* J Exp Med, 2001. **193**(1): p. 13-23.
122. Kraus, M., et al., *Ig-alpha cytoplasmic truncation renders immature B cells more sensitive to antigen contact.* Immunity, 1999. **11**(5): p. 537-45.
123. Torres, R.M. and K. Hafen, *A negative regulatory role for Ig-alpha during B cell development.* Immunity, 1999. **11**(5): p. 527-36.
124. Fruman, D.A., A.B. Satterthwaite, and O.N. Witte, *Xid-like phenotypes: a B cell signalosome takes shape.* Immunity, 2000. **13**(1): p. 1-3.
125. Fu, C., et al., *BLNK: a central linker protein in B cell activation.* Immunity, 1998. **9**(1): p. 93-103.
126. Justement, L.B., *The role of the protein tyrosine phosphatase CD45 in regulation of B lymphocyte activation.* Int Rev Immunol, 2001. **20**(6): p. 713-38.
127. Hata, A., et al., *Functional analysis of Csk in signal transduction through the B-cell antigen receptor.* Mol Cell Biol, 1994. **14**(11): p. 7306-13.
128. Nishizumi, H., et al., *Impaired proliferation of peripheral B cells and indication of autoimmune disease in lyn-deficient mice.* Immunity, 1995. **3**(5): p. 549-60.
129. Turner, M., et al., *Perinatal lethality and blocked B-cell development in mice lacking the tyrosine kinase Syk.* Nature, 1995. **378**(6554): p. 298-302.
130. Khan, W.N., et al., *The role of Bruton's tyrosine kinase in B-cell development and function in mice and man.* Ann N Y Acad Sci, 1995. **764**: p. 27-38.
131. Park, H., et al., *Regulation of Btk function by a major autophosphorylation site within the SH3 domain.* Immunity, 1996. **4**(5): p. 515-25.
132. Saito, K., A.M. Scharenberg, and J.P. Kinet, *Interaction between the Btk PH domain and phosphatidylinositol-3,4,5-trisphosphate directly regulates Btk.* J Biol Chem, 2001. **276**(19): p. 16201-6.
133. Fearon, D.T. and R.H. Carter, *The CD19/CR2/TAPA-1 complex of B lymphocytes: linking natural to acquired immunity.* Annu Rev Immunol, 1995. **13**: p. 127-49.

134. Carter, R.H., et al., *The CD19 complex of B lymphocytes. Activation of phospholipase C by a protein tyrosine kinase-dependent pathway that can be enhanced by the membrane IgM complex.* J Immunol, 1991. **147**(11): p. 3663-71.
135. Buhl, A.M. and J.C. Cambier, *Phosphorylation of CD19 Y484 and Y515, and linked activation of phosphatidylinositol 3-kinase, are required for B cell antigen receptor-mediated activation of Bruton's tyrosine kinase.* J Immunol, 1999. **162**(8): p. 4438-46.
136. Brooks, S.R., et al., *Systematic analysis of the role of CD19 cytoplasmic tyrosines in enhancement of activation in Daudi human B cells: clustering of phospholipase C and Vav and of Grb2 and Sos with different CD19 tyrosines.* J Immunol, 2000. **164**(6): p. 3123-31.
137. Carter, R.H., Y. Wang, and S. Brooks, *Role of CD19 signal transduction in B cell biology.* Immunol Res, 2002. **26**(1-3): p. 45-54.
138. Kurosaki, T., et al., *Regulation of the phospholipase C-gamma2 pathway in B cells.* Immunol Rev, 2000. **176**: p. 19-29.
139. Ponader, S., et al., *The Bruton tyrosine kinase inhibitor PCI-32765 thwarts chronic lymphocytic leukemia cell survival and tissue homing in vitro and in vivo.* Blood, 2012. **119**(5): p. 1182-9.
140. Johnson, G.L. and R. Lapadat, *Mitogen-activated protein kinase pathways mediated by ERK, JNK, and p38 protein kinases.* Science, 2002. **298**(5600): p. 1911-2.
141. D'Ambrosio, D., K.L. Hippen, and J.C. Cambier, *Distinct mechanisms mediate SHC association with the activated and resting B cell antigen receptor.* Eur J Immunol, 1996. **26**(8): p. 1960-5.
142. Ishiai, M., et al., *BLNK required for coupling Syk to PLC gamma 2 and Rac1-JNK in B cells.* Immunity, 1999. **10**(1): p. 117-25.
143. Hashimoto, A., et al., *Involvement of guanosine triphosphatases and phospholipase C-gamma2 in extracellular signal-regulated kinase, c-Jun NH2-terminal kinase, and p38 mitogen-activated protein kinase activation by the B cell antigen receptor.* J Exp Med, 1998. **188**(7): p. 1287-95.
144. Wagner, E.F. and A.R. Nebreda, *Signal integration by JNK and p38 MAPK pathways in cancer development.* Nat Rev Cancer, 2009. **9**(8): p. 537-49.
145. Niiro, H. and E.A. Clark, *Regulation of B-cell fate by antigen-receptor signals.* Nat Rev Immunol, 2002. **2**(12): p. 945-56.
146. Su, T.T., et al., *PKC-beta controls I kappa B kinase lipid raft recruitment and activation in response to BCR signaling.* Nat Immunol, 2002. **3**(8): p. 780-6.
147. Ruland, J. and T.W. Mak, *Transducing signals from antigen receptors to nuclear factor kappaB.* Immunol Rev, 2003. **193**: p. 93-100.
148. Dolmetsch, R.E., et al., *Differential activation of transcription factors induced by Ca2+ response amplitude and duration.* Nature, 1997. **386**(6627): p. 855-8.
149. Antony, P., et al., *B cell receptor directs the activation of NFAT and NF-kappaB via distinct molecular mechanisms.* Exp Cell Res, 2003. **291**(1): p. 11-24.
150. Nishizumi, H., et al., *A double-edged kinase Lyn: a positive and negative regulator for antigen receptor-mediated signals.* J Exp Med, 1998. **187**(8): p. 1343-8.
151. Tamir, I., J.M. Dal Porto, and J.C. Cambier, *Cytoplasmic protein tyrosine phosphatases SHP-1 and SHP-2: regulators of B cell signal transduction.* Curr Opin Immunol, 2000. **12**(3): p. 307-15.

152. Fong, D.C., et al., *Mutational analysis reveals multiple distinct sites within Fc gamma receptor IIB that function in inhibitory signaling.* J Immunol, 2000. **165**(8): p. 4453-62.
153. Hippen, K.L., et al., *Fc gammaRIIB1 inhibition of BCR-mediated phosphoinositide hydrolysis and Ca2+ mobilization is integrated by CD19 dephosphorylation.* Immunity, 1997. **7**(1): p. 49-58.
154. Ehrhardt, G.R., et al., *The inhibitory potential of Fc receptor homolog 4 on memory B cells.* Proc Natl Acad Sci U S A, 2003. **100**(23): p. 13489-94.
155. Schamel, W.W. and M. Reth, *Monomeric and oligomeric complexes of the B cell antigen receptor.* Immunity, 2000. **13**(1): p. 5-14.
156. Cheng, P.C., et al., *Translocation of the B cell antigen receptor into lipid rafts reveals a novel step in signaling.* J Immunol, 2001. **166**(6): p. 3693-701.
157. Gupta, N. and A.L. DeFranco, *Visualizing lipid raft dynamics and early signaling events during antigen receptor-mediated B-lymphocyte activation.* Mol Biol Cell, 2003. **14**(2): p. 432-44.
158. D'Avola, A., et al., *Surface IgM expression and function are associated with clinical behavior, genetic abnormalities, and DNA methylation in CLL.* Blood, 2016. **128**(6): p. 816-26.
159. Cambier, J.C., et al., *B-cell anergy: from transgenic models to naturally occurring anergic B cells?* Nat Rev Immunol, 2007. **7**(8): p. 633-43.
160. Muzio, M., et al., *Constitutive activation of distinct BCR-signaling pathways in a subset of CLL patients: a molecular signature of anergy.* Blood, 2008. **112**(1): p. 188-95.
161. Apollonio, B., et al., *Targeting B-cell anergy in chronic lymphocytic leukemia.* Blood, 2013. **121**(19): p. 3879-88, S1-8.
162. Gabelloni, M.L., et al., *SHIP-1 protein level and phosphorylation status differs between CLL cells segregated by ZAP-70 expression.* Br J Haematol, 2008. **140**(1): p. 117-9.
163. Tibaldi, E., et al., *Lyn-mediated SHP-1 recruitment to CD5 contributes to resistance to apoptosis of B-cell chronic lymphocytic leukemia cells.* Leukemia, 2011. **25**(11): p. 1768-81.
164. Luciano, F., J.E. Ricci, and P. Auberger, *Cleavage of Fyn and Lyn in their N-terminal unique regions during induction of apoptosis: a new mechanism for Src kinase regulation.* Oncogene, 2001. **20**(36): p. 4935-41.
165. Thomas, M.L. and E.J. Brown, *Positive and negative regulation of Src-family membrane kinases by CD45.* Immunol Today, 1999. **20**(9): p. 406-11.
166. Donella-Deana, A., et al., *Spontaneous autophosphorylation of Lyn tyrosine kinase at both its activation segment and C-terminal tail confers altered substrate specificity.* Biochemistry, 1998. **37**(5): p. 1438-46.
167. Caplan, A.J., A.K. Mandal, and M.A. Theodoraki, *Molecular chaperones and protein kinase quality control.* Trends Cell Biol, 2007. **17**(2): p. 87-92.
168. Trentin, L., et al., *Geldanamycin-induced Lyn dissociation from aberrant Hsp90-stabilized cytosolic complex is an early event in apoptotic mechanisms in B-chronic lymphocytic leukemia.* Blood, 2008. **112**(12): p. 4665-74.
169. Messmer, B.T., et al., *In vivo measurements document the dynamic cellular kinetics of chronic lymphocytic leukemia B cells.* J Clin Invest, 2005. **115**(3): p. 755-64.

170. Collins, R.J., et al., *Spontaneous programmed death (apoptosis) of B-chronic lymphocytic leukaemia cells following their culture in vitro.* Br J Haematol, 1989. **71**(3): p. 343-50.
171. Czabotar, P.E., et al., *Control of apoptosis by the BCL-2 protein family: implications for physiology and therapy.* Nature Reviews Molecular Cell Biology, 2014. **15**(1): p. 49-63.
172. Kitada, S., et al., *Expression of apoptosis-regulating proteins in chronic lymphocytic leukemia: correlations with In vitro and In vivo chemoresponses.* Blood, 1998. **91**(9): p. 3379-89.
173. Kuwana, T., et al., *BH3 domains of BH3-only proteins differentially regulate Bax-mediated mitochondrial membrane permeabilization both directly and indirectly.* Mol Cell, 2005. **17**(4): p. 525-35.
174. Green, D.R. and G. Kroemer, *The pathophysiology of mitochondrial cell death.* Science, 2004. **305**(5684): p. 626-9.
175. Chipuk, J.E., et al., *The BCL-2 family reunion.* Mol Cell, 2010. **37**(3): p. 299-310.
176. Faderl, S., et al., *Expression profile of 11 proteins and their prognostic significance in patients with chronic lymphocytic leukemia (CLL).* Leukemia, 2002. **16**(6): p. 1045-52.
177. Kischkel, F.C., et al., *Cytotoxicity-dependent APO-1 (Fas/CD95)-associated proteins form a death-inducing signaling complex (DISC) with the receptor.* EMBO J, 1995. **14**(22): p. 5579-88.
178. Boldin, M.P., et al., *Self-association of the "death domains" of the p55 tumor necrosis factor (TNF) receptor and Fas/APO1 prompts signaling for TNF and Fas/APO1 effects.* J Biol Chem, 1995. **270**(1): p. 387-91.
179. Panayiotidis, P., et al., *Expression and function of the FAS antigen in B chronic lymphocytic leukemia and hairy cell leukemia.* Leukemia, 1995. **9**(7): p. 1227-32.
180. De Fanis, U., et al., *Altered constitutive and activation-induced expression of CD95 by B- and T-cells in B-cell chronic lymphocytic leukemia.* Haematologica, 2002. **87**(3): p. 325-7.
181. Pallasch, C.P. and C.M. Wendtner, *Overexpression of the Fas-inhibitory molecule TOSO: a novel antiapoptotic factor in chronic lymphocytic leukemia.* Leuk Lymphoma, 2009. **50**(3): p. 498-501.
182. Mohr, J., et al., *DNA damage-induced transcriptional program in CLL: biological and diagnostic implications for functional p53 testing.* Blood, 2011. **117**(5): p. 1622-32.
183. Reif, K., et al., *Balanced responsiveness to chemoattractants from adjacent zones determines B-cell position.* Nature, 2002. **416**(6876): p. 94-9.
184. Moser, B. and P. Loetscher, *Lymphocyte traffic control by chemokines.* Nat Immunol, 2001. **2**(2): p. 123-8.
185. Butcher, E.C. and L.J. Picker, *Lymphocyte homing and homeostasis.* Science, 1996. **272**(5258): p. 60-6.
186. Burger, J.A., M. Burger, and T.J. Kipps, *Chronic lymphocytic leukemia B cells express functional CXCR4 chemokine receptors that mediate spontaneous migration beneath bone marrow stromal cells.* Blood, 1999. **94**(11): p. 3658-67.
187. Sipkins, D.A., et al., *In vivo imaging of specialized bone marrow endothelial microdomains for tumour engraftment.* Nature, 2005. **435**(7044): p. 969-73.
188. Bowman, E.P., et al., *Developmental switches in chemokine response profiles during B cell differentiation and maturation.* J Exp Med, 2000. **191**(8): p. 1303-18.

189. Quiroga, M.P. and J.A. Burger, *BCR-mediated decrease of CXCR4 and CD62L in CLL.* Cancer Res, 2010. **70**(12): p. 5194; author reply 5195.
190. de Gorter, D.J., et al., *Bruton's tyrosine kinase and phospholipase Cgamma2 mediate chemokine-controlled B cell migration and homing.* Immunity, 2007. **26**(1): p. 93-104.
191. Burger, J.A., et al., *Blood-derived nurse-like cells protect chronic lymphocytic leukemia B cells from spontaneous apoptosis through stromal cell-derived factor-1.* Blood, 2000. **96**(8): p. 2655-63.
192. Burger, M., et al., *Small peptide inhibitors of the CXCR4 chemokine receptor (CD184) antagonize the activation, migration, and antiapoptotic responses of CXCL12 in chronic lymphocytic leukemia B cells.* Blood, 2005. **106**(5): p. 1824-30.
193. Calissano, C., et al., *In vivo intraclonal and interclonal kinetic heterogeneity in B-cell chronic lymphocytic leukemia.* Blood, 2009. **114**(23): p. 4832-42.
194. Allen, C.D., et al., *Germinal center dark and light zone organization is mediated by CXCR4 and CXCR5.* Nat Immunol, 2004. **5**(9): p. 943-52.
195. Trentin, L., et al., *Homeostatic chemokines drive migration of malignant B cells in patients with non-Hodgkin lymphomas.* Blood, 2004. **104**(2): p. 502-8.
196. Burkle, A., et al., *Overexpression of the CXCR5 chemokine receptor, and its ligand, CXCL13 in B-cell chronic lymphocytic leukemia.* Blood, 2007. **110**(9): p. 3316-25.
197. Till, K.J., et al., *The chemokine receptor CCR7 and alpha4 integrin are important for migration of chronic lymphocytic leukemia cells into lymph nodes.* Blood, 2002. **99**(8): p. 2977-84.
198. Richardson, S.J., et al., *ZAP-70 expression is associated with enhanced ability to respond to migratory and survival signals in B-cell chronic lymphocytic leukemia (B-CLL).* Blood, 2006. **107**(9): p. 3584-92.
199. Calpe, E., et al., *ZAP-70 enhances migration of malignant B lymphocytes toward CCL21 by inducing CCR7 expression via IgM-ERK1/2 activation.* Blood, 2011. **118**(16): p. 4401-10.
200. Trentin, L., et al., *The chemokine receptor CXCR3 is expressed on malignant B cells and mediates chemotaxis.* J Clin Invest, 1999. **104**(1): p. 115-21.
201. Mahadevan, D., et al., *Gene Expression and Serum Cytokine Profiling of Low Stage CLL Identify WNT/PCP, Flt-3L/Flt-3 and CXCL9/CXCR3 as Regulators of Cell Proliferation, Survival and Migration.* Hum Genomics Proteomics, 2009. **2009**: p. 453634.
202. Ocana, E., et al., *The prognostic role of CXCR3 expression by chronic lymphocytic leukemia B cells.* Haematologica, 2007. **92**(3): p. 349-56.
203. Prockop, D.J., *Marrow stromal cells as stem cells for nonhematopoietic tissues.* Science, 1997. **276**(5309): p. 71-4.
204. Pittenger, M.F., et al., *Multilineage potential of adult human mesenchymal stem cells.* Science, 1999. **284**(5411): p. 143-7.
205. Bruder, S.P., N. Jaiswal, and S.E. Haynesworth, *Growth kinetics, self-renewal, and the osteogenic potential of purified human mesenchymal stem cells during extensive subcultivation and following cryopreservation.* J Cell Biochem, 1997. **64**(2): p. 278-94.
206. Friedenstein, A.J., J.F. Gorskaja, and N.N. Kulagina, *Fibroblast precursors in normal and irradiated mouse hematopoietic organs.* Exp Hematol, 1976. **4**(5): p. 267-74.

207. Piersma, A.H., R.E. Ploemacher, and K.G. Brockbank, *Transplantation of bone marrow fibroblastoid stromal cells in mice via the intravenous route.* Br J Haematol, 1983. **54**(2): p. 285-90.
208. Caplan, A.I., *Mesenchymal stem cells.* J Orthop Res, 1991. **9**(5): p. 641-50.
209. Wakitani, S., T. Saito, and A.I. Caplan, *Myogenic cells derived from rat bone marrow mesenchymal stem cells exposed to 5-azacytidine.* Muscle Nerve, 1995. **18**(12): p. 1417-26.
210. Owen, M. and A.J. Friedenstein, *Stromal stem cells: marrow-derived osteogenic precursors.* Ciba Found Symp, 1988. **136**: p. 42-60.
211. Friedenstein, A.J., S. Piatetzky, II, and K.V. Petrakova, *Osteogenesis in transplants of bone marrow cells.* J Embryol Exp Morphol, 1966. **16**(3): p. 381-90.
212. Erices, A., P. Conget, and J.J. Minguell, *Mesenchymal progenitor cells in human umbilical cord blood.* Br J Haematol, 2000. **109**(1): p. 235-42.
213. Katz, A.J., et al., *Cell surface and transcriptional characterization of human adipose-derived adherent stromal (hADAS) cells.* Stem Cells, 2005. **23**(3): p. 412-23.
214. In 't Anker, P.S., et al., *Isolation of mesenchymal stem cells of fetal or maternal origin from human placenta.* Stem Cells, 2004. **22**(7): p. 1338-45.
215. Trubiani, O., et al., *Morphological and cytofluorimetric analysis of adult mesenchymal stem cells expanded ex vivo from periodontal ligament.* Int J Immunopathol Pharmacol, 2005. **18**(2): p. 213-21.
216. Wexler, S.A., et al., *Adult bone marrow is a rich source of human mesenchymal 'stem' cells but umbilical cord and mobilized adult blood are not.* Br J Haematol, 2003. **121**(2): p. 368-74.
217. Lazarus, H.M., et al., *Human bone marrow-derived mesenchymal (stromal) progenitor cells (MPCs) cannot be recovered from peripheral blood progenitor cell collections.* J Hematother, 1997. **6**(5): p. 447-55.
218. Zvaifler, N.J., et al., *Mesenchymal precursor cells in the blood of normal individuals.* Arthritis Res, 2000. **2**(6): p. 477-88.
219. Fernandez, M., et al., *Detection of stromal cells in peripheral blood progenitor cell collections from breast cancer patients.* Bone Marrow Transplant, 1997. **20**(4): p. 265-71.
220. Dominici, M., et al., *Minimal criteria for defining multipotent mesenchymal stromal cells. The International Society for Cellular Therapy position statement.* Cytotherapy, 2006. **8**(4): p. 315-7.
221. Barry, F.P., et al., *The monoclonal antibody SH-2, raised against human mesenchymal stem cells, recognizes an epitope on endoglin (CD105).* Biochem Biophys Res Commun, 1999. **265**(1): p. 134-9.
222. Majumdar, M.K., et al., *Phenotypic and functional comparison of cultures of marrow-derived mesenchymal stem cells (MSCs) and stromal cells.* J Cell Physiol, 1998. **176**(1): p. 57-66.
223. Smith, J.R., et al., *Isolation of a highly clonogenic and multipotential subfraction of adult stem cells from bone marrow stroma.* Stem Cells, 2004. **22**(5): p. 823-31.
224. Cappellesso-Fleury, S., et al., *Human fibroblasts share immunosuppressive properties with bone marrow mesenchymal stem cells.* J Clin Immunol, 2010. **30**(4): p. 607-19.
225. Barry, F., et al., *The SH-3 and SH-4 antibodies recognize distinct epitopes on CD73 from human mesenchymal stem cells.* Biochem Biophys Res Commun, 2001. **289**(2): p. 519-24.

226. Simmons, P.J. and B. Torok-Storb, *Identification of stromal cell precursors in human bone marrow by a novel monoclonal antibody, STRO-1.* Blood, 1991. **78**(1): p. 55-62.
227. Lanza, F., L. Healy, and D.R. Sutherland, *Structural and functional features of the CD34 antigen: an update.* J Biol Regul Homeost Agents, 2001. **15**(1): p. 1-13.
228. Jersmann, H.P., *Time to abandon dogma: CD14 is expressed by non-myeloid lineage cells.* Immunol Cell Biol, 2005. **83**(5): p. 462-7.
229. Jackson, D.E., *The unfolding tale of PECAM-1.* FEBS Lett, 2003. **540**(1-3): p. 7-14.
230. Jiang, Y., et al., *Pluripotency of mesenchymal stem cells derived from adult marrow.* Nature, 2002. **418**(6893): p. 41-9.
231. Scott, M.A., et al., *Current methods of adipogenic differentiation of mesenchymal stem cells.* Stem Cells Dev, 2011. **20**(10): p. 1793-804.
232. Bennett, J.H., et al., *Adipocytic cells cultured from marrow have osteogenic potential.* J Cell Sci, 1991. **99 (Pt 1)**: p. 131-9.
233. Solchaga, L.A., K.J. Penick, and J.F. Welter, *Chondrogenic differentiation of bone marrow-derived mesenchymal stem cells: tips and tricks.* Methods Mol Biol, 2011. **698**: p. 253-78.
234. Manolagas, S.C. and R.L. Jilka, *Bone marrow, cytokines, and bone remodeling. Emerging insights into the pathophysiology of osteoporosis.* N Engl J Med, 1995. **332**(5): p. 305-11.
235. Joo, S., et al., *Myogenic-induced mesenchymal stem cells are capable of modulating the immune response by regulatory T cells.* J Tissue Eng, 2014. **5**: p. 2041731414524758.
236. Woodbury, D., et al., *Adult rat and human bone marrow stromal cells differentiate into neurons.* J Neurosci Res, 2000. **61**(4): p. 364-70.
237. Kotton, D.N., et al., *Bone marrow-derived cells as progenitors of lung alveolar epithelium.* Development, 2001. **128**(24): p. 5181-8.
238. Sato, Y., et al., *Human mesenchymal stem cells xenografted directly to rat liver are differentiated into human hepatocytes without fusion.* Blood, 2005. **106**(2): p. 756-63.
239. Morigi, M., et al., *Mesenchymal stem cells are renotropic, helping to repair the kidney and improve function in acute renal failure.* J Am Soc Nephrol, 2004. **15**(7): p. 1794-804.
240. Zhao, L.R., et al., *Human bone marrow stem cells exhibit neural phenotypes and ameliorate neurological deficits after grafting into the ischemic brain of rats.* Exp Neurol, 2002. **174**(1): p. 11-20.
241. Corcione, A., et al., *Human mesenchymal stem cells modulate B-cell functions.* Blood, 2006. **107**(1): p. 367-72.
242. Dexter, T.M., T.D. Allen, and L.G. Lajtha, *Conditions controlling the proliferation of haemopoietic stem cells in vitro.* J Cell Physiol, 1977. **91**(3): p. 335-44.
243. Sugiyama, T., et al., *Maintenance of the hematopoietic stem cell pool by CXCL12-CXCR4 chemokine signaling in bone marrow stromal cell niches.* Immunity, 2006. **25**(6): p. 977-88.
244. Haynesworth, S.E., M.A. Baber, and A.I. Caplan, *Cytokine expression by human marrow-derived mesenchymal progenitor cells in vitro: effects of dexamethasone and IL-1 alpha.* J Cell Physiol, 1996. **166**(3): p. 585-92.
245. Ruster, B., et al., *Mesenchymal stem cells display coordinated rolling and adhesion behavior on endothelial cells.* Blood, 2006. **108**(12): p. 3938-44.

246. Bensidhoum, M., et al., *[Therapeutic effect of human mesenchymal stem cells in skin after radiation damage].* J Soc Biol, 2005. **199**(4): p. 337-41.
247. Caplan, A.I. and J.M. Sorrell, *The MSC curtain that stops the immune system.* Immunol Lett, 2015. **168**(2): p. 136-9.
248. Jones, B.J. and S.J. McTaggart, *Immunosuppression by mesenchymal stromal cells: from culture to clinic.* Exp Hematol, 2008. **36**(6): p. 733-41.
249. Lazarus, H.M., et al., *Ex vivo expansion and subsequent infusion of human bone marrow-derived stromal progenitor cells (mesenchymal progenitor cells): implications for therapeutic use.* Bone Marrow Transplant, 1995. **16**(4): p. 557-64.
250. Aggarwal, S. and M.F. Pittenger, *Human mesenchymal stem cells modulate allogeneic immune cell responses.* Blood, 2005. **105**(4): p. 1815-22.
251. Le Blanc, K. and O. Ringden, *Immunomodulation by mesenchymal stem cells and clinical experience.* J Intern Med, 2007. **262**(5): p. 509-25.
252. Rasmusson, I., et al., *Mesenchymal stem cells inhibit lymphocyte proliferation by mitogens and alloantigens by different mechanisms.* Exp Cell Res, 2005. **305**(1): p. 33-41.
253. Waterman, R.S., et al., *A New Mesenchymal Stem Cell (MSC) Paradigm: Polarization into a Pro-Inflammatory MSC1 or an Immunosuppressive MSC2 Phenotype.* Plos One, 2010. **5**(4).
254. Devine, S.M., et al., *Mesenchymal stem cells distribute to a wide range of tissues following systemic infusion into nonhuman primates.* Blood, 2003. **101**(8): p. 2999-3001.
255. Ozawa, K., et al., *Cell and gene therapy using mesenchymal stem cells (MSCs).* J Autoimmun, 2008. **30**(3): p. 121-7.
256. Ohtaki, H., et al., *Stem/progenitor cells from bone marrow decrease neuronal death in global ischemia by modulation of inflammatory/immune responses.* Proc Natl Acad Sci U S A, 2008. **105**(38): p. 14638-43.
257. Nauta, A.J. and W.E. Fibbe, *Immunomodulatory properties of mesenchymal stromal cells.* Blood, 2007. **110**(10): p. 3499-506.
258. Di Nicola, M., et al., *Human bone marrow stromal cells suppress T-lymphocyte proliferation induced by cellular or nonspecific mitogenic stimuli.* Blood, 2002. **99**(10): p. 3838-43.
259. Krampera, M., et al., *Bone marrow mesenchymal stem cells inhibit the response of naive and memory antigen-specific T cells to their cognate peptide.* Blood, 2003. **101**(9): p. 3722-9.
260. Glennie, S., et al., *Bone marrow mesenchymal stem cells induce division arrest anergy of activated T cells.* Blood, 2005. **105**(7): p. 2821-7.
261. Meisel, R., et al., *Human bone marrow stromal cells inhibit allogeneic T-cell responses by indoleamine 2,3-dioxygenase-mediated tryptophan degradation.* Blood, 2004. **103**(12): p. 4619-21.
262. Di Ianni, M., et al., *Mesenchymal cells recruit and regulate T regulatory cells.* Exp Hematol, 2008. **36**(3): p. 309-18.
263. Maccario, R., et al., *Interaction of human mesenchymal stem cells with cells involved in alloantigen-specific immune response favors the differentiation of CD4+ T-cell subsets expressing a regulatory/suppressive phenotype.* Haematologica, 2005. **90**(4): p. 516-25.

264. Potian, J.A., et al., *Veto-like activity of mesenchymal stem cells: functional discrimination between cellular responses to alloantigens and recall antigens.* J Immunol, 2003. **171**(7): p. 3426-34.
265. Le Blanc, K., et al., *Treatment of severe acute graft-versus-host disease with third party haploidentical mesenchymal stem cells.* Lancet, 2004. **363**(9419): p. 1439-41.
266. Kierney, P.C. and K. Dorshkind, *B lymphocyte precursors and myeloid progenitors survive in diffusion chamber cultures but B cell differentiation requires close association with stromal cells.* Blood, 1987. **70**(5): p. 1418-24.
267. Glodek, A.M., et al., *Sustained activation of cell adhesion is a differentially regulated process in B lymphopoiesis.* J Exp Med, 2003. **197**(4): p. 461-73.
268. Sotiropoulou, P.A., et al., *Interactions between human mesenchymal stem cells and natural killer cells.* Stem Cells, 2006. **24**(1): p. 74-85.
269. Spaggiari, G.M., et al., *Mesenchymal stem cell-natural killer cell interactions: evidence that activated NK cells are capable of killing MSCs, whereas MSCs can inhibit IL-2-induced NK-cell proliferation.* Blood, 2006. **107**(4): p. 1484-90.
270. Jiang, X.X., et al., *Human mesenchymal stem cells inhibit differentiation and function of monocyte-derived dendritic cells.* Blood, 2005. **105**(10): p. 4120-6.
271. Zhang, W., et al., *Effects of mesenchymal stem cells on differentiation, maturation, and function of human monocyte-derived dendritic cells.* Stem Cells Dev, 2004. **13**(3): p. 263-71.
272. Beyth, S., et al., *Human mesenchymal stem cells alter antigen-presenting cell maturation and induce T-cell unresponsiveness.* Blood, 2005. **105**(5): p. 2214-9.
273. Ramasamy, R., et al., *Mesenchymal stem cells inhibit dendritic cell differentiation and function by preventing entry into the cell cycle.* Transplantation, 2007. **83**(1): p. 71-6.
274. Raffaghello, L., et al., *Human mesenchymal stem cells inhibit neutrophil apoptosis: a model for neutrophil preservation in the bone marrow niche.* Stem Cells, 2008. **26**(1): p. 151-62.
275. Lama, V.N., et al., *Evidence for tissue-resident mesenchymal stem cells in human adult lung from studies of transplanted allografts.* J Clin Invest, 2007. **117**(4): p. 989-96.
276. Hong, I.S., H.Y. Lee, and K.S. Kang, *Mesenchymal stem cells and cancer: friends or enemies?* Mutat Res, 2014. **768**: p. 98-106.
277. Li, H., X. Fan, and J. Houghton, *Tumor microenvironment: the role of the tumor stroma in cancer.* J Cell Biochem, 2007. **101**(4): p. 805-15.
278. Zhu, W., et al., *Mesenchymal stem cells derived from bone marrow favor tumor cell growth in vivo.* Exp Mol Pathol, 2006. **80**(3): p. 267-74.
279. Spaeth, E.L., et al., *Mesenchymal stem cell transition to tumor-associated fibroblasts contributes to fibrovascular network expansion and tumor progression.* PLoS One, 2009. **4**(4): p. e4992.
280. Sato, K., et al., *Nitric oxide plays a critical role in suppression of T-cell proliferation by mesenchymal stem cells.* Blood, 2007. **109**(1): p. 228-34.
281. Djouad, F., et al., *Mesenchymal stem cells inhibit the differentiation of dendritic cells through an interleukin-6-dependent mechanism.* Stem Cells, 2007. **25**(8): p. 2025-32.
282. Nemeth, K., et al., *Bone marrow stromal cells attenuate sepsis via prostaglandin E(2)-dependent reprogramming of host macrophages to increase their interleukin-10 production.* Nat Med, 2009. **15**(1): p. 42-9.

283. Feng, B. and L. Chen, *Review of mesenchymal stem cells and tumors: executioner or coconspirator?* Cancer Biother Radiopharm, 2009. **24**(6): p. 717-21.
284. Qiao, L., et al., *Dkk-1 secreted by mesenchymal stem cells inhibits growth of breast cancer cells via depression of Wnt signalling.* Cancer Lett, 2008. **269**(1): p. 67-77.
285. Abdel aziz, M.T., et al., *Efficacy of mesenchymal stem cells in suppression of hepatocarcinorigenesis in rats: possible role of Wnt signaling.* J Exp Clin Cancer Res, 2011. **30**: p. 49.
286. Khakoo, A.Y., et al., *Human mesenchymal stem cells exert potent antitumorigenic effects in a model of Kaposi's sarcoma.* J Exp Med, 2006. **203**(5): p. 1235-47.
287. Giordano, A., U. Galderisi, and I.R. Marino, *From the laboratory bench to the patient's bedside: an update on clinical trials with mesenchymal stem cells.* J Cell Physiol, 2007. **211**(1): p. 27-35.
288. Ren, C., et al., *Cancer gene therapy using mesenchymal stem cells expressing interferon-beta in a mouse prostate cancer lung metastasis model.* Gene Ther, 2008. **15**(21): p. 1446-53.
289. Reagan, M.R., et al., *Stem Cell Implants for Cancer Therapy: TRAIL-Expressing Mesenchymal Stem Cells Target Cancer Cells In Situ.* J Breast Cancer, 2012. **15**(3): p. 273-82.
290. Both, G.W., *Gene-directed enzyme prodrug therapy for cancer: a glimpse into the future?* Discov Med, 2009. **8**(42): p. 97-103.
291. Ruan, J., et al., *Magnitude of stromal hemangiogenesis correlates with histologic subtype of non-Hodgkin's lymphoma.* Clin Cancer Res, 2006. **12**(19): p. 5622-31.
292. Ding, W., et al., *Bi-directional activation between mesenchymal stem cells and CLL B-cells: implication for CLL disease progression.* Br J Haematol, 2009. **147**(4): p. 471-83.
293. Purroy, N., et al., *Co-culture of primary CLL cells with bone marrow mesenchymal cells, CD40 ligand and CpG ODN promotes proliferation of chemoresistant CLL cells phenotypically comparable to those proliferating in vivo.* Oncotarget, 2015. **6**(10): p. 7632-43.
294. Marquez, M.E., et al., *Bone marrow stromal mesenchymal cells induce down regulation of CD20 expression on B-CLL: implications for rituximab resistance in CLL.* Br J Haematol, 2015. **169**(2): p. 211-8.
295. Lutzny, G., et al., *Protein kinase c-beta-dependent activation of NF-kappaB in stromal cells is indispensable for the survival of chronic lymphocytic leukemia B cells in vivo.* Cancer Cell, 2013. **23**(1): p. 77-92.
296. Ghosh, A.K., et al., *Circulating microvesicles in B-cell chronic lymphocytic leukemia can stimulate marrow stromal cells: implications for disease progression.* Blood, 2010. **115**(9): p. 1755-64.
297. Paggetti, J., et al., *Exosomes released by chronic lymphocytic leukemia cells induce the transition of stromal cells into cancer-associated fibroblasts.* Blood, 2015. **126**(9): p. 1106-17.
298. Pontikoglou, C., et al., *Study of the quantitative, functional, cytogenetic, and immunoregulatory properties of bone marrow mesenchymal stem cells in patients with B-cell chronic lymphocytic leukemia.* Stem Cells Dev, 2013. **22**(9): p. 1329-41.

299. Lagneaux, L., et al., *Chronic lymphocytic leukemic B cells but not normal B cells are rescued from apoptosis by contact with normal bone marrow stromal cells.* Blood, 1998. **91**(7): p. 2387-96.
300. Herishanu, Y., et al., *Biology of chronic lymphocytic leukemia in different microenvironments: clinical and therapeutic implications.* Hematol Oncol Clin North Am, 2013. **27**(2): p. 173-206.
301. Frezzato, F., et al., *HS1, a Lyn kinase substrate, is abnormally expressed in B-chronic lymphocytic leukemia and correlates with response to fludarabine-based regimen.* PLoS One, 2012. **7**(6): p. e39902.
302. Wu, X. and H. Koiwa, *One-step casting of Laemmli discontinued sodium dodecyl sulfate-polyacrylamide gel electrophoresis gel.* Anal Biochem. **421**(1): p. 347-9.
303. Kurtova, A.V., et al., *Diverse marrow stromal cells protect CLL cells from spontaneous and drug-induced apoptosis: development of a reliable and reproducible system to assess stromal cell adhesion-mediated drug resistance.* Blood, 2009. **114**(20): p. 4441-50.
304. Davids, M.S. and J.A. Burger, *Cell Trafficking in Chronic Lymphocytic Leukemia.* Open J Hematol, 2012. **3**(S1).
305. Lopez-Giral, S., et al., *Chemokine receptors that mediate B cell homing to secondary lymphoid tissues are highly expressed in B cell chronic lymphocytic leukemia and non-Hodgkin lymphomas with widespread nodular dissemination.* J Leukoc Biol, 2004. **76**(2): p. 462-71.
306. Brachtl, G., et al., *Differential bone marrow homing capacity of VLA-4 and CD38 high expressing chronic lymphocytic leukemia cells.* PLoS One, 2011. **6**(8): p. e23758.
307. Zhao, Z.G., et al., *Phenotypic and functional comparison of mesenchymal stem cells derived from the bone marrow of normal adults and patients with hematologic malignant diseases.* Stem Cells Dev, 2007. **16**(4): p. 637-48.
308. Trimarco, V., et al., *Cross-talk between chronic lymphocytic leukemia (CLL) tumor B cells and mesenchymal stromal cells (MSCs): implications for neoplastic cell survival.* Oncotarget, 2015. **6**(39): p. 42130-42149.
309. Manabe, A., et al., *Bone marrow-derived stromal cells prevent apoptotic cell death in B-lineage acute lymphoblastic leukemia.* Blood, 1992. **79**(9): p. 2370-7.
310. Burger, J.A. and E. Montserrat, *Coming full circle: 70 years of chronic lymphocytic leukemia cell redistribution, from glucocorticoids to inhibitors of B-cell receptor signaling.* Blood, 2013. **121**(9): p. 1501-9.
311. Ticchioni, M., et al., *Homeostatic chemokines increase survival of B-chronic lymphocytic leukemia cells through inactivation of transcription factor FOXO3a.* Oncogene, 2007. **26**(50): p. 7081-91.
312. Yoon, J.Y., et al., *Association of interleukin-6 and interleukin-8 with poor prognosis in elderly patients with chronic lymphocytic leukemia.* Leuk Lymphoma, 2012. **53**(9): p. 1735-42.
313. Tsukada, S., et al., *Deficient expression of a B cell cytoplasmic tyrosine kinase in human X-linked agammaglobulinemia.* Cell, 1993. **72**(2): p. 279-90.
314. Hendriks, R.W., et al., *Biology and novel treatment options for XLA, the most common monogenetic immunodeficiency in man.* Expert Opin Ther Targets, 2011. **15**(8): p. 1003-21.
315. Mohamed, A.J., et al., *Bruton's tyrosine kinase (Btk): function, regulation, and transformation with special emphasis on the PH domain.* Immunol Rev, 2009. **228**(1): p. 58-73.

316. Hyvonen, M. and M. Saraste, *Structure of the PH domain and Btk motif from Bruton's tyrosine kinase: molecular explanations for X-linked agammaglobulinaemia.* EMBO J, 1997. **16**(12): p. 3396-404.
317. Genevier, H.C., et al., *Expression of Bruton's tyrosine kinase protein within the B cell lineage.* Eur J Immunol, 1994. **24**(12): p. 3100-5.
318. Smith, C.I., et al., *Expression of Bruton's agammaglobulinemia tyrosine kinase gene, BTK, is selectively down-regulated in T lymphocytes and plasma cells.* J Immunol, 1994. **152**(2): p. 557-65.
319. Kim, Y.J., et al., *Mechanism of B-cell receptor-induced phosphorylation and activation of phospholipase C-gamma2.* Mol Cell Biol, 2004. **24**(22): p. 9986-99.
320. Takesono, A., L.D. Finkelstein, and P.L. Schwartzberg, *Beyond calcium: new signaling pathways for Tec family kinases.* J Cell Sci, 2002. **115**(Pt 15): p. 3039-48.
321. Herman, S.E., et al., *Bruton tyrosine kinase represents a promising therapeutic target for treatment of chronic lymphocytic leukemia and is effectively targeted by PCI-32765.* Blood, 2011. **117**(23): p. 6287-96.
322. Kurosaki, T. and M. Hikida, *Tyrosine kinases and their substrates in B lymphocytes.* Immunol Rev, 2009. **228**(1): p. 132-48.
323. Khan, W.N., et al., *Defective B cell development and function in Btk-deficient mice.* Immunity, 1995. **3**(3): p. 283-99.
324. Brorson, K., et al., *xid affects events leading to B cell cycle entry.* J Immunol, 1997. **159**(1): p. 135-43.
325. Kil, L.P., et al., *Btk levels set the threshold for B-cell activation and negative selection of autoreactive B cells in mice.* Blood, 2012. **119**(16): p. 3744-56.
326. Tsukada, S., et al., *Binding of beta gamma subunits of heterotrimeric G proteins to the PH domain of Bruton tyrosine kinase.* Proc Natl Acad Sci U S A, 1994. **91**(23): p. 11256-60.
327. Jiang, Y., et al., *The G protein G alpha12 stimulates Bruton's tyrosine kinase and a rasGAP through a conserved PH/BM domain.* Nature, 1998. **395**(6704): p. 808-13.
328. de Rooij, M.F., et al., *The clinically active BTK inhibitor PCI-32765 targets B-cell receptor- and chemokine-controlled adhesion and migration in chronic lymphocytic leukemia.* Blood, 2012. **119**(11): p. 2590-4.
329. Campbell, D.J., C.H. Kim, and E.C. Butcher, *Chemokines in the systemic organization of immunity.* Immunol Rev, 2003. **195**: p. 58-71.
330. Calissano, C., et al., *Intraclonal complexity in chronic lymphocytic leukemia: fractions enriched in recently born/divided and older/quiescent cells.* Mol Med, 2011. **17**(11-12): p. 1374-82.
331. Herishanu, Y., et al., *The lymph node microenvironment promotes B-cell receptor signaling, NF-kappaB activation, and tumor proliferation in chronic lymphocytic leukemia.* Blood, 2011. **117**(2): p. 563-74.
332. Dubovsky, J.A., et al., *Ibrutinib is an irreversible molecular inhibitor of ITK driving a Th1-selective pressure in T lymphocytes.* Blood, 2013. **122**(15): p. 2539-49.
333. Fiorcari, S., et al., *Ibrutinib modifies the function of monocyte/macrophage population in chronic lymphocytic leukemia.* Oncotarget, 2016. **7**(40): p. 65968-65981.
334. Byrd, J.C., et al., *Three-year follow-up of treatment-naive and previously treated patients with CLL and SLL receiving single-agent ibrutinib.* Blood, 2015. **125**(16): p. 2497-506.

335. Burger, J.A., et al., *Ibrutinib as Initial Therapy for Patients with Chronic Lymphocytic Leukemia.* N Engl J Med, 2015. **373**(25): p. 2425-37.
336. Byrd, J.C., S. O'Brien, and D.F. James, *Ibrutinib in relapsed chronic lymphocytic leukemia.* N Engl J Med, 2013. **369**(13): p. 1278-9.
337. Farooqui, M.Z., et al., *Ibrutinib for previously untreated and relapsed or refractory chronic lymphocytic leukaemia with TP53 aberrations: a phase 2, single-arm trial.* Lancet Oncol, 2015. **16**(2): p. 169-76.
338. O'Brien, S., et al., *Ibrutinib for patients with relapsed or refractory chronic lymphocytic leukaemia with 17p deletion (RESONATE-17): a phase 2, open-label, multicentre study.* Lancet Oncol, 2016. **17**(10): p. 1409-1418.
339. Eichhorst, B., et al., *Chronic lymphocytic leukaemia: ESMO Clinical Practice Guidelines for diagnosis, treatment and follow-up.* Ann Oncol, 2015. **26 Suppl 5**: p. v78-84.
340. Jain, P., et al., *Outcomes of patients with chronic lymphocytic leukemia after discontinuing ibrutinib.* Blood, 2015. **125**(13): p. 2062-7.
341. Cheson, B.D., et al., *Novel targeted agents and the need to refine clinical end points in chronic lymphocytic leukemia.* J Clin Oncol, 2012. **30**(23): p. 2820-2.
342. Chen, S.S., et al., *BTK inhibition results in impaired CXCR4 chemokine receptor surface expression, signaling and function in chronic lymphocytic leukemia.* Leukemia, 2016. **30**(4): p. 833-43.
343. Woyach, J.A., et al., *Resistance mechanisms for the Bruton's tyrosine kinase inhibitor ibrutinib.* N Engl J Med, 2014. **370**(24): p. 2286-94.
344. Liu, T.M., et al., *Hypermorphic mutation of phospholipase C, gamma2 acquired in ibrutinib-resistant CLL confers BTK independency upon B-cell receptor activation.* Blood, 2015. **126**(1): p. 61-8.
345. Trimarco, V., et al., *Cross-talk between chronic lymphocytic leukemia (CLL) tumor B cells and mesenchymal stromal cells (MSCs): implications for neoplastic cell survival.* Oncotarget, 2015. **6**(39): p. 42130-49.
346. Herman, S.E., et al., *Ibrutinib inhibits BCR and NF-kappaB signaling and reduces tumor proliferation in tissue-resident cells of patients with CLL.* Blood, 2014. **123**(21): p. 3286-95.
347. Cheng, S., et al., *BTK inhibition targets in vivo CLL proliferation through its effects on B-cell receptor signaling activity.* Leukemia, 2014. **28**(3): p. 649-57.
348. Woyach, J.A., et al., *Prolonged lymphocytosis during ibrutinib therapy is associated with distinct molecular characteristics and does not indicate a suboptimal response to therapy.* Blood, 2014. **123**(12): p. 1810-7.
349. Herman, S.E.M., et al., *Treatment with Ibrutinib Inhibits BTK- and VLA-4-Dependent Adhesion of Chronic Lymphocytic Leukemia Cells In Vivo.* Clinical Cancer Research, 2015. **21**(20): p. 4642-4651.
350. Lyons, J.J., J.D. Milner, and S.D. Rosenzweig, *Glycans Instructing Immunity: The Emerging Role of Altered Glycosylation in Clinical Immunology.* Front Pediatr, 2015. **3**: p. 54.
351. Forum, U.C., *Ibrutinib for Relapsed / Refractory CLL: A UK and Ireland Analysis of Outcomes in 315 patients.* Haematologica, 2016.
352. Coelho, V., et al., *Identification in CLL of circulating intraclonal subgroups with varying B-cell receptor expression and function.* Blood, 2013. **122**(15): p. 2664-72.
353. Krysov, S., et al., *Surface IgM of CLL cells displays unusual glycans indicative of engagement of antigen in vivo.* Blood, 2010. **115**(21): p. 4198-205.

354. Dwek, R.A., *Glycobiology: Toward Understanding the Function of Sugars.* Chem Rev, 1996. **96**(2): p. 683-720.
355. Takata, M. and T. Kurosaki, *A role for Bruton's tyrosine kinase in B cell antigen receptor-mediated activation of phospholipase C-gamma 2.* J Exp Med, 1996. **184**(1): p. 31-40.
356. Fluckiger, A.C., et al., *Btk/Tec kinases regulate sustained increases in intracellular Ca2+ following B-cell receptor activation.* EMBO J, 1998. **17**(7): p. 1973-85.
357. Bojarczuk, K., et al., *BCR signaling inhibitors differ in their ability to overcome Mcl-1-mediated resistance of CLL B cells to ABT-199.* Blood, 2016. **127**(25): p. 3192-201.
358. Gobessi, S., et al., *Inhibition of constitutive and BCR-induced Syk activation downregulates Mcl-1 and induces apoptosis in chronic lymphocytic leukemia B cells.* Leukemia, 2009. **23**(4): p. 686-97.
359. Wodarz, D., et al., *Kinetics of CLL cells in tissues and blood during therapy with the BTK inhibitor ibrutinib.* Blood, 2014. **123**(26): p. 4132-5.